

THE TRANSIENT RESPONSE OF A HELMHOLTZ RESONATOR
WITH APPLICATION TO SONIC BOOM
RESPONSE STUDIES

By

JAMES DONALD SIMPSON, JR.

Bachelor of Science
Oklahoma State University
Stillwater, Oklahoma
1962

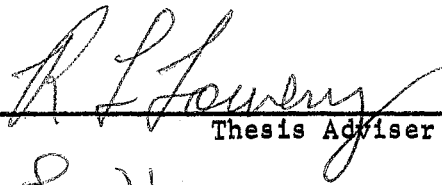
Master of Science
Oklahoma State University
Stillwater, Oklahoma
1963

Submitted to the Faculty of the Graduate School of
the Oklahoma State University
in partial fulfillment of the requirements
for the degree of
DOCTOR OF PHILOSOPHY
May, 1966


OKLAHOMA
STATE UNIVERSITY
LIBRARY
NOV 10 1966


THE TRANSIENT RESPONSE OF A HELMHOLTZ RESONATOR
WITH APPLICATION TO SONIC BOOM
RESPONSE STUDIES

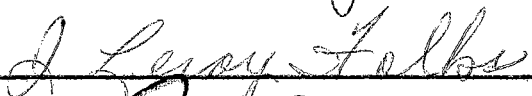
Thesis Approved:

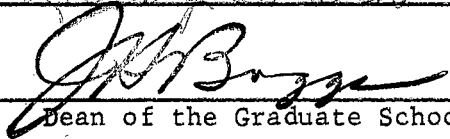


Thesis Adviser









Dean of the Graduate School

321814

ACKNOWLEDGEMENTS

The author wishes to extend his sincere appreciation to several people for their parts in the completion of this work.

Dr. R. L. Lowery who served as my thesis advisor is due particular thanks for his interest, encouragement, and guidance in the preparation of this work. Thanks are due Dr. Lee Harrisberger and Professor L. J. Fila for their helpful comments in the editing of the thesis, and also to Dr. Leroy Folks the remaining committee member.

Mr. Gerald Whitehouse is thanked for his aid in the design and construction of the experimental apparatus. Mrs. Bob Bose is thanked for her help in editing. Mr. Eldon Hardy is thanked for his help with the drafting work. Mrs. Betty Stewart is thanked for the typing of the final manuscript.

I am forever indebted to my wife, Pat, for her interest and encouragement, and for her many sacrifices during my years of graduate study.

TABLE OF CONTENTS

Chapter	Page
I. INTRODUCTION	1
Definition of the Problem	2
The Purpose and Scope of the Study	3
Previous Work	4
II. SONIC BOOMS AND TRANSIENT ACOUSTIC RESPONSES	6
Sonic Boom Signatures	6
Occurrence of Acoustic Resonators in Structures	6
The Sonic Boom and Dynamic Response	10
Evidence from the Oklahoma City Tests	17
III. ANALYSIS OF THE HELMHOLTZ RESONATOR	22
Low Frequency Theory	22
Frequency Limitations	26
Application of Frequency Limitations	27
Higher Modes	30
IV. TRANSIENT RESPONSE	32
Fourier Analysis	32
Frequency Limitations for Transient Response	36
Participation Factors	40
Damping Effects	41
Validity of the Lumped Parameter Model	43
V. EXPERIMENTAL APPARATUS	45
A Plane Wave Tube	45
Generating the Pressure Pulse	47
Test Resonators and Recording Instrumentation	50
Performance of the Test Facility	50
Improved Apparatus and Sonic Boom Simulation	54
VI. EXPERIMENTAL PROCEDURE AND RESULTS	58
Natural Frequency and Damping Measurements	60
Time Response Studies	64

Chapter	Page
Maximax Study	79
Higher Mode Response.	83
The Frequency Criteria.	83
The Effect of Leakage	86
VII. CONCLUSIONS AND RECOMMENDATIONS.	93
SELECTED BIBLIOGRAPHY.	97
BIBLIOGRAPHY	99
APPENDICES	
A. List of Symbols	102
B. List of Major Instrumentation	105
C. Derivations Relating to Frequency Limitations . .	106
D. Calibrations.	135

LIST OF TABLES

Table	Page
3-1. f_L and f_0 for Several Resonator Configurations	29
6-1. Natural Frequency Comparisons	61
6-2. Comparison of Measurements from Figures 6-19 and 6-20 . . .	87
C-1. Values of f_n	113
C-2. Selected Numerical Values of Δ	126
C-3. Summary of Frequency Dependent Approximations	134
D-1. Microphone Sensitivity Comparison	136

LIST OF FIGURES

Figure	Page
1-1. N-Wave Idealized Sonic Boom Signature	2
2-1. Typical Free Ground Overpressure Signatures--Four Types Aircraft	7
2-2. Typical Overpressure Signatures--Same F-101 Flight--Four Locations	8
2-3. Typical Overpressure Signatures Which Do Not Conform Well to the N-Wave Idealization	9
2-4. Simple Acoustic Networks Which Could Be Found in a Typical Home	11
2-5. Typical Residence Floor Plan	12
2-6. Normalized Response of a Simple Oscillator with Natural Period T to a N-Wave of Duration τ	14
2-7. Normalized Maximax Response of a Damped Oscillator to an N-Wave	15
2-8. Laboratory Trace Showing Input and Response Out of Phase .	16
2-9. Laboratory Trace Showing a Response Which is Lightly Damped and Persists for Many Cycles	16
2-10. Sonic Boom Record for Oklahoma City Tests. The Response Persists for Several Cycles	18
3-1. General Helmholtz Resonator	22
4-1. Normalized Amplitude Density Spectrum for an N-Wave	34
4-2. Normalized Energy Density Spectrum for an N-Wave	35
5-1. The Plane Wave Tube	46
5-2. Block Diagram of Pulse Generating Apparatus	48

Figure	Page
5-3. General View of Instrumentation	49
5-4. Bank of Small Loudspeakers Used for a Driving Unit	49
5-5. Test Resonator in Position for Testing	51
5-6. Microphone Comparison Fixture and Test Resonator	51
5-7. Smaller Test Resonator	52
5-8. End Plate Used for Evaluating the Plane Wave Assumption . .	52
5-9. Representative Pulse Produced by the Test Apparatus	55
5-10. Representative Pulse Produced by the Test Apparatus	55
5-11. Representative Pulse Produced by the Test Apparatus	56
5-12. Representative Pulse Produced by the Test Apparatus	56
6-1. Typical Laboratory Trace Used in Measuring Natural Frequency and Damping	60
6-2. Time Response Measurement	60
6-3. Straight Line Approximation of Input and Predicted Response Corresponding to Figure 6-2	66
6-4. Resonator Configuration Used in Testing	67
6-5. Time Response Measurement	69
6-6. Time Response Measurement	69
6-7. Time Response Measurement	71
6-8. Time Response Measurement	71
6-9. Straight Line Approximation of Input and Predicted Response Corresponding to Figure 6-8	72
6-10. Time Response Measurement	74
6-11. Straight Line Approximation of Input and Predicted Response Corresponding to Figure 6-10	75
6-12. Time Response Measurement	76
6-13. Time Response Measurement	76

Figure	Page
6-14. Straight Line Approximation of Input and Predicted Response Corresponding to Figure 6-12	77
6-15. Straight Line Approximation of Input and Predicted Response Corresponding to Figure 6-13	78
6-16. Time Response Measurement	80
6-17. X_F Measurement for One Cycle Sinusoidal Input	80
6-18. X_F Curves for One Cycle Sinusoidal Input	82
6-19. Response Variation Within the Cavity #2 Microphone in the #5 Hole, Near Edge	85
6-20. Response Variation Within the Cavity #2 Microphone in the #1 Hole, Near Center	85
6-21. Time Response Measurement with Leakage or a Second Acoustic Mass	88
6-22. Acoustical and Mechanical Systems with Leakage or a Second Mass	89
C-1. Cross Section of a Circular Symmetrical Resonator Configuration	107
C-2. Geometric Configuration of the Cavity of the Resonator . .	108
C-3. Neck Configuration	115
C-4. Wave Length and Frequency Relationship for Sinusoidal Motion	121
C-5. Electrical Circuit Analogous to a Helmholtz Resonator at Low Frequencies	125
C-6. Mechanical System Analogous to a Helmholtz Resonator at Low Frequencies	127
C-7. Analogous Electrical Circuit for the Neck for $\lambda > L_e/16$. .	130

CHAPTER I

INTRODUCTION

An investigation of the data obtained from the sonic boom tests conducted by the Federal Aviation Administration in Oklahoma City, Oklahoma, during 1964 indicates that many structures may respond to sonic booms in the manner of a Helmholtz resonator. The data obtained from these tests, however, was not complete enough to permit a thorough study of internal pressure responses. No tests were conducted specifically to investigate the mechanism or properties of these pressure responses. While the available data indicated the presence of such phenomena, it ~~was~~ not adequate to permit a comprehensive study.

The Helmholtz resonator in its simplest form consists of an enclosed volume which communicates with the external air through a neck. The response of a Helmholtz resonator to sound, that is more or less steady state pressure oscillations, was studied by Lord Rayleigh [1]¹, and various aspects of the problem have since been studied by other investigators. Rayleigh showed that at low frequencies the resonator could be described by a lumped parameter oscillator with the air in the neck providing mass and that in the cavity providing elasticity. He also pointed out that an exact solution was impossible because of

¹ Numbers in parentheses refer to references in the selected bibliography.

the inadequacy of existing mathematics. This observation has been altered little by developments since his time. More recent investigators have considered various shapes of necks, various damping mechanisms, and the effects of varied positioning of the neck. Very little interest has been shown, however, in the transient response problem which is the object of this work.

Definition of the Problem

It will be shown in Chapter III that the frequency limitation which must accompany the lumped parameter description of the resonator usually becomes effective at frequencies in the neighborhood of the resonant frequency of the resonator. The response of such a lumped parameter oscillator to a pulse such as an N-wave representing an idealized sonic boom would be expected to be greatest when the duration of the pulse and the natural period of the oscillator are approximately the same.

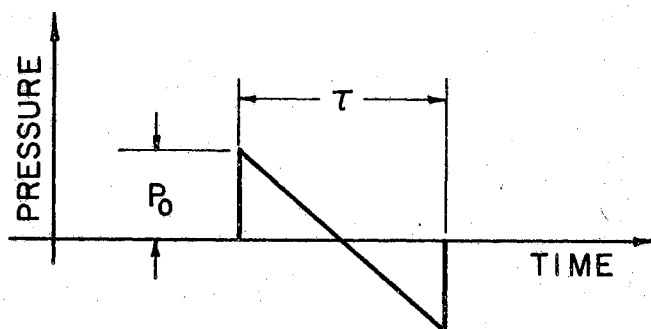


Figure 1-1. N-Wave Idealized Sonic Boom Signature

A Fourier analysis of a pulse shows that the energy of the pulse is not concentrated at a single frequency but is distributed over all frequencies. The frequency limitation on the lumped parameter

description which is given in Chapter III is easily applied to the steady state problem for which the input frequency is well defined, but the meaning of this frequency limitation is not clear in the transient case. On the basis of previous work dealing with Helmholtz resonators it is not possible to state if, or with what accuracy, the lumped parameter description is applicable to study of transient response phenomena. A theoretical and experimental study of the transient response properties of the Helmholtz resonator is needed.

The Purpose and Scope of the Study

The purpose of this study is to investigate the transient response spectra of a Helmholtz resonator in an infinite baffle to a plane wave pressure pulse at normal incidence. The study consists of two phases: theoretical and experimental. The results of the study have application in the area of acoustic responses to sonic booms. Other applications might include acoustic response to blasting or other types of explosions, response to gusts produced by storms, and possible response to noise generated by rocket launchings.

The scope of the theoretical study includes the derivation of a more exact solution for a circularly symmetric resonator in transfer function form and Laplace transformation notation; a discussion of frequency limitations of several models; Fourier analysis of pulses with application to response of an Helmholtz resonator; a qualitative discussion of damping effects and their effect on higher mode response; and a Fourier or Laplace synthesis study of the response of a simple oscillator to an N-wave or the first few harmonics thereof.

The scope of the experimental phase of the study consists of the design and construction of a plane wave tube; development of apparatus for producing pressure pulses; design and construction of a test resonator; instrumentation to measure and record input pressure and internal pressure of a test resonator as functions of time; and two series of tests which demonstrate, first, that a Helmholtz resonator responds to pressure pulses generally as a lumped parameter oscillator responds to a shock input, and secondly, that higher mode responses with attendant magnitude and phase differences of internal pressure are of minor importance.

Previous Work

There is no known previous work dealing with the transient response of a Helmholtz resonator which includes any consideration of the possibility of higher mode response or deficiency of the lumped parameter model. Olson [2] briefly examined transient response of a lumped parameter acoustical resonator, but he simply accepted the lumped parameter model with no discussion, justification or study of frequency limitations. There is no known experimental work in the area.

Rayleigh [1] presented the lumped parameter analysis for the steady state case and low frequency.

Beranek [3] gave some discussion of approximately what the frequency limitations should be in the steady state problem.

Ingard [6] in a comprehensive paper examined the effects of different neck cross sections, different cavity geometry, different positioning of the neck, and different damping mechanisms, all pertaining to

the steady state case. Ingard [7] examined the near field of a spherical Helmholtz resonator exposed to a steady plane wave. Lambert [8] presented a systematic study of damping effects.

Albert and McGinnis [9] discussed several-degrees-of-freedom acoustical networks built up from multiple Helmholtz resonators. Lagrange's equations were used to develop the equations of motion. The lumped parameter model was accepted. The work done by Albert and McGinnis coupled with the present study which verifies the lumped parameter model in the transient situation form an excellent basis for handling the transient response of an acoustical network with several-degrees-of-freedom.

Much work has been done with the transient response of linear systems and there are many good sources in the literature. References used for this work included Jacobsen and Ayre [5] and Thompson [10]. Cheng [11] did some extensive theoretical work with the response of simple oscillators, beams, and plates to N-wave inputs. Arde Associates [12] presented a great deal of theoretical work with sonic boom response including some good work on the response of a simple oscillator to various types of idealized booms.

In the report published by Andrews Associates [13] the probability of Helmholtz resonator type response to sonic booms was discussed. The section of the report which contains this discussion was originally written by J. D. Simpson who was serving as consultant to Andrews Associates of Oklahoma City. A paper [14] dealing specifically with the area of this thesis, written by J. D. Simpson and Dr. R. L. Lowery, is to be presented at the 70th meeting of the Acoustic Society of America in November, 1965.

CHAPTER II

SONIC BOOMS AND TRANSIENT ACOUSTIC RESPONSES

The problem of the transient response of a Helmholtz resonator was first encountered by the author in 1964 when he and Dr. R. L. Lowery were consulting with Andrews Associates of Oklahoma City on their contract for recording and reporting data from the Federal Aviation Agency's sponsored sonic boom tests in Oklahoma City in 1964.

Sonic Boom Signatures

The pressure pulse referred to as a sonic boom is often idealized as an N-wave as shown in Figure 1-1. Figures 2-1 and 2-2 are recorded sonic boom signatures from the 1964 tests in Oklahoma City. These recorded signatures are reasonably close in shape to the idealized N-wave. These figures were taken from reference [13]. Figure 2-3 shows recorded signatures from the Oklahoma City tests which are also fairly typical but are not approximated well by the N-wave. They could be better approximated perhaps by one cycle of a sine wave or of a triangular wave.

Occurrence of Acoustic Resonators in Structures

Any typical home and many commercial buildings contain enclosed volumes and openings which could function as Helmholtz resonators

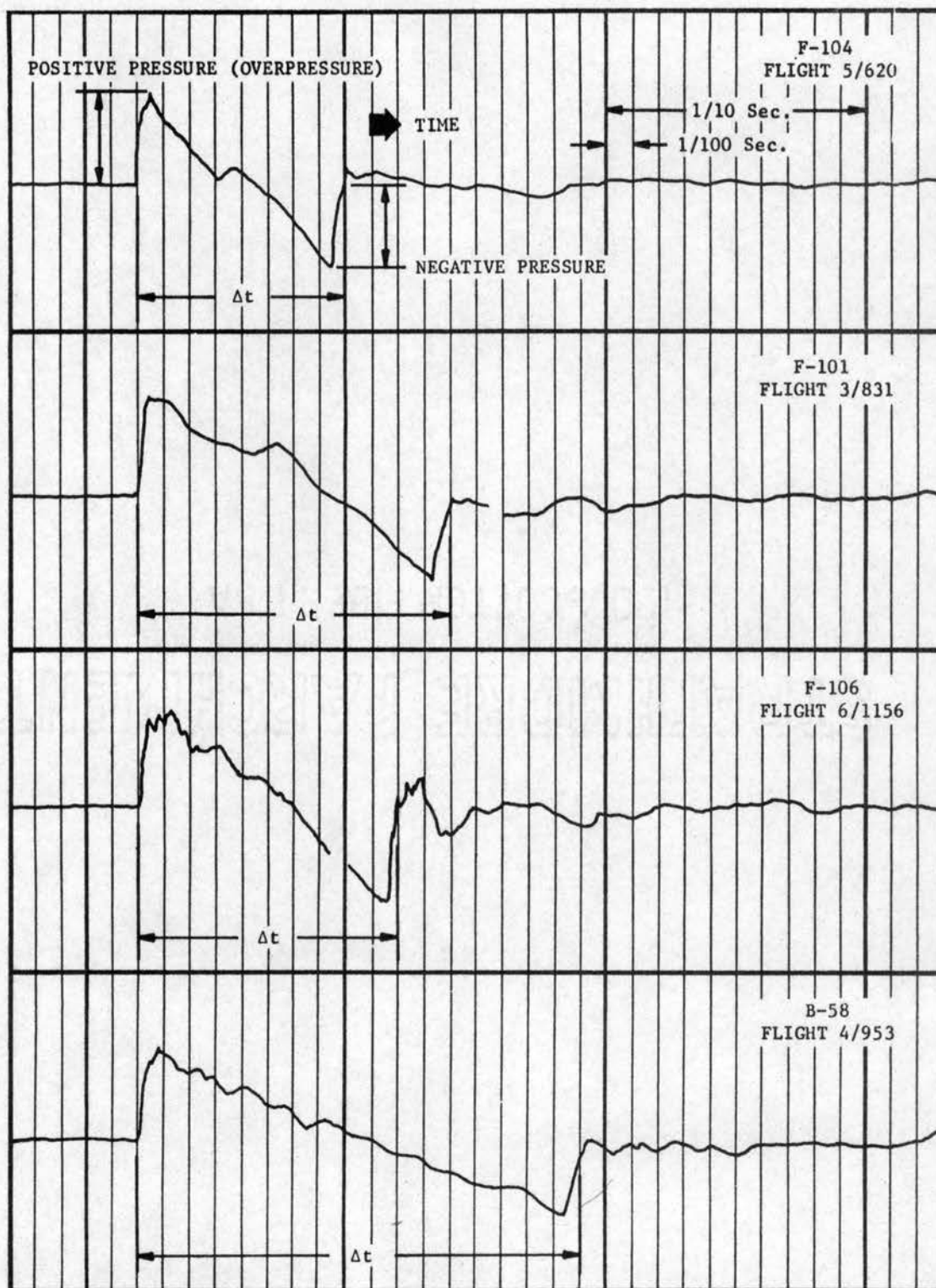


Figure 2-1. Typical Free Ground Overpressure Signatures
Four Types Aircraft

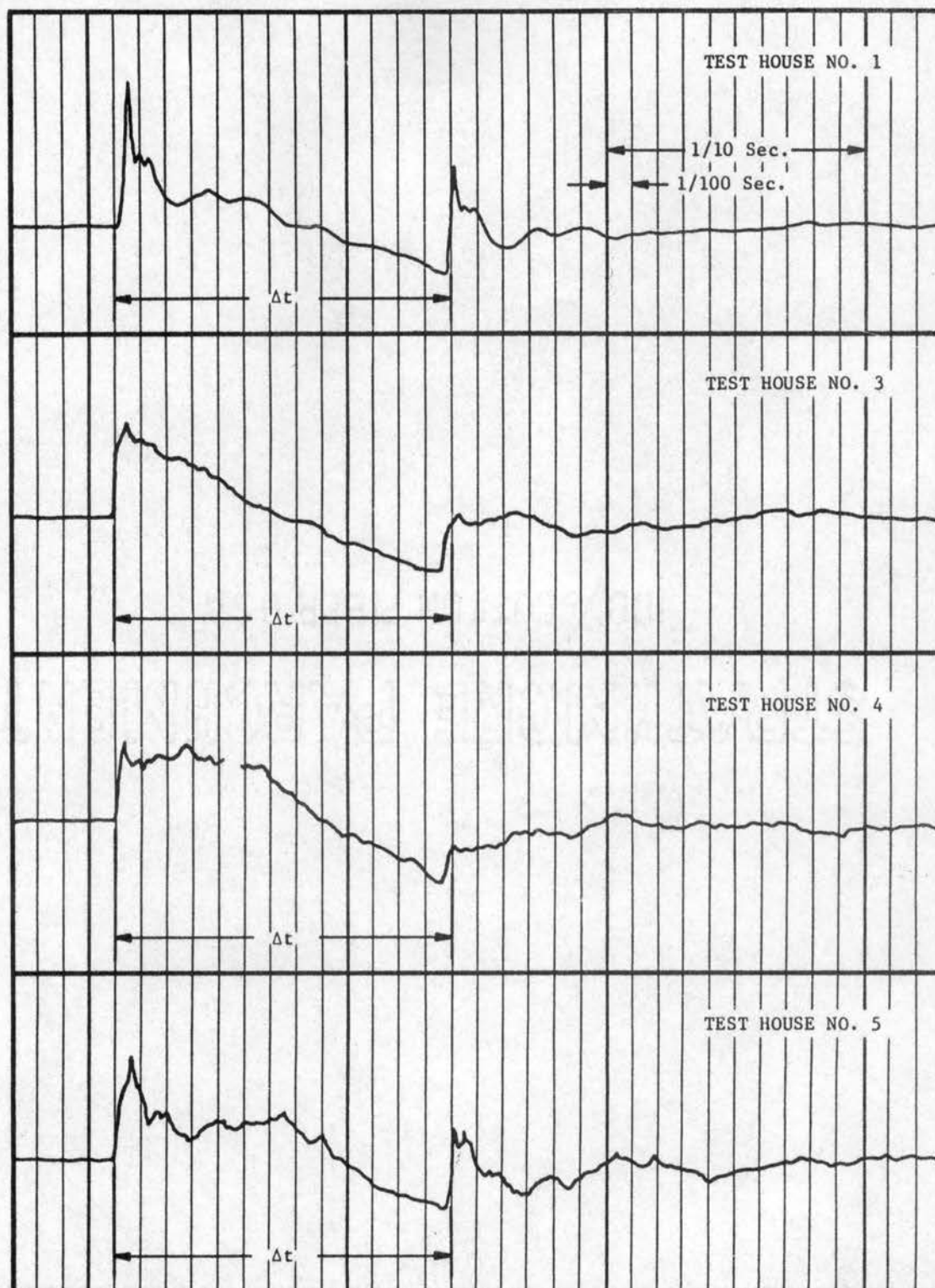


Figure 2-2. Typical Overpressure Signatures
Same F-101 Flight
Four Locations

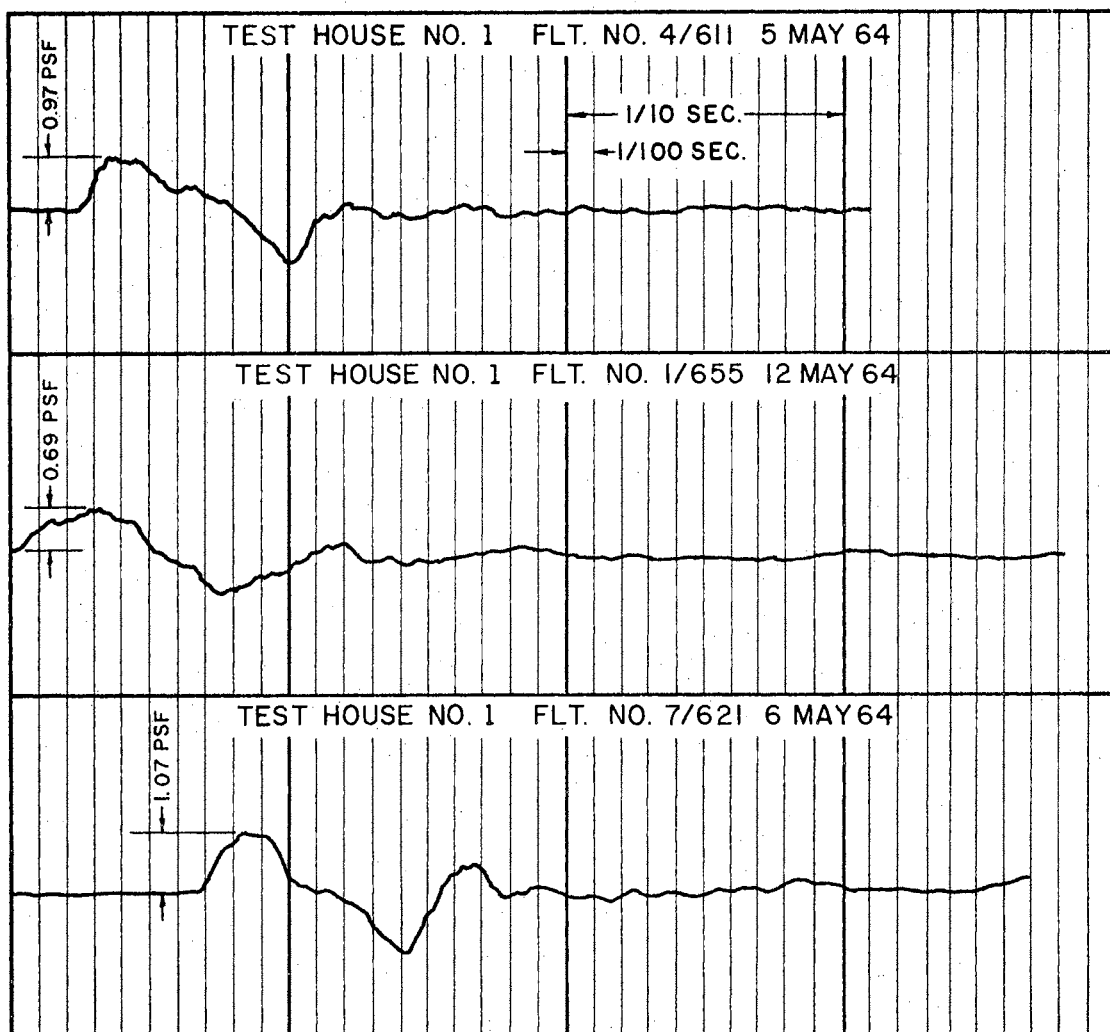


Figure 2-3. Typical Overpressure Signatures Which Do Not Conform Well to the N-Wave Idealization

and would have resonant frequencies in the region where considerable excitation could be expected from sonic booms. Natural frequencies of individual rooms with one open door or window would typically be in the range from five to fifteen cycles per second which would correspond to periods of approximately 0.07 to 0.20 seconds. Very large rooms with large openings could have lower natural frequencies, perhaps as low as one cycle per second. The time duration of the sonic booms recorded in the Oklahoma City tests ranges from approximately 0.08-0.18 seconds.

Various combinations of rooms, hallways, windows, and doors would produce acoustical systems of several degrees of freedom which if properly tuned could be strongly excited by sonic booms. Three very simple possible configurations are shown in Figure 2-4. Casual inspection of the floor plan of any typical home will reveal many such simple possibilities as well as much more complicated acoustical networks. Figure 2-5, which was taken from reference [13], exhibits many possibilities for simple, one-degree-of-freedom resonators and more complicated acoustical systems. The resonance properties of rooms or groups of rooms will be influenced to some extent by the flexibility of the structure, a factor which is not included in this study.

The Sonic Boom and Dynamic Response

An idealized pressure signature of a sonic boom is shown in Figure 1-1. The duration of the boom depends mostly on the length of the aircraft which generated the boom. The measured durations

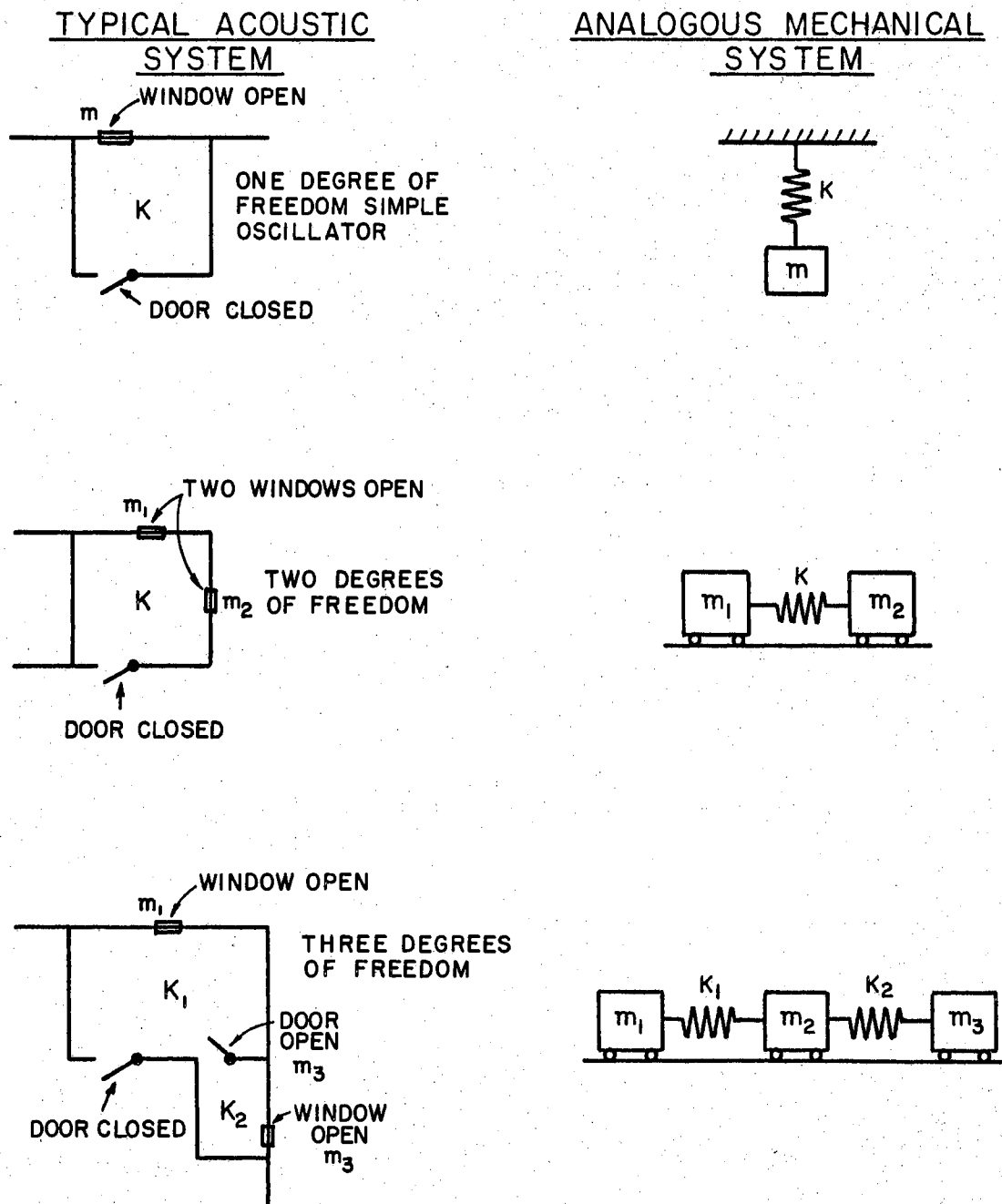


Figure 2-4. Simple Acoustic Networks Which Could Be Found in a Typical Home

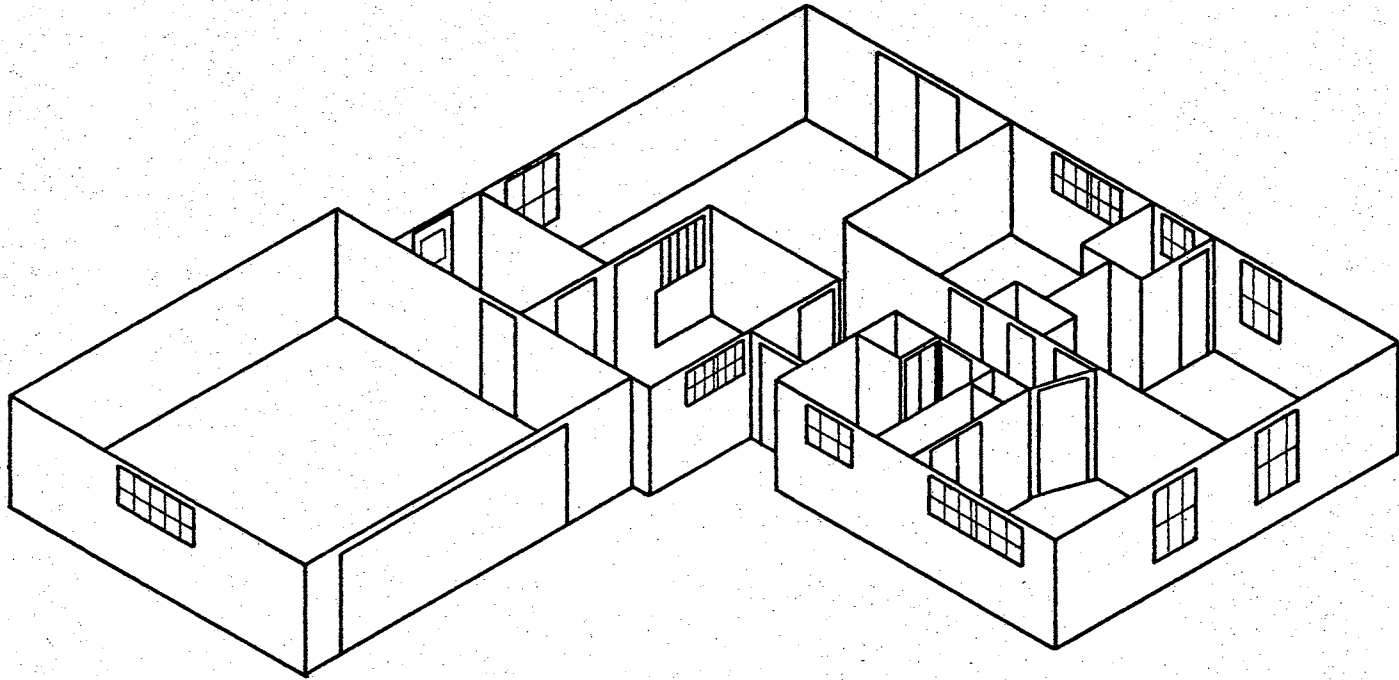


Figure 2-5. Typical Residence Floor Plan

of booms in the Oklahoma City tests were approximately 0.08, 0.10, 0.12, and 0.18 seconds corresponding to the four types of aircraft used in the tests. It is expected that the duration of the boom generated by the proposed supersonic transport will be on the order of 0.25 seconds. The amplitude of the pressure pulse which is considered "safe" at this time is approximately 2 psf [13]. The normalized response of a simple mechanical oscillator to an N-wave force pulse is shown in Figure 2-6. The developments presented in Chapter III show that the differential equations which govern the Helmholtz resonator are identical in form with those which describe a simple mechanical oscillator. Thus, the curves shown in Figure 2-6 also apply to the normalized internal pressure response of a Helmholtz resonator to a N-wave pressure pulse. From the figure it can be seen that pressure magnification on the order of two may be expected to occur in a properly tuned resonator. It is safe to assume that higher pressure differentials will mean higher damage probabilities so that the importance of the doubling of the pressure by the resonator is obvious. Figure 2-7 shows the effect of a small amount of viscous damping on the response of a simple oscillator to a N-wave. Timing effects can be very important also. If the pressure rise inside reaches a maximum when the outside pressure swings through a minimum, a maximum possible pressure differential is developed across windows or wall panels. This timing effect is shown in Figure 2-8 which is a laboratory response.

A complicated acoustical network such as a house could very easily demonstrate rather unusual dynamic response properties. As

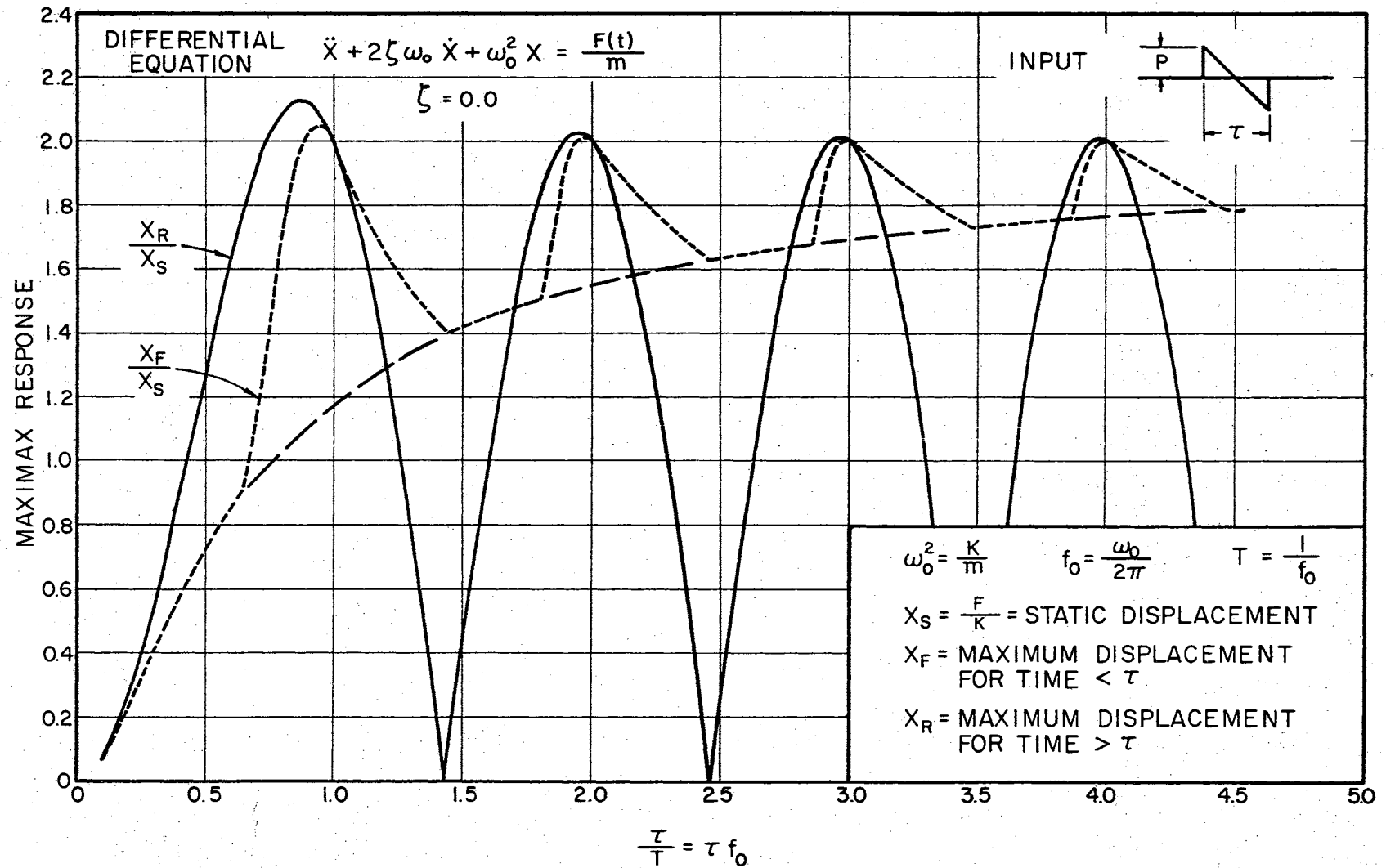


Figure 2-6. Normalized Response of a Simple Oscillator With Natural Period T to a N-Wave of Duration τ

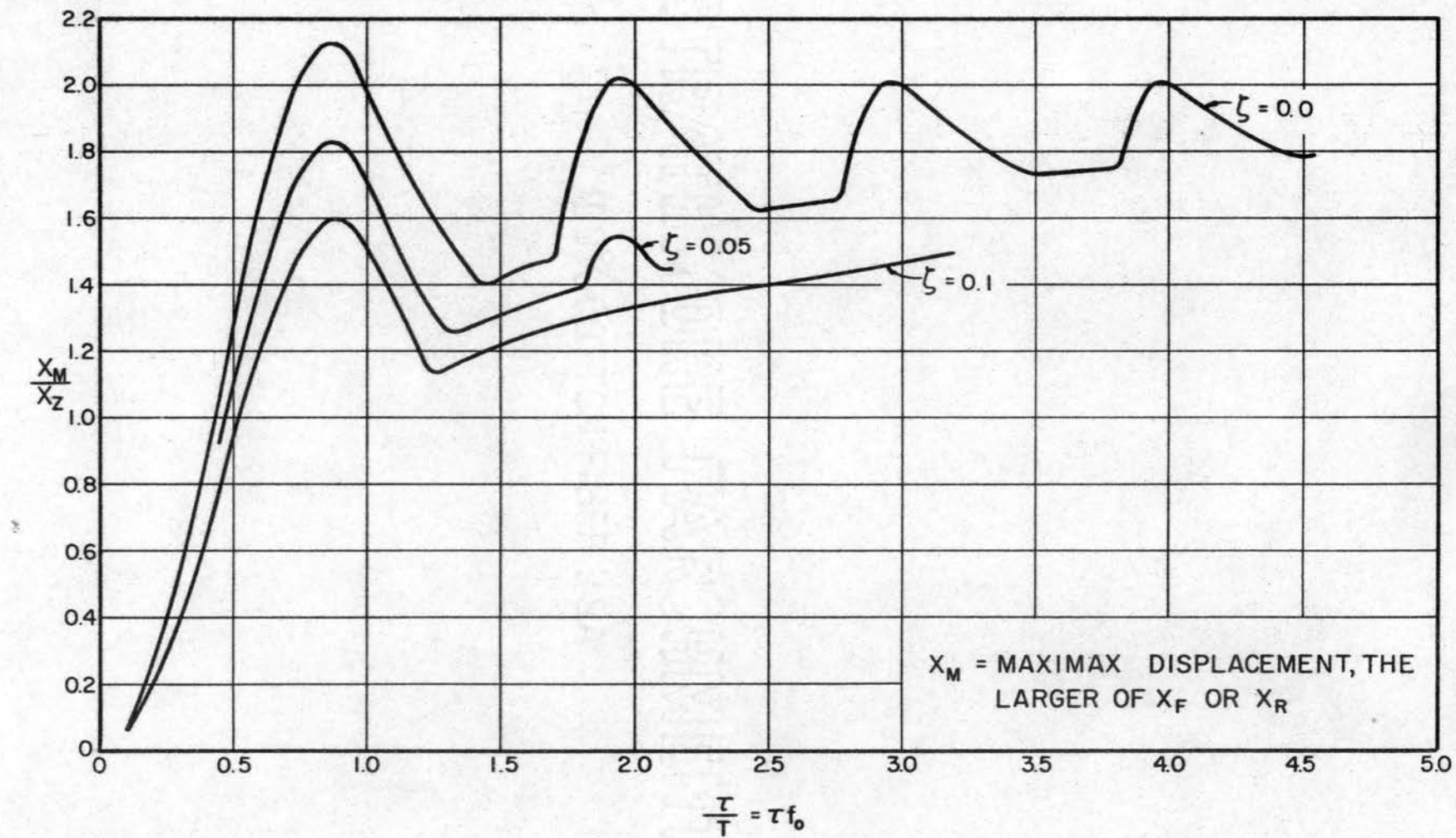


Figure 2-7. Normalized Maximax Response of a Damped Oscillator to a N-Wave

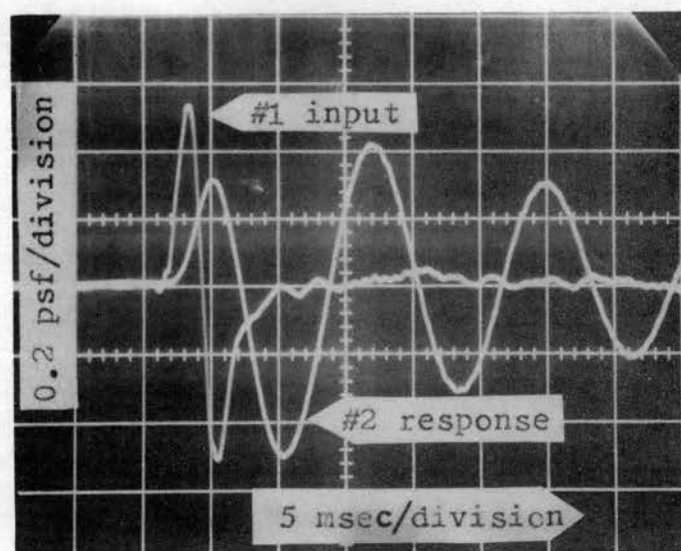


Figure 2-8. Laboratory Trace Showing Input and Response Out of Phase

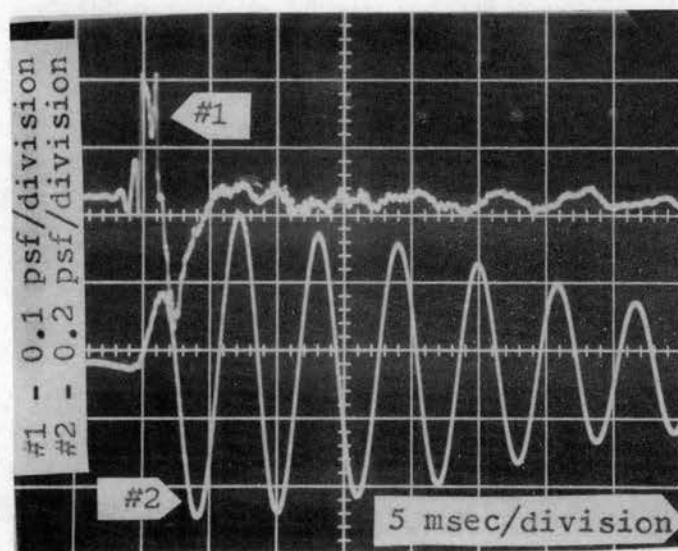


Figure 2-9. A Laboratory Trace Showing a Response Which is Lightly Damped and Persists for Many Cycles

an example, beating could be expected and was in fact observed in the Oklahoma City tests.

Pressure amplification resulting from reflections from the ground and nearby buildings coupled with acoustic amplifications within the structure could easily result in greatly amplified pressure differentials across wall panels or windows. Conditions favorable to very large amplifications may not occur frequently but, on the other hand, it is statistically probable that some situations resulting in considerable amplification will occur when a boom is generated over a large urban area.

The presence of many cycles of acoustic vibrations might excite any critically tuned system to considerably more amplitude than could the incident pulse. In other words, it is possible that a sonic boom could set up pressure oscillations within a structure which could persist for ten or more cycles; these pressure oscillations could in turn act as the driving force on any other systems within the house which were capable of vibration. This possibility is illustrated in Figure 2-10 which is a recorded response from a sonic boom and in Figure 2-9 which is a laboratory response.

Evidence of Acoustic Responses From the Oklahoma City Tests

Examination of the data obtained from the Oklahoma City tests revealed considerable evidence of acoustic resonance phenomena. The inside microphone in Test House #1 which was located directly under the flight path recorded pressure oscillations which persisted for a

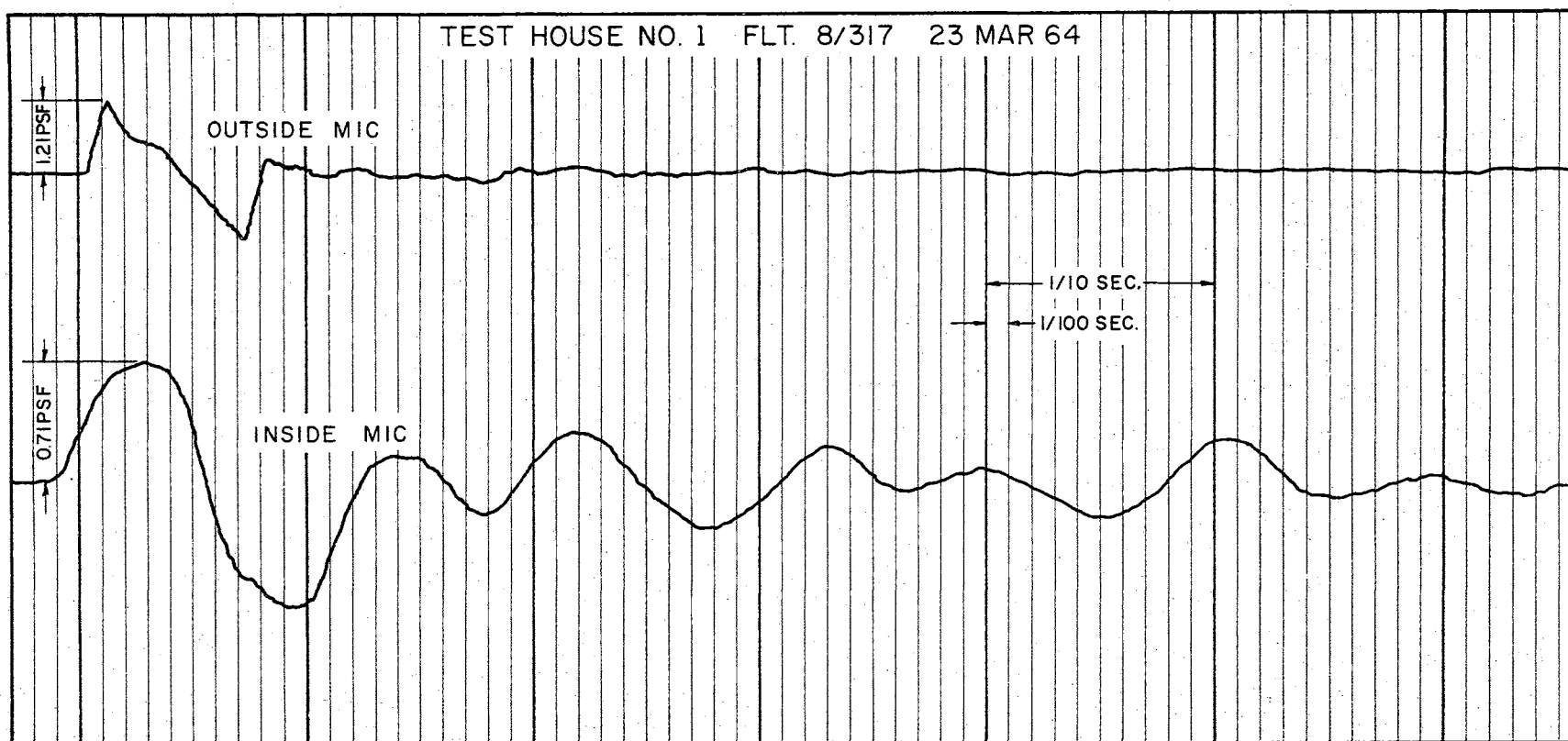


Figure 2-10. Sonic Boom Record for Oklahoma City Tests.
The Response Persists for Several Cycles.

considerable time after the passage of the boom. Figure 2-10 shows one such recorded response. Beating was frequently observed; the pressure oscillations seeming to disappear entirely for a time and then reappear. The inside pressure was occasionally a little larger than the outside pressure. The ceiling and window of the front room in Test House #5 often appeared to be driven to considerable amplitude by something other than the incident boom. The following discussion is taken directly from reference [13]. The figures used in the discussion are not included in this paper.

c. Window Glass - Test House No. 5

In the typical oscillograph records shown for July 28th [Figure 52-1 through 52-8], several basic wave forms are shown, indicating that there is considerable variance in the nature of the pressure signature [wave form], and it is to be expected that different types would produce different responses in a given element.

From the graph [Figure 57 in Section III] it is observed that peak overpressure does not necessarily produce peak displacement or strain. This is to be expected since the shape of the pressure signatures vary significantly as mentioned above. The response of a simple structure depends upon both the amplitude of excitation and the time duration. The principle and theory of this statement is discussed more fully in following subsections of this report.

Aside from the obvious variations due to inconsistencies in the shape of the pressure wave, another unusual effect was observed in some of the displacement recordings. On the records corresponding to Flights 4, 5, 6, 7, and 8 of July 28 [Figures 52-4 through -8], relatively high readings were taken for both the differential transformer and the strain gage. The fact that both readings were high suggests that the window actually was driven by some force to a considerable amplitude and that the instruments were not in error.

The strain and displacement traces show the window to be vibrating at a low frequency, about 5 cps. This is unexpected since the natural frequency of the window was found to be on the order of 25 cps, in shock excitation tests. This figure of 25 cps also checks with the calculated natural frequency.

It can be seen in some of the recordings that the peak strain [and displacement] can occur after the pressure wave is past. The logical explanation for this is that a secondary driving function has been generated and continues to drive the window at a low frequency, after the wave has passed.

Considering the possibility of a pressure fluctuation, or oscillation, in the living room, it can be seen that the ceiling of the room, on which a strain gage [#1] was installed, should also be excited at the same frequency.

Figure 76 is a tracing of the oscillograph record for Flight 7 of July 28 showing responses only for pressure signature, differential transformer [#1] and strain gage [#7] on the window, plus living room ceiling [Strain Gage #1].

This frequency of about 5 cps can be detected in the strain recordings [Strain Gage #1] for the living room ceiling. The amplitude of vibration of the ceiling is low, which is to be expected in view of massive construction. [The ceiling carries the floor joists for the room above.] The shock excitation tests demonstrated that the natural frequency of the ceiling is far above 5 cps which rules out the possibility of any other explanation for the correlation of motion between the window and ceiling. It can also be seen that the motion of the ceiling is reasonably well in phase with the motion of the window. That is, when the window moves outward, the ceiling is moving upward. This is to be expected since both of these members appear to be driven by a forcing function well below either of their respective natural frequencies.

At this point it can be reasonably well established that a pressure fluctuation is responsible for the relatively high readings for these particular flights. The most credible explanation at this time is that the living room and the connecting passageways, doors, and windows constitute an acoustic resonator similar to a Helmholtz Resonator. The natural frequency of such a device is a function of the total volume of a cavity [the room], the length of connecting passages [the doors and hallways] and the temperature and humidity of the ambient air. While it would be difficult to arrive at exact values for the various variables presented here, preliminary calculations show that this room can easily have a natural frequency of 5 cps.

The exact tuning of the room would depend upon the number of doors and windows open and possibly upon the position of doors and windows in other parts of the house. This could explain why most of these unusual recordings were taken on simultaneous flights; no windows or doors would likely be closed or opened between flights.

The question arises as to the occurrence of the pressure fluctuations on one day and not on another. This can be explained by the fact that the temperature and humidity of the air varies widely from one day to the next, and more important, it is not likely that the same combination of doors and windows would be open or closed on any two days. Part of these flights were made on some of the hottest days of the year which made it necessary to open many of the windows in the back part of the house. Also, it is thought that the shape of the pressure signature has a direct bearing on the excitation of Helmholtz resonance.

It might be possible for considerable stresses to be built up in a window having a natural frequency close to the Helmholtz resonance. While the pressure fluctuation inside the room is probably very slight, it could continue for a sufficiently long period to allow potentially dangerous resonant vibrations to be developed in anything having the

same natural frequency. That is, the energy input to the window could last for several times the duration of the pressure signature.

Additional investigation is indicated in this area of Helmholtz resonance.

CHAPTER III

ANALYSIS OF THE HELMHOLTZ RESONATOR

The electrical or mechanical analog representation of the Helmholtz resonator as well as the most suitable mathematical model are dependent on the frequency of the input sound.

Low Frequency Theory

The resonator consists of an enclosed volume V which communicates with the external air through a neck of area A and length L' .

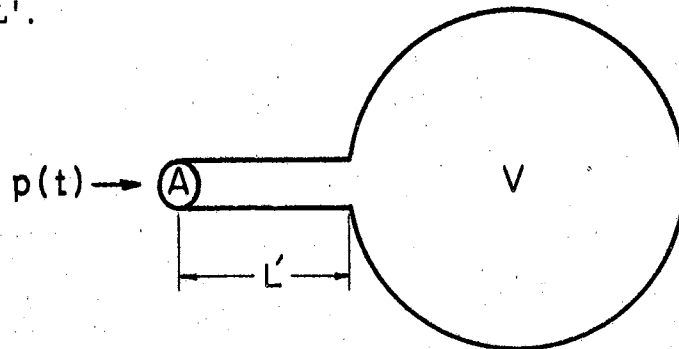


Figure 3-1. General Helmholtz Resonator

If it is assumed that the wavelength of pressure variations is long enough, then the pressure everywhere inside the volume is essentially the same. Very little velocity is attained within the volume so that there is very little change in kinetic energy within the volume. The air in the volume acts as a spring alternately absorbing and relinquishing potential energy by virtue of its

resistance to compression or dilatation. Since acoustic level pressure variations are relatively small, the temperature variations caused by the alternate compression and rarefaction will also be small as will be the temperature gradients. Due to the small temperature gradients and large distances between regions of compression and rarefaction and the limited time during which the temperature gradients exist, there is very little heat transfer. Thus, it is reasonable to assume that the compression takes place adiabatically. Adiabatic compression is expressed mathematically as

$$PV^\gamma = \text{constant}. \quad (3-1)$$

The differential of equation (3-1) is

$$dPV^\gamma + \gamma PV^{\gamma-1} dV = 0, \quad (3-2)$$

which can be solved for dP as

$$dP = -\frac{\gamma P}{V} dV. \quad (3-3)$$

In the neck, the air attains appreciable velocity and thus kinetic energy. If the neck (the space through which the kinetic energy is sensible) is very small in comparison with the wavelength, the air moves in response to the differential pressure across it and to its own inertia very much as an incompressible fluid would. Thus, the air in the neck behaves as a mass while that in the enclosed volume behaves as a spring. Therefore, if x is the displacement of the air plug in the neck, then a Newtonian force balance on that air mass leads to the differential equation of motion,

$$(\rho_0 L_e A) \frac{d^2 x}{dt^2} + \frac{\gamma P_0}{V} A^2 x = P(t) A, \quad (3-4)$$

where L_e the effective length of the neck, which includes the end effects, has been used instead of the actual length L' . If $\rho_0 P_0$ is replaced by its equivalent $\rho_0 c^2$ and a variable change,

$$\bar{X} = Ax = \text{volume displacement}, \quad (3-5)$$

is made, the equation of motion may be written as

$$\left(\frac{\rho_0 L_e}{A}\right) \frac{d^2 \bar{X}}{dt^2} + \left(\frac{\rho_0 c^2}{V}\right) \bar{X} = P_1(t), \quad (3-6)$$

or

$$\left(\frac{\rho_0 L_e}{A}\right) \frac{dU}{dt} + \left(\frac{\rho_0 c^2}{V}\right) \int U dt = P_1(t), \quad (3-7)$$

where U is the volume velocity. From either of these equations the natural frequency is seen to be

$$f_0 = \frac{c}{2\pi} \sqrt{\frac{A}{VL_e}}. \quad (3-8)$$

The incident pressure $P_1(t)$ has been assumed to be sinusoidal and the steady state situation has also been assumed in the above derivation. Similar derivations may be found in references [1], [3], and [4].

The effective length of the neck is used rather than the actual length since some of the air on either end of the neck moves in unison with that in the neck. The effective length is given by

$$L_e = L' + \Delta_1 + \Delta_2, \quad (3-9)$$

where Δ_1 and Δ_2 are end corrections. The neck corrections depend on the shape of the neck cross section, the geometric configuration of the resonator, and the frequency of the sound. Generally they are taken as $.85A$ for an infinite baffle termination and $.6A$ for an unflanged termination.

In the frequency domain, equation (3-7) becomes

$$U(S) = \frac{P_1(S)}{\left(\frac{\rho_0 L_e}{A}\right)S + \frac{\rho_0 c^2}{VS}} \quad (3-10)$$

The pressure within the cavity is given by

$$P(S) = \frac{P_1(S)}{\frac{S^2}{\omega_0^2} + 1}, \quad (3-11)$$

where ω_0 is the natural frequency of the resonator in radians per second and is given

$$\omega_0 = c \sqrt{\frac{A}{VL_e}} \quad (3-12)$$

It can be seen that the natural frequency of the resonator depends on the area and length of the neck and the volume of the cavity. The shape of the neck is a rather minor factor as long as the cross section is not greatly elongated. The geometric configuration of the cavity does not enter into the problem, that is the cavity might be spherical, cubical, or cylindrical with no change in the properties of the resonator as long as the volume remains constant.

There are a number of refinements or corrections which can be included in the description of the resonator. The end corrections depend not only on the area and termination of the neck but also on the shape and on how and where the neck is joined with the cavity and also on the geometry of the cavity. Damping should be considered to improve the description. Damping mechanisms include reradiation of energy from the mouth of the resonator, viscous losses, thermal losses to a conducting surface and mechanical losses to a non-rigid shell.

These refinements are useful in some cases, but for the most part the very simple description already given is quite adequate as long as the frequency limitation is observed.

At higher frequencies this simple model becomes inadequate. The resonator is actually a continuous system with distributed mass, elasticity and damping. The resonator is capable of response in higher modes which are much more strongly tied to the detailed geometric configuration of a given resonator.

Frequency Limitations

The derivations presented in Appendix C permit a mathematical statement of the frequency limitations which must be associated with the lumped parameter description of the Helmholtz resonator. The procedure used in establishing these frequency limitations follows closely along the lines used by Beranek [3]. The lumped parameter model which is described in the section on low frequency theory is shown to be accurate within approximately five percent for frequencies low enough so that the wavelength is greater than about sixteen times the characteristic dimension of the resonator. The characteristic dimension is normally taken as the largest dimension of the resonator. Analogous electrical and mechanical systems which are valid if the frequency limitation is satisfied are shown in Figures C-5 and C-6.

As the frequency of the input sound is increased it becomes necessary to use a more complicated mathematical or analog description of the resonator. The geometric configuration of the resonator becomes more important as the frequency is increased. It was shown in the previous

section that at low frequencies the Helmholtz resonator could be described by the cross sectional area and length of the neck and the volume of the cavity. The neck cross section might be round, square, or triangular and the cavity might be spherical, cubical or etc. with only very minor effects on the properties of the resonator. At higher frequencies this is no longer true; the geometric configuration becomes all important in determining the higher modes. A solution which is valid for higher frequencies is thus tied to a particular geometric configuration. The mathematics involved in the higher frequency solution become very difficult even for a very simple geometric situation. If the geometry is not extremely simple, the mathematics become unmanageable. The solution obtained may be questionable because of assumptions which must be made to permit a solution at all. Also, the complexity of the higher frequency solution may be such that it is almost impossible to use. The tremendous mathematical difficulties involved in the higher frequency solution might be tolerated if the problem could be solved once and the results applied thereafter to any Helmholtz resonator. However, this is not the case; each different geometric situation requires a separate solution.

Any study of the general Helmholtz resonator for which the geometric details are unimportant must rely on the lumped parameter model which implies a frequency restriction.

Application of Frequency Limitations

The relationship between the limiting frequency, f_L , below which the simple low frequency lumped parameter model is assumed to

be valid and the natural frequency of the resonator, f_0 , is in many cases more important than the relationship between f_L and characteristic dimension of the resonator. The latter relationship is given by

$$\lambda > 16 D, \quad (3-13)$$

or

$$f_L < \frac{c}{16D}, \quad (3-14)$$

where D is the characteristic dimension of the resonator. The relationship between f_L and f_0 varies with the geometric configuration of the resonator and cannot be expressed by a single equation. Some idea of the range of variation may be obtained, however, by looking at a few examples.

The expression for the natural frequency of an Helmholtz resonator was given previously as

$$f_0 = \frac{c}{2\pi} \sqrt{\frac{A}{VL_e}}. \quad (3-15)$$

In order to evaluate equation (3-15) for f_0 , it is necessary to make some arbitrary assumptions about the geometry of the resonator. As good a choice as any to examine is the circularly symmetric resonator discussed in Appendix C and used in the experimental part of this work. Table 3-1 gives some calculated values of f_L , f_0 and f_L/f_0 for several geometric configurations. The range of values of f_L/f_0 is about 0.4 to 1.5. Often the limiting frequency is less than the natural frequency. Maximum amplitudes can be expected in either the steady state situation or the transient situation when the period or

TABLE 3-1

 f_L AND f_o FOR SEVERAL RESONATOR CONFIGURATIONS

Cavity Length (Inches)	Neck Diameter (Inches)	Neck Length (Inches)	D (Inches)	$f_L = \frac{852}{D}$ (cps)	f_o (cps)	$\frac{f_L}{f_o}$
2.5	1.0	2.0	5.5	155	148	1.05
		0.0			270	.57
	1.5	2.0			206	.75
		0.0			331	.47
	3.0	2.0			350	.44
		0.0			468	.33
5.0	1.0	2.0	5.5	155	104	1.49
		0.0			191	.81
	1.5	2.0			146	1.06
		0.0			234	.66
	3.0	2.0			247	.64
		0.0			331	.47
7.5	1.0	2.0	7.5	113	85	1.33
		0.0			156	.76
	1.5	2.0			119	.95
		0.0			191	.59
	3.0	2.0			202	.56
		0.0			270	.42
10.0	1.0	2.0	10.0	85	74	1.15
		0.0			135	.63
	1.5	2.0			103	.83
		0.0			165	.52
	3.0	2.0			175	.49
		0.0			234	.36

Cavity Diameter = 5.5 inches

frequency of the input is about the same as the natural period or natural frequency of the resonator. The validity of the lumped parameter model may well be questionable at the resonant frequency.

Higher Modes

The higher modes in which the Helmholtz resonator is capable of responding are standing wave type modes and are thus very closely associated with the geometry of the cavity. Some comparison between the natural frequencies of the Helmholtz mode and these higher modes is needed. In the previous section it was shown that the Helmholtz resonant frequency would be very approximately equal to the limiting frequency which can be expressed mathematically as

$$f_0 \approx f_L = \frac{c}{16D} , \quad (3-16)$$

where c is the velocity of sound and D is the largest or characteristic dimension of the resonator. The above formula is approximate; nevertheless, it is a useful answer and would undoubtedly be good within a factor of two in either direction.

The higher modes are of a standing wave nature and the lowest possible of these modes might be estimated by the condition

$$\frac{\lambda}{2} = D, \quad (3-17)$$

or

$$f = \frac{c}{2D} . \quad (3-18)$$

Comparison of equations (3-16) and (3-18) shows that the higher modes may be expected to have natural frequencies of eight or more times

the Helmholtz frequency. This comparison is admittedly subject to considerable error, but it is impossible to do any better without considering a particular resonator and comparing the resonant frequencies. This would be a very difficult task and the results would only apply to the particular geometric configuration considered. The results could be extended to a general resonator only crudely and would be no better than the comparison already established.

CHAPTER IV

TRANSIENT RESPONSE

In the steady-state response analysis, frequency limitations are applied by considering the frequency domain description of the input sound. It would seem logical to apply frequency limitations in the transient problem in the same way. However, the frequency domain description of a pulse is continuous rather than discrete so that no single frequency is available from the Fourier analysis which characteristically describes a pulse. In the transient problem, however, the natural frequency of the resonator is more important than the frequency description of the input pulse in determining the accuracy of the lumped parameter description.

Fourier Analysis

An aperiodic function $f(t)$ is best described in the frequency domain by the Fourier integral which can be defined [16] as

$$F(\omega) = \frac{1}{2\pi} \int_{-\infty}^{\infty} f(t) e^{-j\omega t} dt. \quad (4-1)$$

The frequency domain representation $F(\omega)$ is not discrete but is a continuous function of the angular frequency ω and in general is complex. Usually the amplitude density spectrum and phase density spectrums are more useful than the complex form. In many cases the

amplitude density spectrum which is simply the absolute value of $F(\omega)$ is the most useful. A description of the energy and frequency relationship is given by the energy density spectrum which can be defined [16] as

$$\bar{\Phi}(\omega) = 2\pi |F(\omega)|^2 \quad (4-2)$$

The amplitude density spectrum $|F(\omega)|$ is not an actual amplitude characteristic of $f(t)$ because all amplitudes are of infinitesimal magnitude; it is rather a characteristic which shows relative magnitudes only. The same is true for the energy density spectrum. The Fourier integral can be used only approximately to predict response of a single-degree-of-freedom linear system and its correlation with the response of a several-degrees-of-freedom system is virtually impossible.

The amplitude density spectrum and the energy density spectrum for a N-wave pulse are presented in normalized form in Figures 4-1 and 4-2. The spectra for other pulses similar to a N-wave will be generally similar to Figures 4-1 and 4-2. It is difficult to obtain much information from these curves which would be of any use towards predicting the importance of higher mode response. A pulse which contained a large amplitude high frequency signal would show this high frequency energy on either an amplitude density spectrum or an energy density spectrum, but the same information is available from the pulse itself and is perhaps more apparent there.

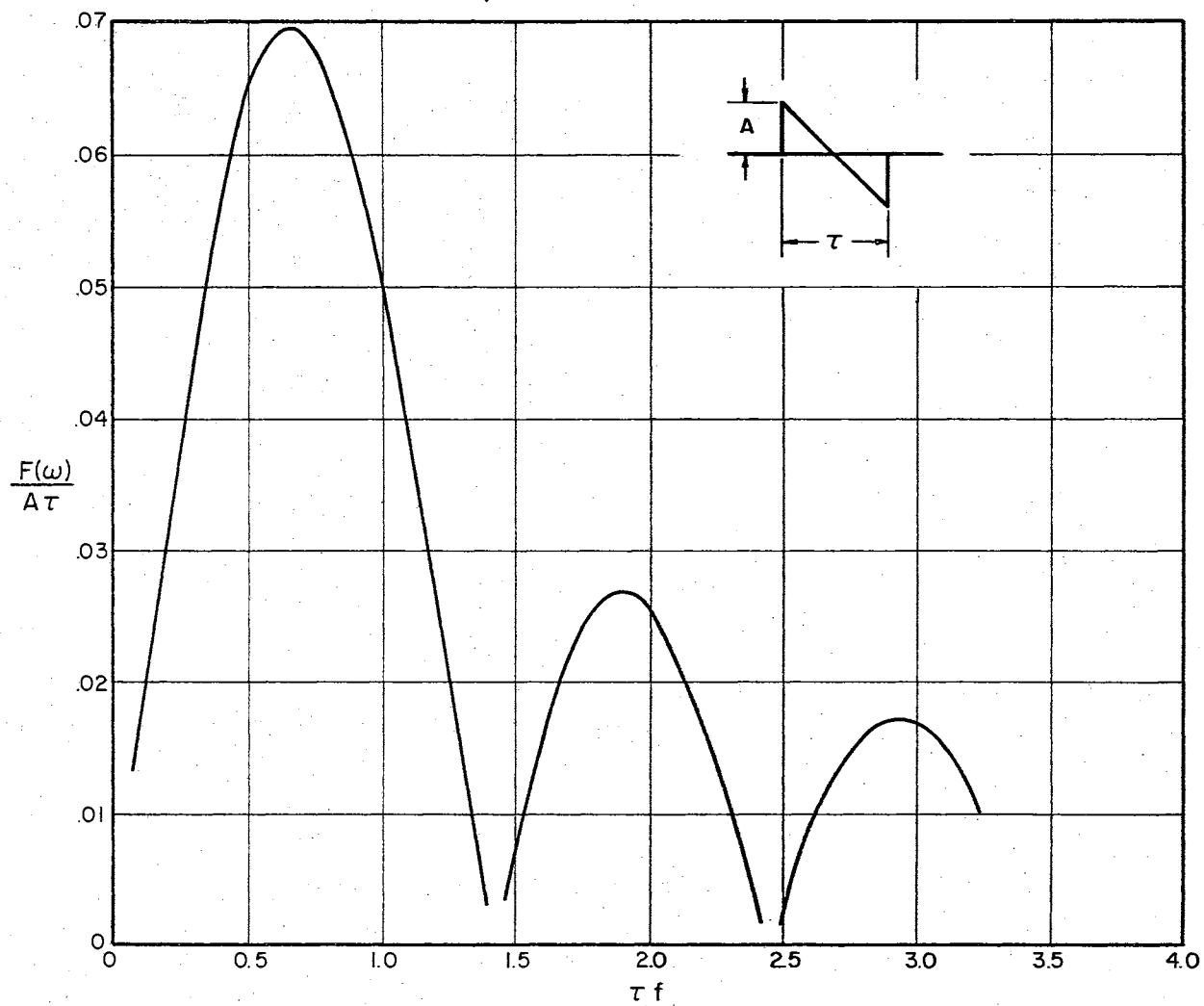


Figure 4-1. Normalized Amplitude Density Spectrum For a N-Wave

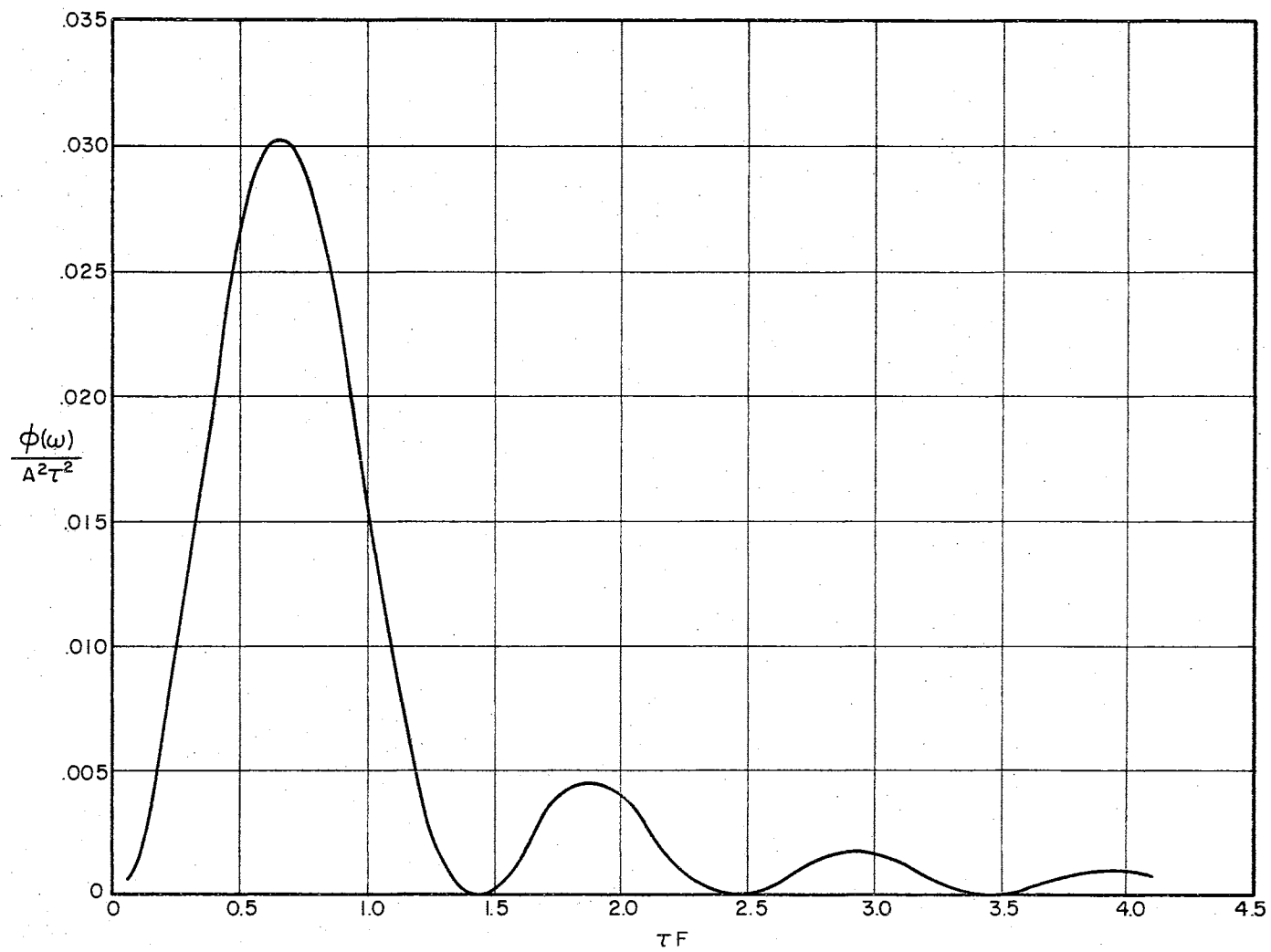


Figure 4-2. Normalized Energy Density Spectrum For a N-Wave

Frequency Limitations for Transient Response

In the steady state situation the frequency limitation has been used to differentiate between frequencies for which the response of the Helmholtz resonator can be adequately described by the simple lumped parameter model, that is for which the pressure everywhere within the cavity is in phase and has the same magnitude for all practical purposes. At frequencies above the limit frequency the higher mode responses begin to become important, with phase and magnitude differences in pressure; magnitude differences in pressure associated with the fundamental mode also become important.

It is important to determine what sort of frequency limitations are necessary in the transient problem. The frequency limitations developed previously for the steady-state problem applied to the frequency of the input. Since the frequency domain description of a pulse is continuous rather than discrete, it is apparent that it will be difficult to apply the previously derived frequency limitations to the frequency domain description of the transient input.

The results of the experimental work reported in Chapter IV indicate that the response of the Helmholtz resonator to transient pulses is limited for all practical purposes to response in the fundamental mode. Residual vibrations are simply relaxation oscillations in the fundamental mode. The time or frequency properties of the input pulse are thus not nearly so important in determining the acceptability of the simple lumped parameter description as is the case for steady-state excitation. The natural frequency of the resonator is the frequency which may be used in determining the

approximate accuracy of the lumped parameter description. In Chapter III it was shown that the limiting frequency may very often be somewhat below the natural frequency of the resonator. If this is the case, the differences in the magnitude of pressures at various points inside the resonator cavity may be expected to acquire some importance. The response is still essentially in the fundamental mode so that no phase differences are expected. The physical situation has deviated from that discussed under low frequency theory in Chapter III in that the velocity and thus the kinetic energy have become sensible to some extent in the cavity in the neighborhood of the neck opening. The appropriate mass to be used in the derivations in Chapter III has therefore increased somewhat. The appropriate spring constant has also increased somewhat with the result that the natural frequency estimate given by Equation (3-8) is still reasonably good. However, the pressures at points in the cavity remote from the neck will be slightly larger than at points near the neck opening. Points remote from the neck opening store and release potential energy but acquire little velocity and thus kinetic energy. Points near the neck also store and release potential energy but not quite so much since there is also some interchange of kinetic energy in this region.

An estimate of the magnitude of this effect may be obtained by studying the derivations for the cavity in Appendix C. From Equation (C-34) the internal pressure is seen to be a function of the axial coordinate x according to the expression,

$$\frac{\cosh \frac{S}{c} (L-x)}{\sinh \frac{S}{c} L} \quad (4-3)$$

where only the first value of α_η has been considered. The ratio of the pressure at the back of the cavity to that at the front is then approximated by

$$\frac{P_R}{P_N} \approx (1/\sinh \frac{S}{c} L) / (1/\tanh \frac{S}{c} L) = 1/\cosh(\frac{S}{c} L). \quad (4-4)$$

Substitution of $j2\pi\omega$ for S yields the relationship

$$\frac{P_R}{P_N} \approx \frac{1}{\cos(\frac{2\pi f L}{c})}, \quad (4-5)$$

or

$$\frac{P_R}{P_N} \approx \frac{1}{\cos(\frac{2\pi L}{\lambda})}. \quad (4-6)$$

If L is $\lambda/16$ then equation (4-6) may be evaluated as

$$\frac{1}{0.925} \approx 1.08,$$

which indicates about 8% difference. In Appendix C an estimate was made following Beranek [3] which indicated about 5% difference for this case. Beranek's estimate is less accurate but the difference is not great enough to warrant argument. The above discussion would tighten the frequency limitation for 5% accuracy to about $D < \lambda/20$ where D is again the characteristic dimension of the resonator. Equation (4-6) can be approximated to a general geometric configuration as an expression of the ratios of the pressure at points remote from the neck opening to pressure at the neck opening as

$$\frac{P_R}{P_N} \approx \frac{1}{\cos(\frac{2\pi D}{\lambda})}, \quad (4-7)$$

where D' is the distance from the mouth of the resonator to the remote point of interest. It may be observed that D' is probably a more meaningful characteristic dimension of the resonator than is D which is simply the largest dimension.

In the transient situation equation (4-7) may be used to predict expected values of internal pressure differences by using the wavelength corresponding to the natural frequency; however, it is probably more convenient to rearrange the expression as

$$\frac{P_R}{P_N} \approx \frac{1}{\cos\left(\frac{2\pi f_0 D'}{c}\right)} \quad (4-8)$$

Equations (4-8) and (3-14) could be combined to yield

$$\frac{P_R}{P_N} \approx \frac{1}{\cos\left(.39 \frac{f_0}{f_L}\right)} \quad (4-9)$$

From table (3-1) it may be seen that f_0/f_L will rarely be greater than 2, which would yield a value of P_R/P_N of 1.33. For a reasonably small neck area, a nonzero neck length, and an approximately cubical or spherical cavity, f_0/f_L may be expected to be near unity in which case the maximum internal variation will be closer to 8 or 10%. Generally the internal pressure variations in the transient situation will be on the order of 10% or less, although in the more extreme geometric situations this variation may be somewhat greater. An estimate of the magnitude of the pressure variations may be obtained from equation (4-8) or (4-9).

The preceding discussions indicate that the frequency limitations developed for the steady state situation may be adopted to the transient

problem. In the transient application the frequency domain description of the input is not an important consideration. The natural frequency of the resonator assumes much greater importance. A relationship between the natural frequency of the resonator and the resonator geometry determines the accuracy of the lumped parameter model. In the steady state situation it was a relationship between the input frequency and the resonator geometry which determined the accuracy of the lumped parameter model.

The use of the frequency limitation in the transient situation is quite different from the use in the steady state situation described in the beginning of this section. The term, frequency limitation, is perhaps a misnomer in the transient situation since it is not used to restrict the frequency content of the input so that the lumped parameter model is acceptable. In the transient case the frequency limitation is used only to estimate variation of internal response pressure from that predicted by the simple model. These variations are generally on the order of 10% or less and are therefore of limited importance.

Participation Factors

It is pointed out in reference [12] that the dynamic response of any structure can be described as the sum of products \sum (normal mode shape) \cdot X (corresponding dynamic response function). It is also noted that if the shape of the load distribution is spacewise constant, the above sum of products takes the form

$$\left\{ \begin{array}{l} \text{contribution of the } j^{\text{th}} \\ \text{mode to the static} \\ \text{deflection} \end{array} \right\} X \left\{ j^{\text{th}} \text{ dynamic response function} \right\}.$$

If the Helmholtz resonator is assumed to be a structure capable of dynamic response in many modes, then the dynamic responses could be described by the equation

$$\left\{ \begin{array}{c} \text{dynamic} \\ \text{response} \end{array} \right\} = \sum_{j=1}^{\infty} \left\{ \begin{array}{c} \text{participation factor} \\ \text{for the } j^{\text{th}} \text{ mode} \end{array} \right\} \times \left\{ \begin{array}{c} j^{\text{th}} \text{ dynamic response} \\ \text{function} \end{array} \right\}.$$

The participation factor is defined in reference [12] as the fractional contribution of the given mode to the maximum static stress due to a uniform pressure on the top surface. In reference [12] this procedure is applied to beams and plates.

In the case of the Helmholtz resonator, the only mode which would contribute to static deflection would be the first mode or what has been previously termed the Helmholtz mode. The participation factors for all the other modes would be zero. On the basis of this reasoning, it would seem that the fundamental mode of the Helmholtz resonator would be the only mode excited for whatever type pulse was applied. If this reasoning is valid, then there is no need for any sort of frequency limitations for the transient response problem of the Helmholtz resonator at least in the case of normal incidence of the pulse. The validity of the participation factor theory with reference to the acoustic problem is questioned by the author, but its result does seem to be in fairly good agreement with the experimental results which will be reported in Chapter VI.

Damping Effects

It is not the purpose of this section to examine in any detail the various damping mechanisms which can be present in the Helmholtz

resonator or to comment on their relative importance but rather to discuss the effects of damping on the various mode responses of which the Helmholtz resonator is capable. If damping of all modes at all frequencies was about the same the effect on the higher frequency modes would be much more pronounced than the effect on the Helmholtz mode. This can be best illustrated by an example: A resonator with a natural frequency of 100 cps is excited by N-wave of amplitude 1.0 and duration 0.01; also, a higher mode which has a frequency of 1,000 cps is excited and the maximum amplitude of this higher mode excitation is about 0.2; the damping factor for all modes is estimated to be $\zeta = 0.05$; after 0.05 seconds the Helmholtz mode response would be about 1.0 as the damping has had very little time to take effect; the higher frequency oscillations have already gone through 5 cycles, however, and have been reduced by damping by about $e^{-0.05 \times 2\pi \times 5} = e^{-1.57} = .21$. Or, in other words, the high frequency oscillations have been reduced to about one fifth their initial amplitude by the time the Helmholtz response is passing through its first maximum. High frequency responses excited for example by a step input would be damped out very rapidly. Since the degree of excitation of the higher modes can be expected to be considerably less than that of the fundamental, it would seem that damping should greatly reduce the importance of higher mode response.

The damping also tends to increase with frequency. Kinsler and Frey [4] consider reradiation of energy from the mouth of the resonator as the major damping source. Their expression for the damping coefficient increases as the square of frequency. Ingard [6] shows that viscosity

losses increase as the square root of frequency if the velocity amplitude remains constant. He also shows that heat conduction losses to the surfaces of the resonator increase as the square root of frequency if the sound pressure magnitude at the surface remains constant. It can be generally expected, therefore, that the higher modes will be damped as much or more than the fundamental mode.

Validity of the Lumped Parameter Model

With reference to the sonic boom there is very little interest in the case when the ratio of the boom length to the resonator natural period is less than about 0.4 since for small values of τ/T there will be little excitation of the fundamental mode. In general the most interesting cases are those in which there can be significant dynamic amplification in the fundamental mode. The experimental results which follow in Chapter V show that for values of τ/T greater than about 0.4 or 0.5 the response of the Helmholtz resonator to pressure pulses is that of a simple oscillator. Higher mode response is generally very small except when the pulse has a high frequency sinusoidal component superimposed upon it. This high frequency driving input results in what amounts to steady state high frequency response. Even this type of high frequency response can be ignored in determining the overall response of the resonator. Sharpness of rise of the input pulse does not seem to increase high frequency response significantly.

Response in the fundamental mode may exhibit some pressure variations inside the resonator cavity as pointed out previously in

this chapter. The presence of these pressure variations can be predicted on the basis of the natural frequency of the resonator and the geometry of the resonator and is not strongly dependent on the time or frequency properties of the input pulse. Normally these pressure differences may be expected to be about 10% or less.

The experimental results of Chapter IV bear out the minor importance of the higher modes but also indicate that in some cases internal pressure differences associated with the fundamental mode may assume some importance.

The simple lumped parameter description is therefore a reasonably good engineering approximation of the Helmholtz resonator in the transient excitation problem.

CHAPTER V

EXPERIMENTAL APPARATUS

In order to study the response of a Helmholtz resonator to transient pressure pulses, one had to devise apparatus capable of producing appropriate pressure pulses whose shape, amplitude, and time duration were within limits which permitted easy study. To facilitate the study the pulse needed to be as reproducible as possible. The ability to vary the shape, amplitude and time duration as much as possible was highly desirable. There had to be sufficient time following the arrival of the pulse at the resonator to study its response before the arrival of reflections which would provide additional input to the resonator.

The apparatus described in this chapter performed in accordance with the above needs quite well. The test apparatus could be improved considerably with a moderate outlay for equipment. Although this equipment is a prototype, the successes with it encourage the belief that the equipment could be developed into an excellent sonic boom simulation apparatus.

A Plane Wave Tube

The plane wave tube, or traveling wave tube, used as a basic part of the test apparatus had a cross section area of about 14

inches square and the tube was 32 feet long. The cross sectional area was chosen rather arbitrarily; however, there were several requirements which influenced the choice. It was desired to have a plane wave front at the test end. This requirement does not place any limits on the cross sectional area except that the length of the tube must be a great deal longer than either of the cross section dimensions. The plane wave front criteria requires driving at the input end in a reasonably evenly distributed way. It was also desired to minimize the feedback effect caused by introducing the test resonator. It was highly desirable that the test resonator should not influence the input. This was accomplished by making the cross section of the tube considerably larger than the cross section of the resonator neck. A photograph of the tube taken from the driver end is shown in Figure 5-1.

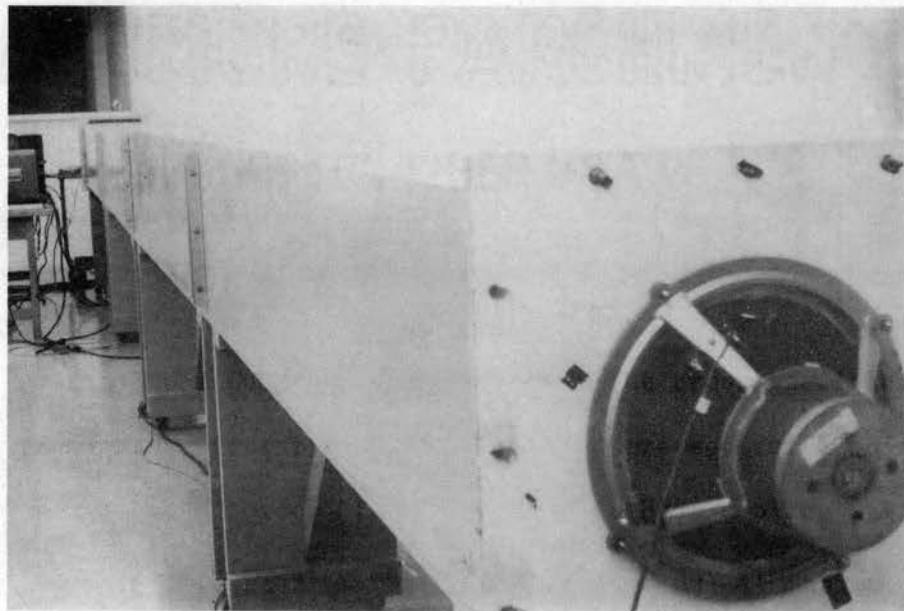


Figure 5-1. The Plane Wave Tube

All of the sizing of the tube was influenced by consideration of frequency ranges within which the various components of the test apparatus would work best. The loudspeakers produced transients reasonably well in the range from about 50 to 300 cps. The microphone response was flat for frequencies above 50 cps. Test resonators with natural frequencies from about 100 to 200 cps were compatible with the above limits and were of convenient size (about 6 in. diameter and up to 10 in. long). The neck diameter of the test resonators of 1 to 2 inches influenced the choice of the cross sectional area of the tube in accordance with the criteria that the tube cross section should be much larger than the neck cross section. The natural frequency of the test resonators dictated the required length of the tube. For example, if the natural frequency of the resonator is 100 cps, primary interest will be in pulses whose duration is from about .5 up to about 3 times the natural period of 0.01 seconds. If the length of the input pulse were .03 seconds, then about .06 seconds would be enough time to study the forced response and about 3 cycles of free vibration. The speed of sound is approximately 10 ft. per 0.01 sec., which requires approximately a 60 foot path for the reflected wave to travel before rearrival at the resonator if there are to be 0.06 seconds between arrival times of the pulse and the first reflection.

Generating the Pressure Pulse

Various means of generating pressure pulses are considered before deciding to use direct-radiator loudspeakers. The electronic system using loudspeakers has the advantage of good reproducibility. Also,

variations in the shape, amplitude, and duration of the pulse can be accomplished much easier with the electronic system. Control of explosives or shock tube apparatus is, at best, difficult; reproducibility is difficult and usually each pulse must be individually set up. The electronic system can produce identical successive pulses, as many as desired. A block diagram of the system is shown in Figure 5-2. Figure 5-3 is a general view showing most of the instrumentation which was used in generating pulses and measuring responses. The low frequency function generator is capable of producing low frequency sine, triangular or square waves. The signal from the function generator may be fed directly into the gate or through rectifying or differentiating circuits into the gate. The purpose of the extra circuitry is to obtain greater flexibility of electronic input. For example, a differentiated square wave yields spikes which produce fast-rise pulses. The gate permits conversion from a steady state input to a transient. The signal from the gate after being amplified is fed to a loudspeaker or bank of smaller loudspeakers. The loudspeaker is shown in Figure 5-1 and the bank of smaller loudspeakers is shown in Figure 5-4. The main difference in the two loudspeaker systems was that the larger tended to produce cleaner

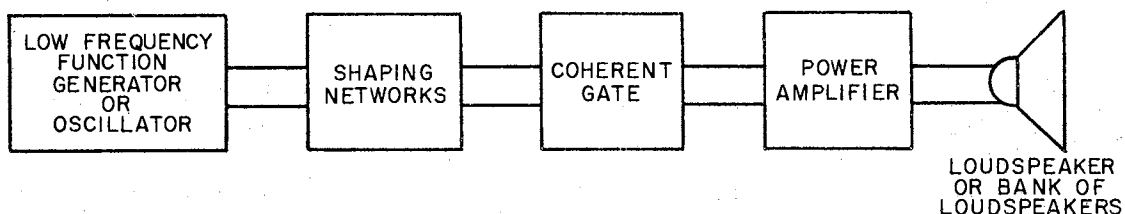


Figure 5-2. Block Diagram of Pulse Generating Apparatus

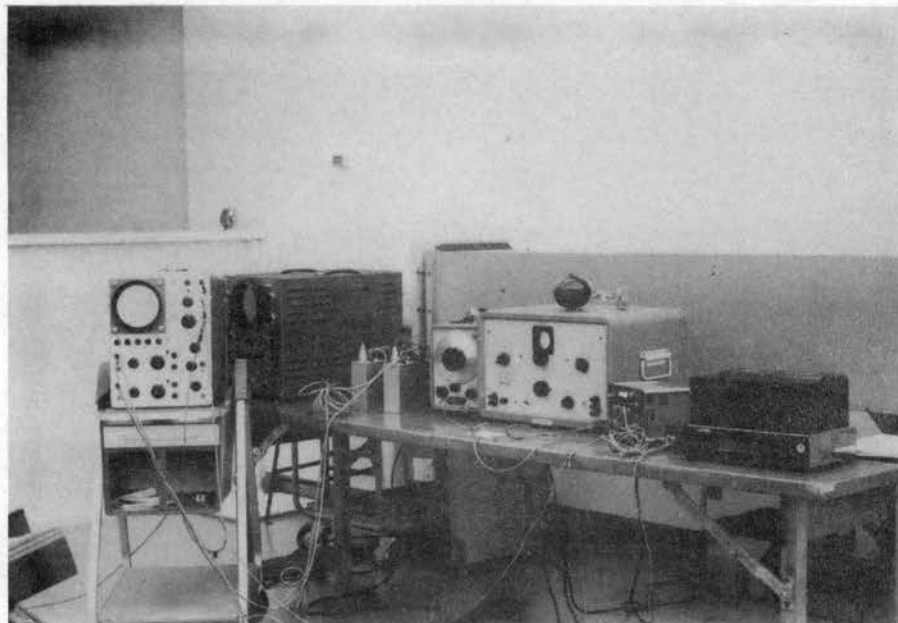


Figure 5-3. General View of Instrumentation

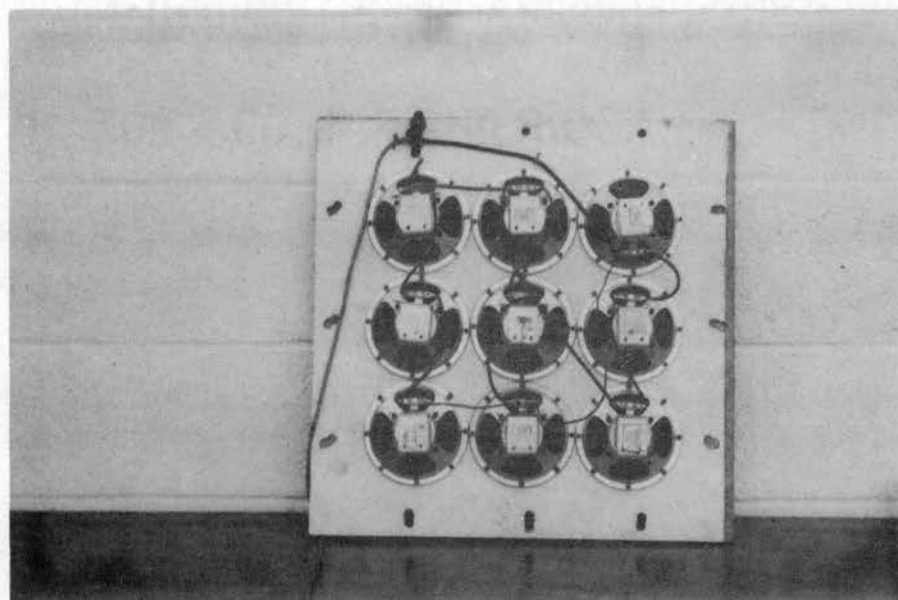


Figure 5-4. Bank of Small Loudspeakers Used
As a Driving Unit

low frequency pulses while the bank of smaller loudspeakers tended to produce better pulses at higher frequencies.

Test Resonators and Recording Instrumentation

The test resonator used for almost all the work was a circularly symmetric one as described in Appendix C, made of plexiglass. The diameter of the cavity was 5.5 inches and the length could be varied from zero to 10 inches. The neck was detachable so that the neck length and cross section could be easily varied. Holes were drilled at intervals along the cavity to permit microphone access. Holes and junctions were usually sealed with paraffin during operation to eliminate leaks. Figures 5-5, 5-6, and 5-7 show various views of test resonators. Figure 5-5 shows the test resonator in position for testing with microphones in position for measuring the input pressure pulse and the response of the resonator. Figure 5-6 shows another view of the test resonator and also a plug in position to permit comparison of microphone sensitivities. Figure 5-7 shows a view of another resonator of smaller diameter. The neck of the resonator simply slips into the hole in the plate on the end of the tube. The position of the microphone measuring the input pressure pulse is shown clearly.

The microphones shown in the figures are Altec model BR-150. The output of the microphones was easily viewed on an oscilloscope and could be photographed if desired.

Performance of the Test Facility

In general the performance of the test apparatus may be termed satisfactory. Of course, the experience of using the apparatus

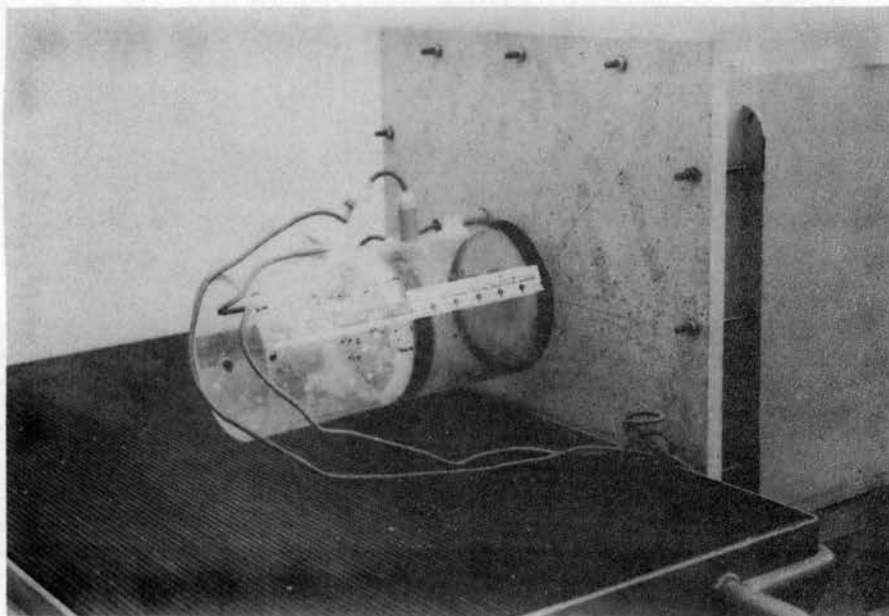


Figure 5-5. Test Resonator in Position for Testing

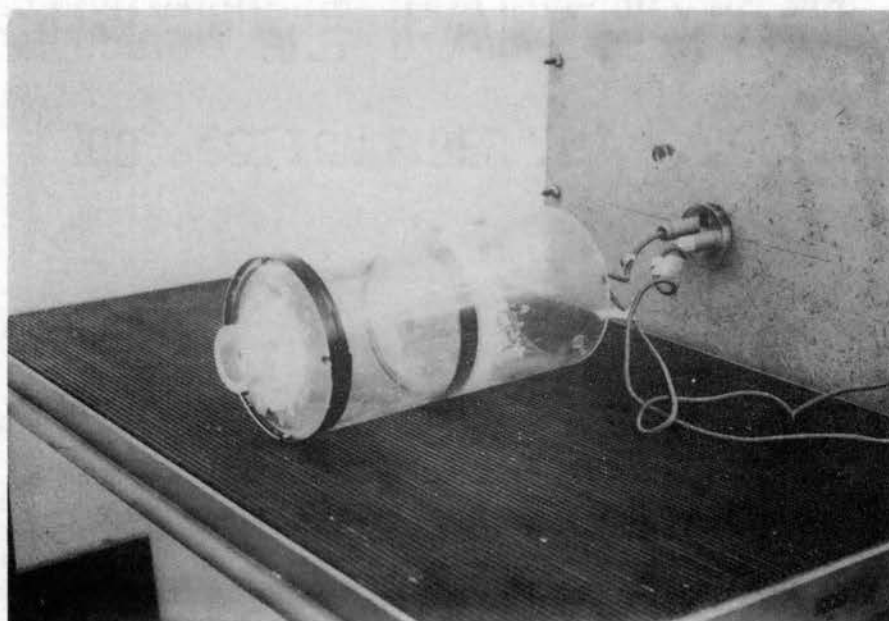


Figure 5-6. Microphone Comparison Fixture and Test Resonator

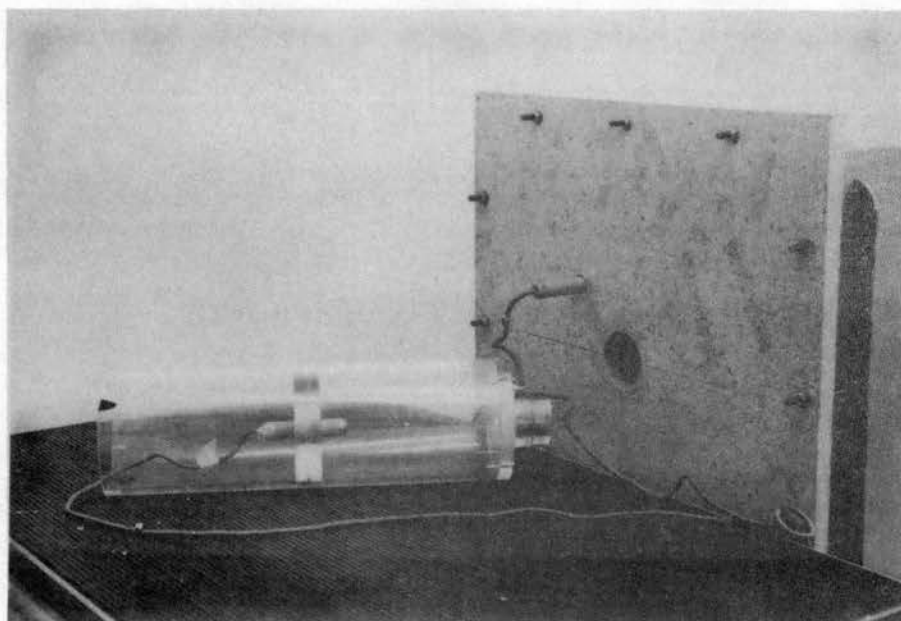


Figure 5-7. Smaller Test Resonator

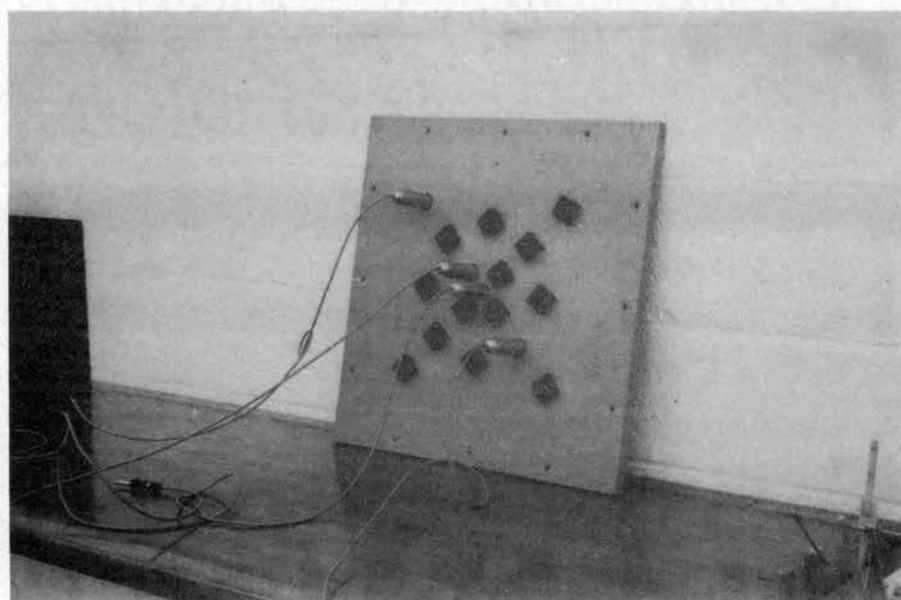


Figure 5-8. End Plate Used for Evaluating the Plane Wave Assumption

disclosed possibilities for improvement. Improvement in pulse shaping would increase the usefulness of the equipment. Nevertheless for the present needs the equipment was adequate.

All of the analysis in this work assumed that the input pressure pulse was invariant in both amplitude and phase, at least in the immediate neighborhood of the neck of the resonator and the input microphone. In other words, it was assumed that the wave front was plane at the test end of the tube. This was checked out experimentally and found to be a very good assumption. The back plate shown in Figure 5-8 was used to check out how planar the wave was. By moving the microphones around from hole to hole while keeping the other holes plugged, one could easily compare microphone sensitivities and pressure measurements at the various holes. This was done with a steady sinusoidal input of varying frequencies up to about 400 cps and with a variety of pulse inputs. There was no discernible difference of magnitude or phase for readings in the central part of the plate. There was a small drop in magnitude on the order of 5 to 10% for readings taken in the four corner holes. For the central part of the back plate which includes all but the corners the wave front is very nearly planar.

The question of whether the variation of impedance at the test end caused by changing the resonator configuration produced any effect on the input must be answered with reference to the testing situation. An attempt was made to use the tube with a steady state sinusoidal input to make measurements on the natural frequencies and damping factors for various resonator configurations. The results were in good agreement with both theory and the results of transient tests, but it was

observed that variation of the resonator tuning did affect the input amplitude also. This was not true however in the transient case. Using various input pulses, one could not detect any variation in the input readings when the resonator tuning was varied. In fact, the hole in the back plate where the resonator neck is inserted could be plugged or left completely open or the resonator inserted and the tuning varied with no observable effect upon the recorded input.

There were limitations on what sort of pulse could be obtained. This situation could be greatly improved by using a more sophisticated driving system as will be discussed in the next section. However, a large variety of pulses could be produced. A representative sampling of the types of pulses which were successfully produced are shown in Figures 5-9 through 5-12 and also in many of the figures in Chapter VI. The loudspeaker driving units do not accurately follow the input electronic signal since the loudspeaker is a complicated dynamic system with electrical, mechanical, and acoustical components which possesses several-degrees-of-freedom. For this study, the electronic input was varied until a useful pulse response was obtained. By trial it was thus possible to find several pulses which were well suited for testing. Improved control of the pulse shape could be established by better control of the loudspeaker system or of the electronic input.

Recommendations for Improved Apparatus and Sonic Boom Simulation

There are several means by which the test apparatus could be improved, but the path to really good sonic boom simulation is an easily

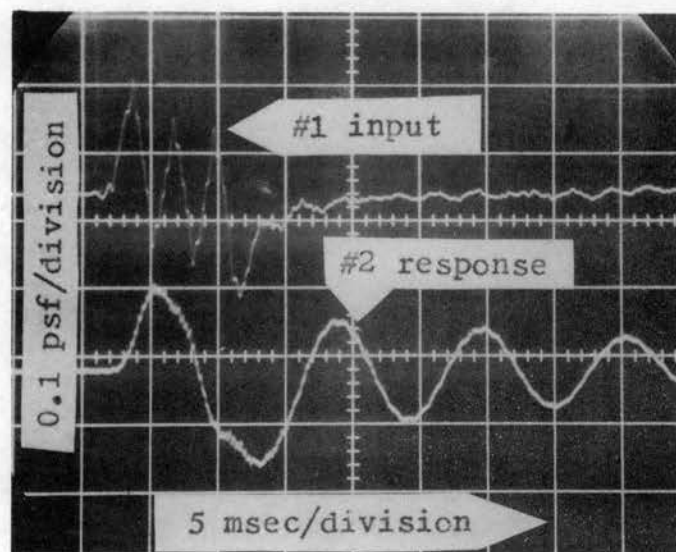


Figure 5-9. Representative Pulse Produced by the Test Apparatus

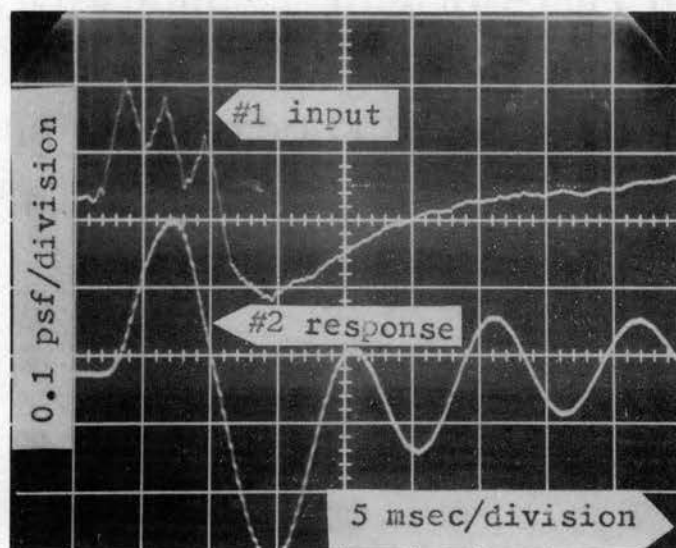


Figure 5-10. Representative Pulse Produced by the Test Apparatus

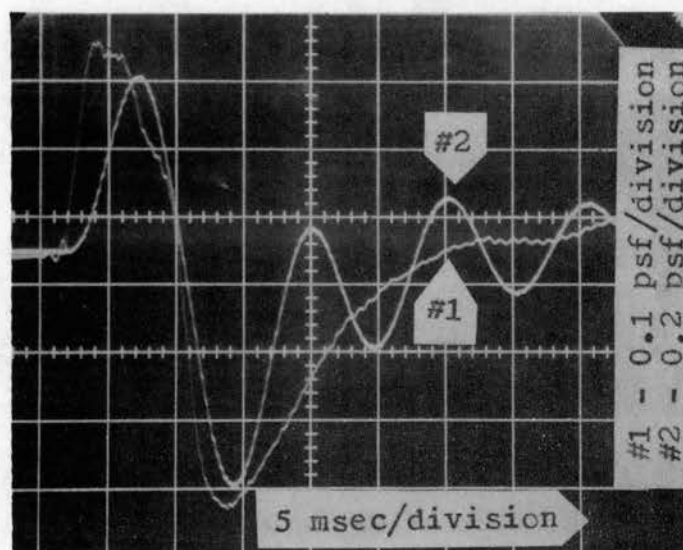


Figure 5-11. Representative Pulse Produced by the Test Apparatus

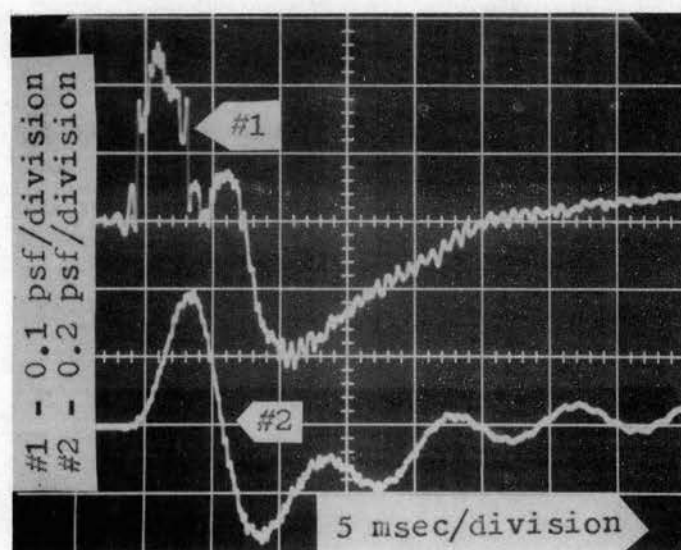


Figure 5-12. Representative Pulse Produced by the Test Apparatus

controlled situation has been shown. There is a need for this simulation. There are many acoustical, structural, and dynamic problems associated with sonic booms which are deserving of study because of the ever increasing number of supersonic flights. It appears that an excellent simulation facility could be built when sufficient funds become available.

There is no reason why the cross sectional area of the plane wave tube might not be increased many times, thereby permitting testing of fairly large specimens. The ability to control and shape the pulses could be improved greatly in several ways. Rigid diaphragm transducers could reduce unwanted responses of the driving units. Increased variability of the input electronic signal would add greatly in the shaping of the resultant pressure pulse. Probably the optimum situation would be rigid diaphragm transducer with servo controls permitting good control of the diaphragm motion and thus control of the pressure pulse.

This sort of system would be far superior to any which depend on explosive or shock tube techniques to produce the pressure pulse because of the control over pulse shape and the very good reproducibility.

One limitation of such a system as proposed might be that it could not easily produce a pressure pulse whose time duration was as long as actual booms due to poor acoustic coupling between the driving transducers and the adjacent air at low frequencies. This is only a scaling problem however. The important feature is the relationship between the time or frequency properties of the pulse and the time or frequency properties of the test piece.

CHAPTER VI

EXPERIMENTAL RESULTS

The several purposes of the experimental work may be listed as follows:

- (1) to determine if the overall response of a Helmholtz resonator to a pressure pulse is generally the same as the response of a simple oscillator to transients;
- (2) to obtain information on the importance of higher mode response;
- (3) to establish some basis for making statements regarding how good the simple lumped parameter description of the Helmholtz resonator is, that is to establish restrictions similar to the frequency limitations of the steady state solution.

It is very difficult to categorize the individual tests as falling under one of the above stated purposes. It is more often the case that any given test sheds some light towards answering all three questions. There is, in fact, considerable overlap in the stated purposes. The experimental results are therefore presented by simply discussing the various tests performed and pointing out what sort of information the tests contribute towards answering the questions of interest.

From preliminary tests which were conducted simply to prove the test facility, it appeared that the low frequency theory would

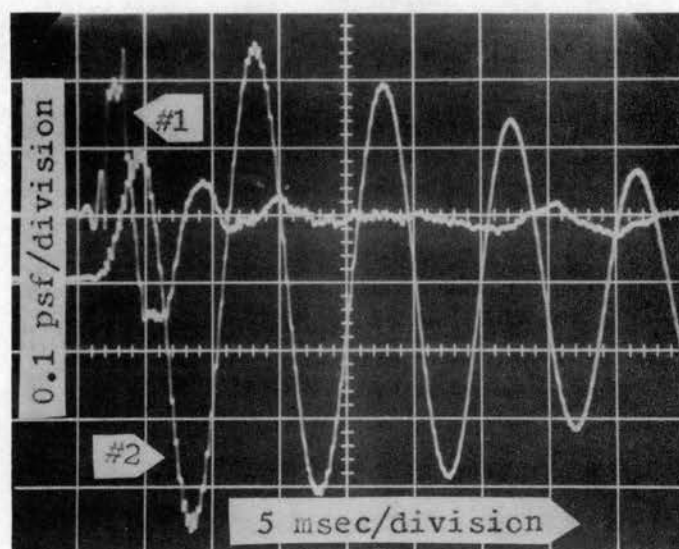


Figure 6-1. Typical Laboratory Trace Used in Measuring Natural Frequency and Damping

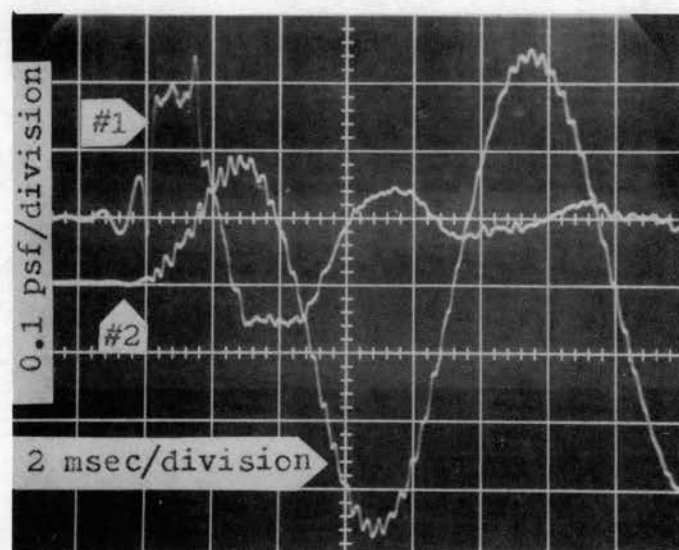


Figure 6-2. Time Response Measurement

hold fairly well in the transient situation. Therefore, the low frequency lumped parameter description was assumed and the tests were conducted to either substantiate this assumption or to find fault with it.

Natural Frequency and Damping Measurements

A logical first test was the check of the natural frequencies. The test procedure consisted of exciting the resonator with some sort of transient pulse and observing the ringing or residual free relaxation oscillations. Figure (6-1) shows input (#1) and response (#2) traces. From the response trace it is easy to compute the damped natural frequency of the resonator, ω_d , knowing the sweep rate of the scope. Most of these measurements were made by simply reading the trace on the oscilloscope. The damped natural frequency ω_d is related to the undamped natural frequency ω_0 through the equation

$$\omega_d = \sqrt{1 - \zeta^2} \omega_0, \quad (6-1)$$

where ζ is the damping factor. Since the damping was quite small, ω_d and ω_0 are equal for all practical purposes.

A theoretical estimate of the natural frequencies was made from equation (3-8). The end corrections were taken as 0.85A for a wide flange or infinite baffle termination. This end correction tends to be a little high which results in estimates of the natural frequency which are a little low. Table 6-1 gives a comparison of measured natural frequencies versus theoretical for various resonator configurations.

TABLE 6-1

NATURAL FREQUENCY COMPARISONS

cavity diameter - 5.5 in., neck diameter - 1.5 in., neck length - 2 in.

Cavity Length Inches	Theoretical Natural Frequencies cps	Measured Natural Frequencies cps
3.0	189	194
4.0	163	169
5.0	146	149
6.0	133	135
7.0	123	125
8.0	115	117
9.0	109	111
10.0	103	105

cavity diameter - 5.5 in., neck diameter - 1 in., neck length - 2 in.

3.0	135	137
4.0	117	119
5.0	104	107
6.0	95	95

All of the measurements recorded in the table were taken with all of the joints and holes in the cavity sealed with paraffin. The results were quite repeatable as long as the cavity was tightly sealed. The total spread of measured values between several trials was usually only two or three cycles per second. The agreement between theoretical and measured values is good.

If the resonator was not sealed, the natural frequencies were observed to increase on the order of eight to ten percent and the results were less repeatable because the amount of leakage was not controllable. The damping also increased considerably. These results will be discussed in a later section.

Measurements of both the natural frequency and damping were also made with a steady sinusoidal input. The results were in good agreement with both theory and the values obtained from transient tests. It was however a little more difficult to pinpoint the natural frequencies. For example, there might be a frequency range of five or ten cycles for which the response was a maximum and very nearly the same. At times the resonator produced a feedback effect in that the input pressure was affected by reradiation from the resonator. In this situation an accurate estimate of the input was not available. In general, the transient tests were much easier to make.

A study of damping effects was not included in the objectives of this study because of the works of Ingard [6] and Lambert [8]. Since damping characteristics are readily evaluated from the tests, a comparison of damping in steady and transient cases can lend support to the equivalence of the two systems. The logarithmic decrement of the transient and the amplitude of the steady state can be converted into the damping coefficient. The damping factor was found to lie in the range of $\zeta = 0.025$ to 0.030 , being slightly higher for the larger cavities. Damping could also be estimated from steady state tests at resonance since the magnitude of the amplification factor

at resonance is controlled solely by damping. The results were in close agreement with those obtained from the transient tests.

There is nothing new about measuring the natural frequency or the damping of an Helmholtz resonator; the measurements were made more to establish confidence in the logic and equipment than for the measurements themselves. The measurements did however produce some useful results which support the preliminary theorizing of this work. If any of the higher modes of the resonator were excited to amplitudes comparable with that of the fundamental or Helmholtz mode, this would show up noticeably on the recorded decay curves. The wave form would be distorted showing any higher frequency component of comparable magnitude clearly. The frequency would appear to be changing due to the presence of more than one frequency. Some high frequency excitation can be observed in Figure 6-1 and in many other figures showing response curves. The amplitude of the high frequency components is always very small in comparison with the amplitude of the Helmholtz mode so that for all practical purposes the Helmholtz mode determines the response of the resonator. From the response traces it is difficult to say if the high frequency response is excited by the sharp rise of the input pulse or by the small amplitude high frequency oscillations superimposed on the input pulse.

Many types of pulses were used to excite the resonator to make the natural frequency tests with no control maintained over the pulse shape. The free vibration decay curves were always the smooth classical decay curves typical of a simple oscillator. The frequency of the

Helmholtz mode was always the only frequency present with a significant amplitude. These natural frequency tests although carried out mainly to check the natural frequencies accomplished more than their purpose. This was primarily because the tests amounted to studying the relaxation oscillations of a resonator excited by a pulse, which had not been done before. The tests contributed something towards all the listed purposes of the experimental work. The importance of the higher modes appears generally negligible and no frequency limitation on the input is apparent.

Time Response Studies

One method of determining how well the Helmholtz resonator is described by the simple low frequency model in the transient situation is to subject the resonator to various pulses and compare theoretical and measured responses. Significant differences between predicted and measured responses would indicate the possible presence of other effects such as higher mode responses. Several studies of response traces are presented, all of which show excellent agreement between predicted and recorded traces and further demonstrate the relatively minor importance of higher mode responses. The predicted response curves are derived using a straight line approximation of the pulse. The measured values of natural frequency and damping are used to define the resonator. The response is then solved for using Laplace transform techniques and a digital computer. The response pressure is given by

$$P(S) = G(S) P_1(S), \quad (6-2)$$

where $G(S)$ is the transfer function of the resonator and is defined by the natural frequency and the damping factors, and $P_1(S)$ is the input pulse description. A correction factor is used to account for the slight difference in the sensitivities of the microphones as noted in Appendix D. When the damping is very small, the phase plane techniques presented by Jacobsen [5] may be used to predict the response.

Figure 6-2 shows the same trace as Figure 6-1 except that the sweep rate has been decreased. The sweep rate in Figure 6-2 is 2 msec/line. The natural frequency and damping factor may be taken from Figure 6-1 as $f_0 \approx 105$ cps and $\zeta \approx 0.03$.

Figure 6-3 shows a straight line approximation of the input pulse and the computed response. The separations between scale divisions in Figures 6-2 and 6-3 correspond, the time scale for each figure being 2 m sec/division, while the amplitude scale is approximately 0.1 psf/division. The difference in microphone sensitivities is taken into account in computing the predicted response shown in Figure 6-3. The agreement between the measured and predicted responses is excellent. The period of the first push-pull cycle in the input is about 6 m sec. so that the value of the non-dimensional time parameter τ/T is about 0.63. The magnification obtained in this case is about 1.75. This considerable magnification for tuning which is not close to critical can be attributed to the fact that the pulse approaches a square wave which produces maximum amplification [13].

Figure 6-4 shows the resonator configuration when Figures 6-1 and 6-2 were recorded.

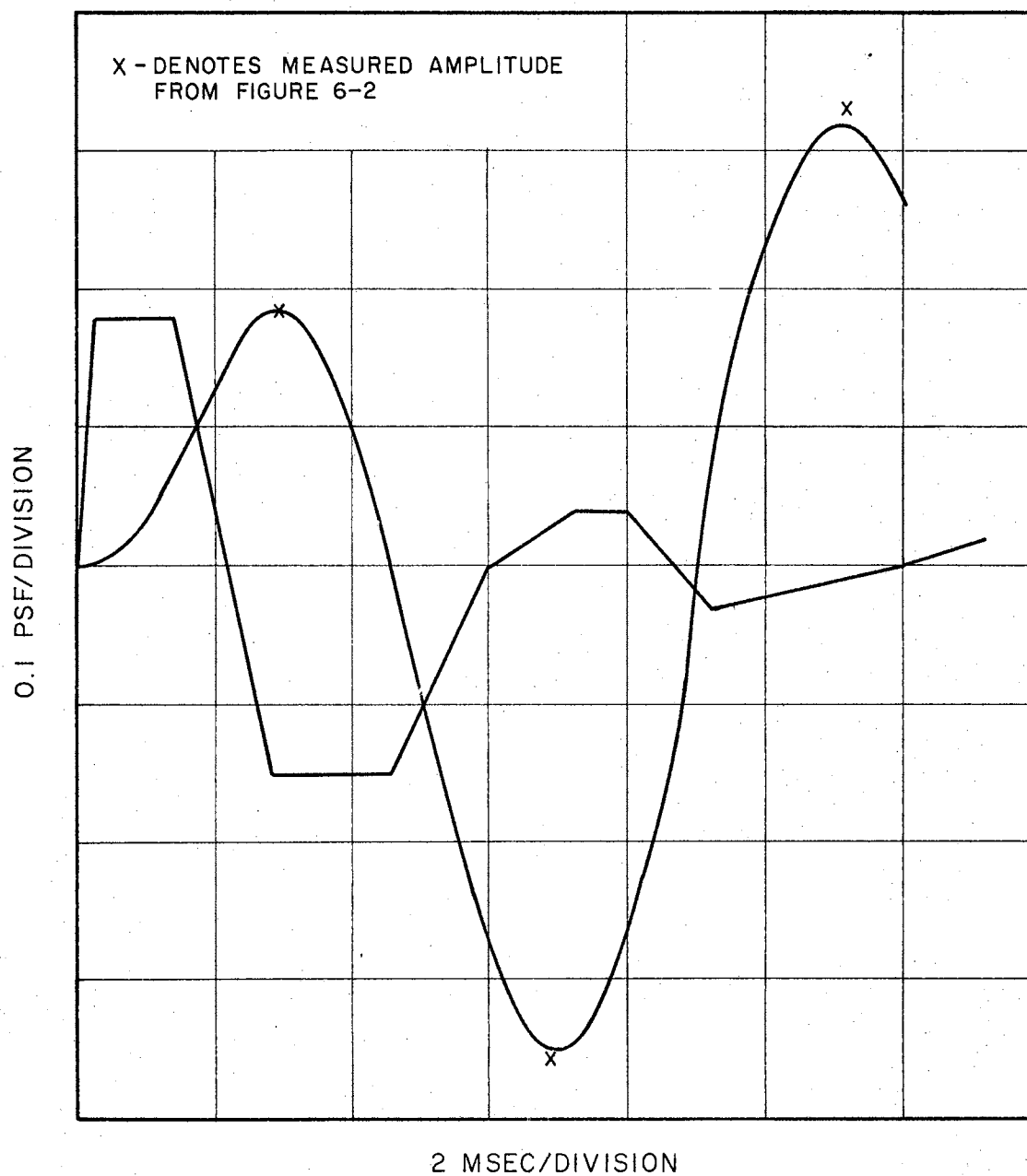


Figure 6-3. Straight Line Approximation of Input and Predicted Response Corresponding to Figure 6-2.

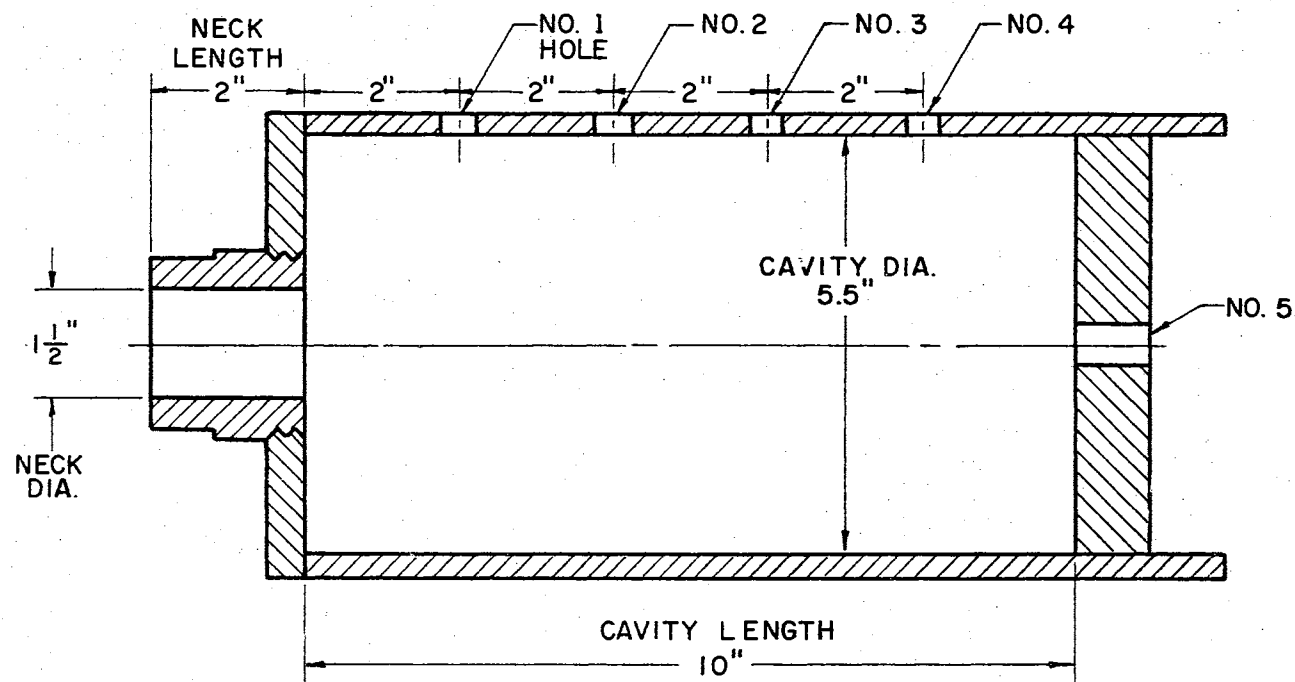


Figure 6-4. Resonator Configuration Used in Testing

When Figures 6-1 and 6-2 were recorded the measuring microphone was in the No. 1 hole close to the center of the cavity. For this particular configuration f_o/f_L is about 1/0.83 from Table 3.1; thus from equation (4-9) the ratio P_R/P_N would be predicted to be approximately 1.12.

Figure 6-5 and 6-6 are pressure recordings inside the cavity for the same pulse input as shown in Figures 6-1 and 6-2. Traces obtained with the microphones near the axial center exhibit larger amplitude high frequency response which is, however, still quite minor as far as the overall response of the resonator is concerned, the amplitude ratio being about $.4/7 \approx 5\%$. This amount of high frequency response was about as much as was ever observed.

The amplitudes of the traces shown in both figures appear to be very nearly equal. The number 2 microphone is, however, about 1.1 times as sensitive as the number 1 microphone so that the pressure at the rear of the cavity is about 1.1 times that at the front as predicted. This was as much amplitude variation inside the resonator as was ever observed. This resonator configuration is the most extreme ever used. The cavity length is nearly twice the diameter and the distance from the neck to the back plate is nearly 4 times the distance from the neck to the side walls. The resonator theory could not be expected to be very accurate if the length/diameter ration were greater than about 2.

The study of this particular time response has indicated that in general the simple oscillator representation is good, that the higher mode response is of very limited importance, and that the internal

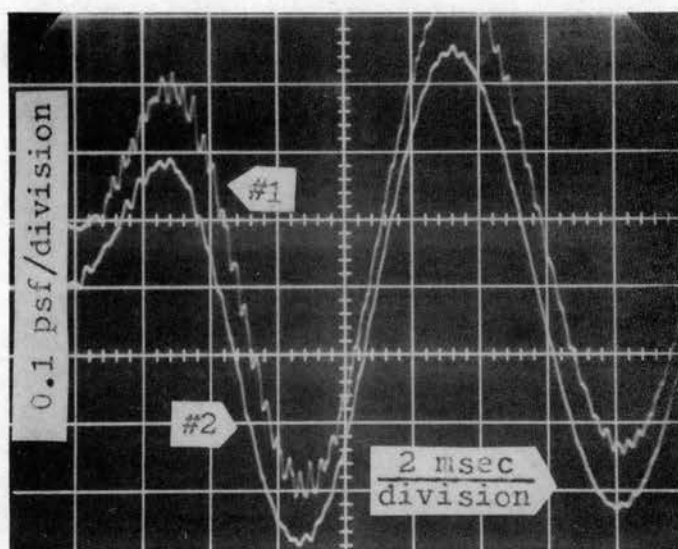


Figure 6-5. Time Response Measurement
 #1 Microphone in #5 Hole Near Edge
 #3 Microphone in #1 Hole Near Edge

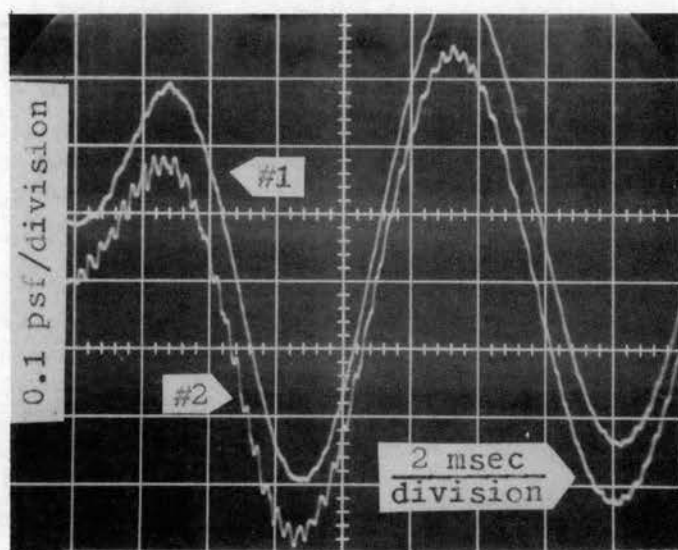


Figure 6-6. Time Response Measurement
 #1 Microphone in #4 Hole Near Edge
 #2 Microphone in #1 Hole Near Center

pressure differences associated with the first mode are present and could in extreme cases become important but can generally be expected to be about 10% or less.

Figures 6-7 and 6-8 are response traces for the same resonator configuration as Figures 6-1 and 6-2. Figure 6-9 shows a straight line approximation of the input pulse and the predicted response. Generally the agreement between predicted and measured response is, again, very good. The recorded peaks are about 10% higher than the predicted peaks. The measurements were taken with the microphone in the number 4 hole at the rear of the resonator. According to the previous discussion these measurements should be about 10% higher.

The pulse studied in these figures has some resemblance to a sonic boom complicated by a reflection. The frequency properties of this pulse are considerably different from the pulse shown in Figure 6-1, yet the pressure amplitude variation is still approximately 10%, a fact which to some extent tends to substantiate the claim that the relationship between the natural frequency of the resonator and the geometry of the resonator determine the amount of pressure amplitude variation and that the frequency properties of the pulse do not enter significantly.

Figure 6-10 is the same trace as Figure 2-10 except that the sweep rate has been slowed to 2 m sec/division. The resonator configuration used here was the same as in Figure 6-4 except that the cavity length was shortened to 4 inches. The natural frequency and damping factor for this configuration may be taken from Figure 2-10 as approximately $f_0 \approx 169$ cps and $\zeta \approx 0.024$. From equation (4-8),

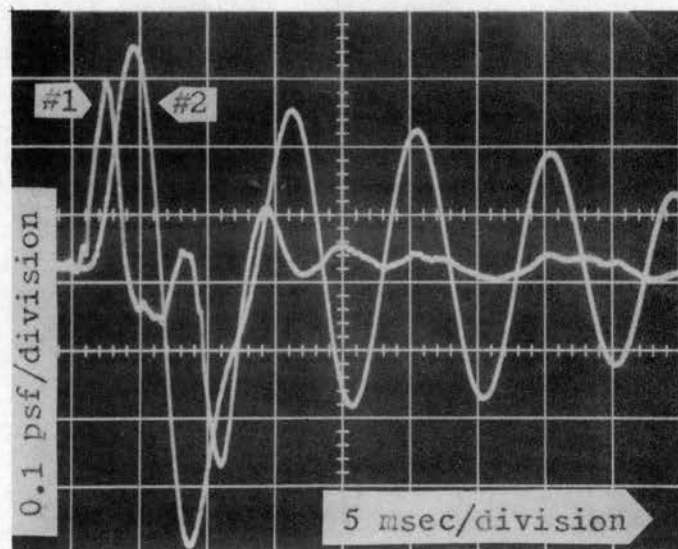


Figure 6-7. Time Response Measurement

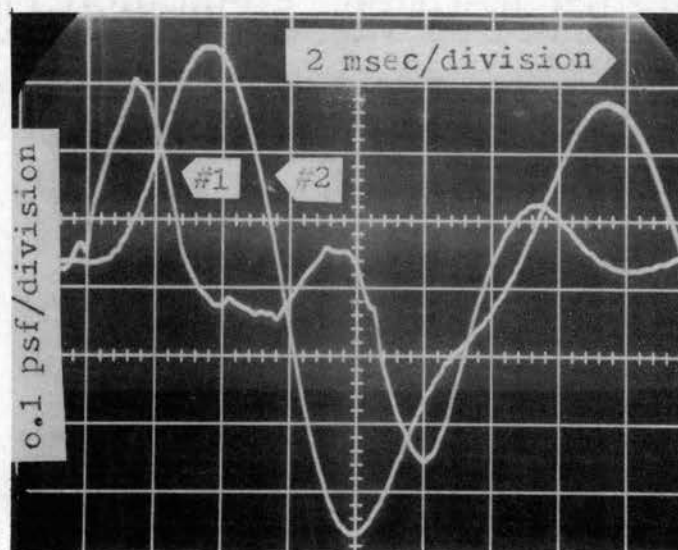


Figure 6-8. Time Response Measurement

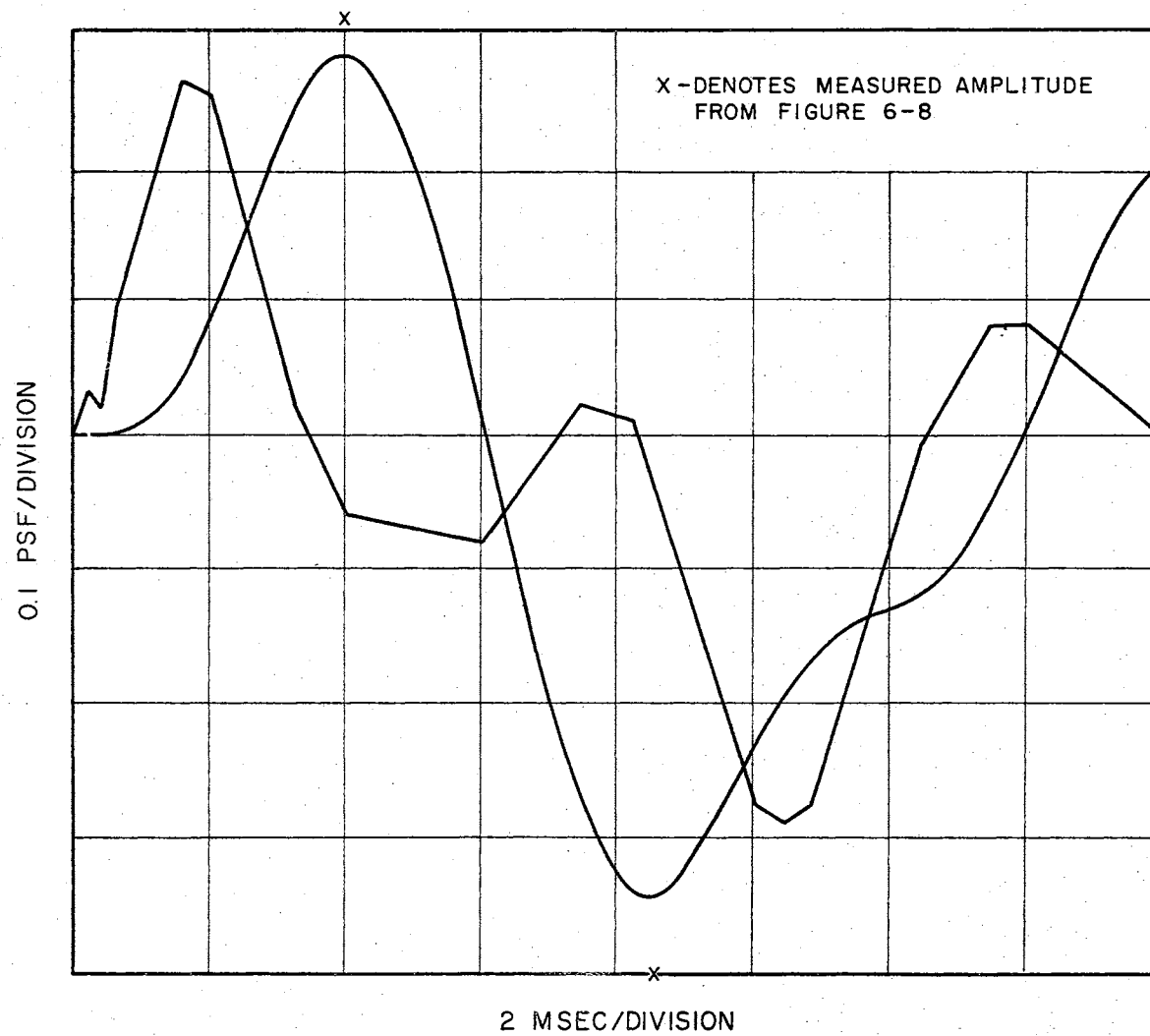


Figure 6-9. Time Response Measurement

$P_R/P_N \approx 1.05$, so that pressure variations inside the cavity may be expected to be minor. It was difficult to observe any variation at all.

Figure 6-11 shows a straight line approximation of the input pulse and predicted response. In these two figures the amplitude scale for the response is twice that for the input. The resonator and the input are fairly closely tuned and the magnification is about $(2.2/1.7) \times 2 \times .91 = 2.35$.

The input in Figure 6-12 is similar to a sonic boom input with a reflection. The resonator configuration was the same as for Figure 6-10. The response sensitivity is one fifth the input sensitivity. The period of the push-pull cycle of the input pulse and the natural period of resonator are nearly equal in this case so that there is considerable amplification. The amplification is approximately $(1.8/2.1) \times 5 \times .91 = 3.9$. Figure 6-14 shows the straight line approximation and predicted response. Sonic booms with a reflection can look very much like this input pulse so that pressure amplification on the order of 4 resulting from the Helmholtz resonator effect are not unrealistic.

Figure 6-13 shows an input pulse which is a fairly good approximation of a N-wave at least until the minimum is reached. The high frequency spikes have little effect since their frequencies are far above the resonant frequency of the resonator. The resonator configuration is the same as for Figures 6-10 and 6-12. Figure 6-15 shows a straight line approximation of the pulse and the predicted response; agreement between the predicted and measured responses is

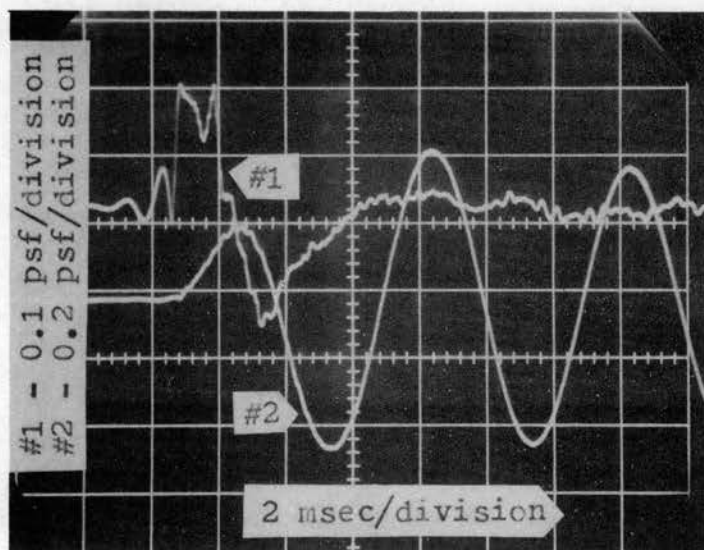


Figure 6-10. Time Response Measurement

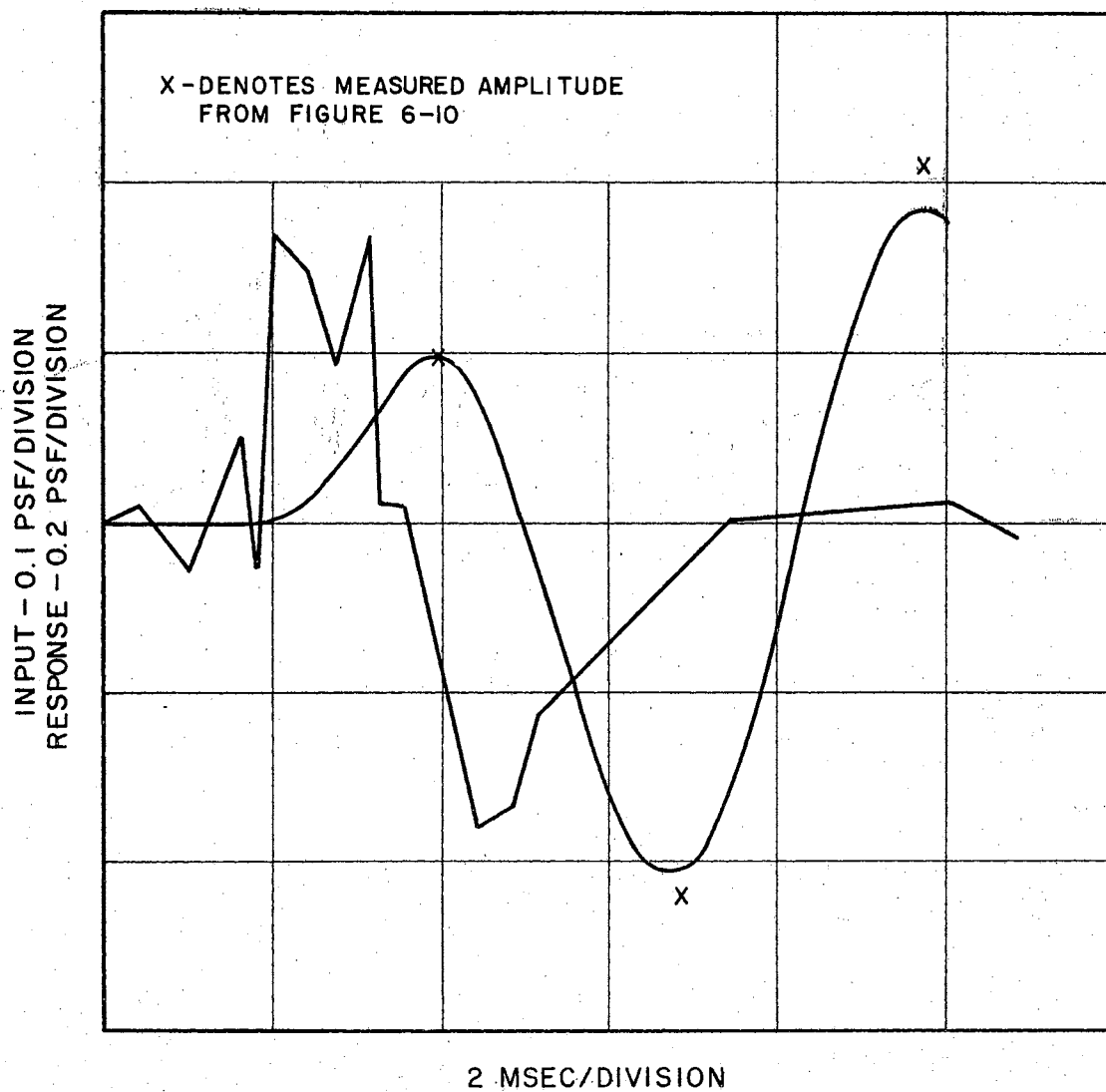


Figure 6-11. Straight Line Approximation of Input and Predicted Response Corresponding to Figure 6-10.

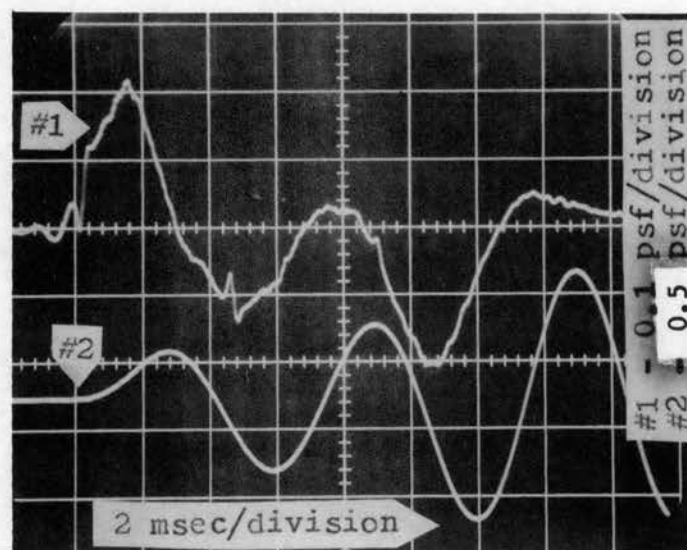


Figure 6-12. Time Response Measurement

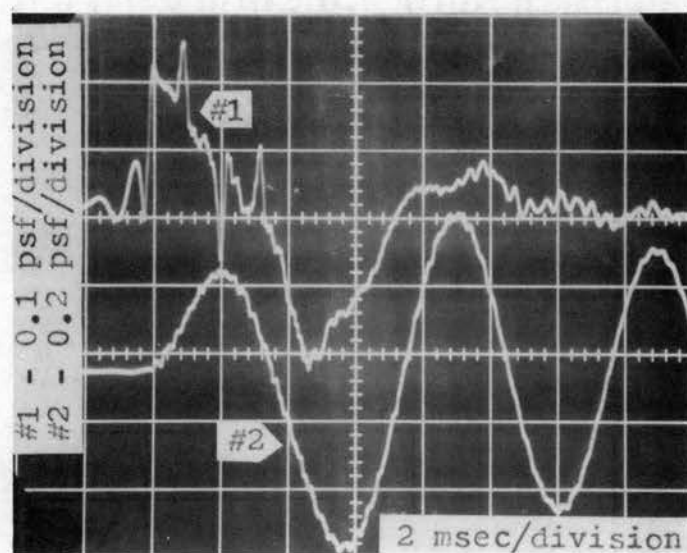


Figure 6-13. Time Response Measurement

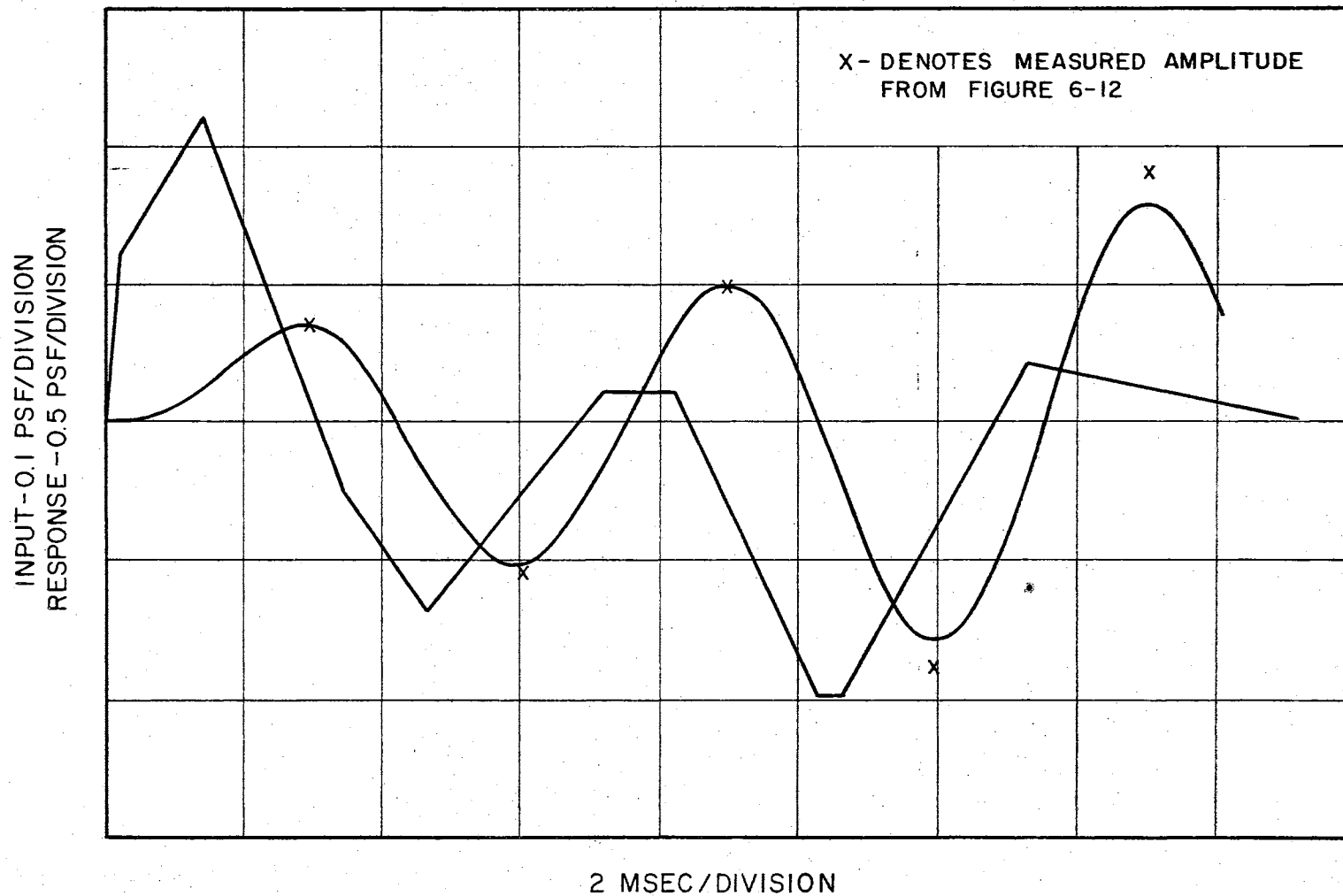


Figure 6-14. Straight Line Approximation of Input and Predicted Response Corresponding to Figure 6-12

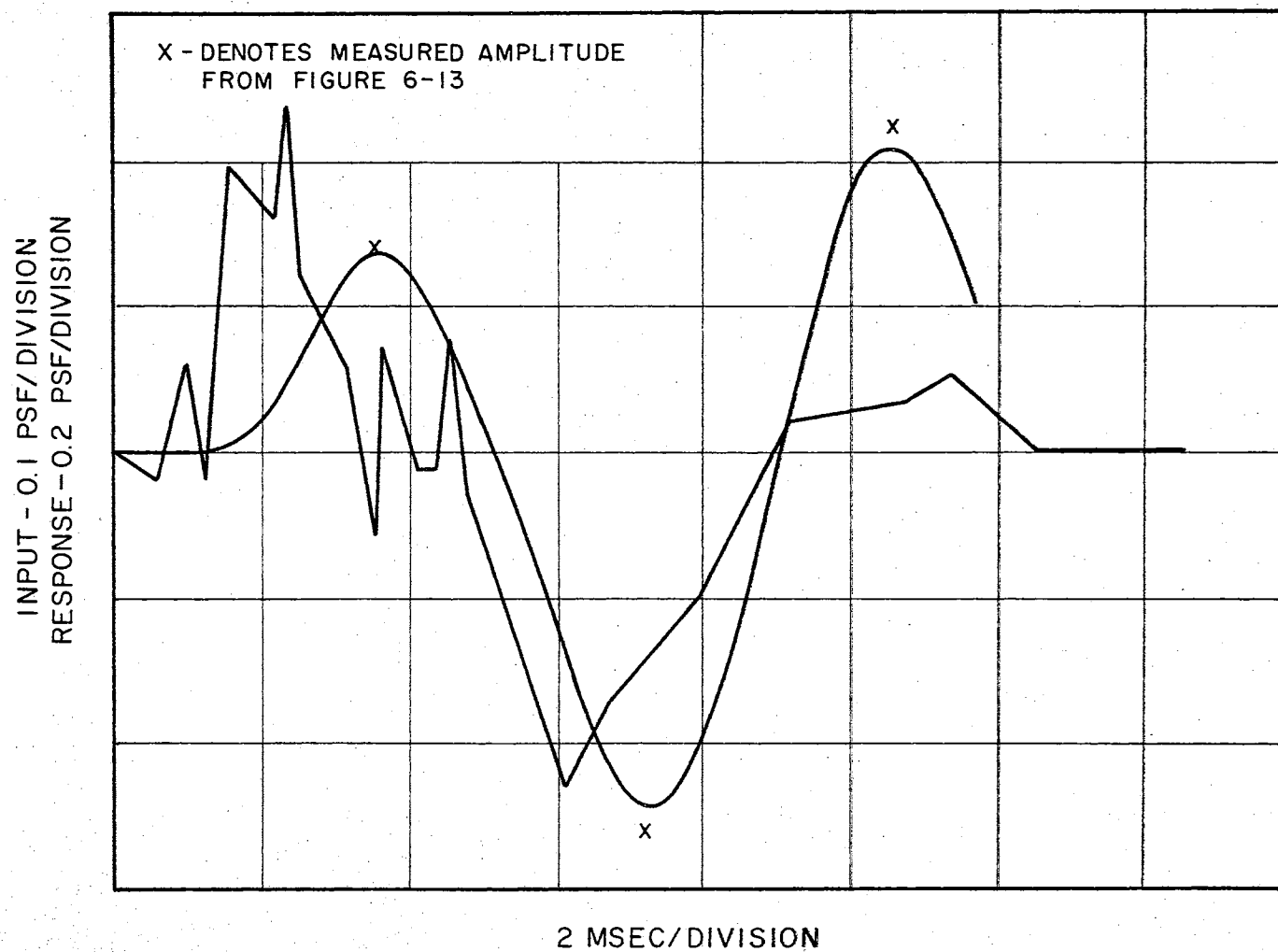


Figure 6-15. Straight Line Approximation of Input and Predicted Response Corresponding to Figure 6-13

again good. The sensitivities for the responses are half that for the inputs. The magnification in this case is about $(2.5/2) \times 2 \times .91 = 2.3$.

Figure 6-16 shows an input pulse with three well defined push-pull cycles. Reflections could produce such a signature for a sonic boom. The response sensitivity is one fifth the input sensitivity so that the magnification is about $(2.9/2.1) \times 5 \times .91 = 6.3$.

There are several conclusions which can be drawn from the time response studies. The time response of the resonator to transient input pulses can be predicted quite satisfactorily with the simple lumped parameter model. The influence of higher modes appears to be minor. Pressure amplitudes at points remote from the neck opening may be expected to be slightly higher than given by the simple theory. Although the differences are often noticeable, normally they will not be large. These pressure differences can be predicted fairly well on the basis of either equation (4-8) or (4-9). Considerable pressure amplification can be achieved for pulses with more than one push-pull cycle as would be expected theoretically. This has important application in sonic boom response analysis.

Maximax Study

A check on how the Helmholtz resonator responds as a simple oscillator can be accomplished by checking how well the resonator response traces out maximax curves such as given by Jacobsen and Ayre [5]. The only pulse which could be produced well enough to perform this test with the existing experimental apparatus was one

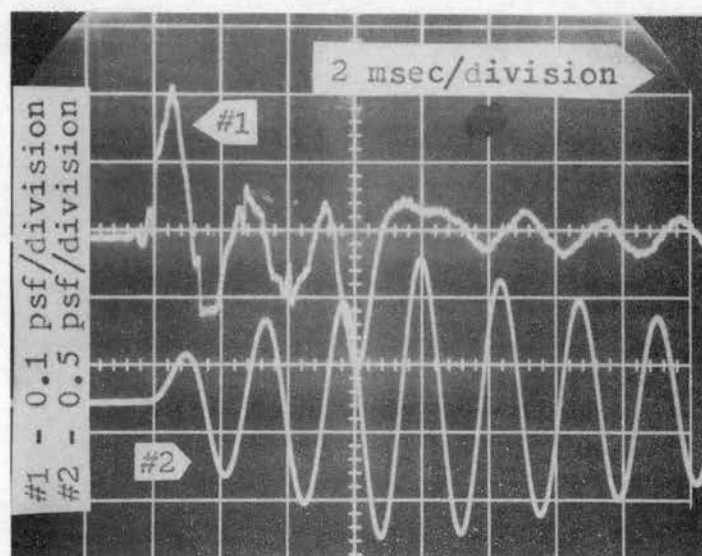


Figure 6-16. Time Response Measurement

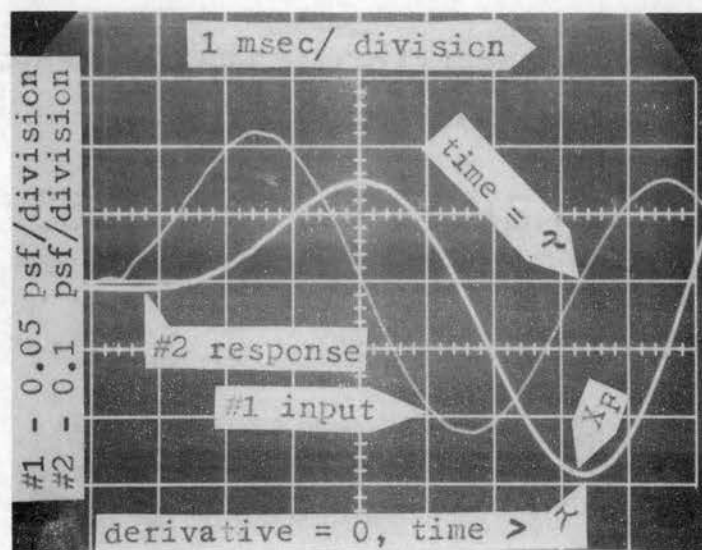


Figure 6-17. X_F Measurement for One Cycle Sinusoidal Input

cycle of a sine wave and this could not be shut off so that the study had to be restricted to the maximum displacement of the resonator during the forcing era, denoted by X_F (page 160, ref. 5).

Figure 6-17 shows input and response curves as used in making these measurements although most of the measurements were made by reading an oscilloscope trace. The results of these tests are shown in Figure 6-18. The agreement between theory and measurements is satisfactory. The theoretical curves agree with the curve given by Jacobsen and Ayre (5, page 165) except in the neighborhood of $\tau/T = 1.0$. The pertinent curve from Jacobsen and Ayre has been replotted in Figure 6-18. The error in Jacobsen and Ayre's curve may be explained by examining Figure 6-17. The maximum amplitude of resonator response during the forcing era is seen to occur at the end of the forcing era. The time rate of change is not zero at this point, however. Perhaps Jacobsen and Ayre considered only those maxima for which the first derivative is zero. This test adds nothing new; it merely adds more weight to the argument that generally the simple lumped parameter description of the resonator is quite good in the transient situation.

There has been some discussion concerning the proposed supersonic transport as to the possibility of shaping the boom so that it resembles one cycle of a sine wave rather than a N-wave. Comparison of Figures 6-18 and 2-6 shows that the sine wave pulse can produce more amplification than the N-wave for near critical tuning (i.e., $\tau/T \approx 1.0$) but not much amplification for cases where the tuning is not good. The N-wave, on the other hand, produces

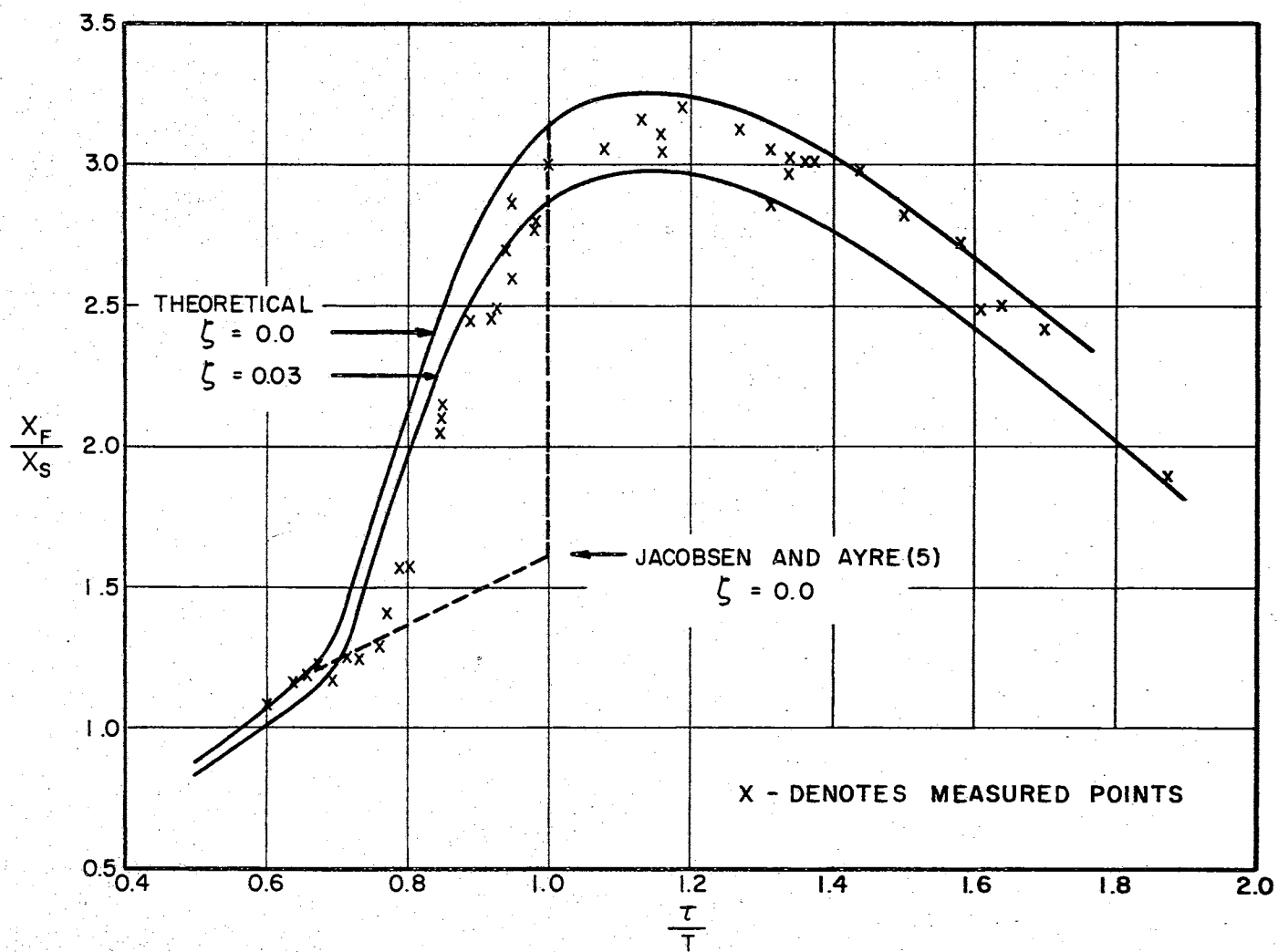


Figure 6-18. X_F Curves for One Cycle Sinusoidal Input

significant amplification any time the dimensionless parameter τ/T is greater than about 0.5.

Higher Mode Response

The higher mode response was discussed at some length in the first two sections of this chapter. Generally the amplitude of the higher mode response was found to be on the order of 5% or less, of the Helmholtz mode response. The only procedure which proved successful in exciting a greater magnitude higher order response was the use of an input pulse such as shown in Figure 5-12. This in fact, however, amounted to driving the resonator with many cycles of high frequency input and does not belong in this study.

The higher mode response should not be confused with the variations in pressure amplitude from point to point inside the resonator cavity associated with the fundamental mode.

Generally there is interest in the transient response of the Helmholtz resonator only when the time or frequency properties of the input pulse are such that considerable excitation of the fundamental mode is expected. The higher mode response is not at all significant under these conditions. Higher mode response is very often present but is not of the same order of magnitude as the response in the fundamental mode.

The Frequency Criteria

In the steady state situation, the representation of the Helmholtz resonator as a simple oscillator is restricted by frequency limitations

on the input. The restrictions on the frequency or time properties of the input are not nearly so critical in the transient case. In the transient case the input is limited in two ways, however. First, there must be only a very few push-pull cycles in the input pulse. If there were many cycles in the input, the steady state situation would be approached. Also, the input pulse must have a period which is long enough so that considerable excitation of the fundamental or Helmholtz mode occurs. If these two restrictions are satisfied, then the response of the resonator can be described quite well by the simple oscillator model.

The frequency of interest in the transient response problem is the natural frequency of the resonator rather than any frequency associated with the input. The relationship between the natural frequency of the resonator and the resonator geometry determines the importance of pressure amplitude differences from point to point inside the resonator cavity. These pressure differences which are associated with the fundamental mode are predicted approximately by equation (4-8) or (4-9).

The experimental results discussed under time response studies substantiate the above statements fairly well. Figures 6-19 and 6-20 further substantiate the fact that the internal pressure differences are related to the natural frequency of the cavity. The resonator configuration was as shown in Figure 6-4 when these results were obtained. The input pulse for both sets of traces is nearly identical. In Figure 6-19 the response was recorded at the back of the resonator while in Figure 6-20 the response was recorded with the microphone in

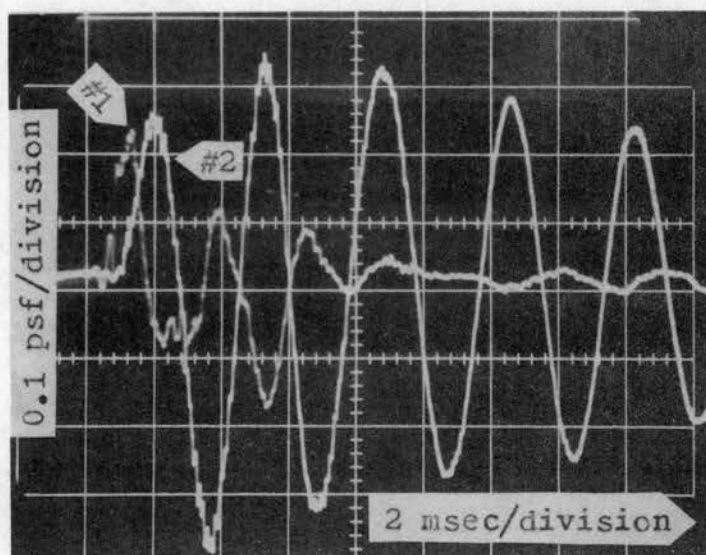


Figure 6-19. Response Variation Within the Cavity
#2 Microphone in #5 Hole Near Edge

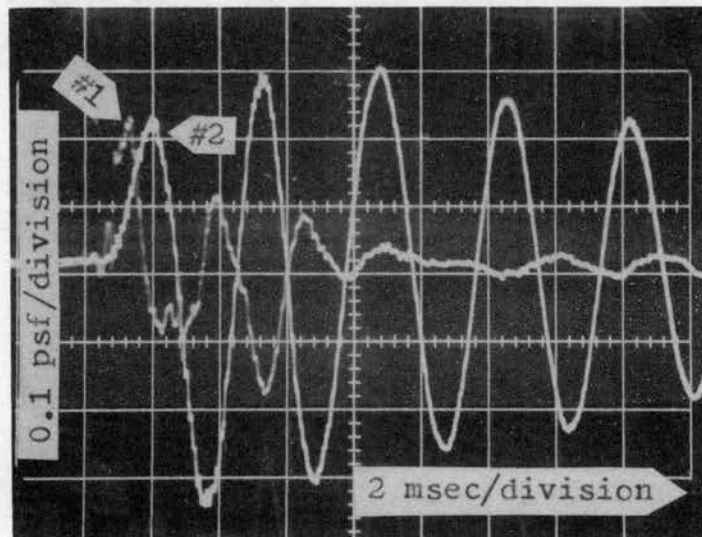


Figure 6-20. Response Variation Within the Cavity
#2 Microphone in #1 Hole Near Center

the number 1 hole near the center of the resonator. Table 6-2 shows the ratio of the peaks obtained from (6-19) to those obtained from (6-20) for the first nine peaks. During the forcing era and also the relaxation era this ratio is always about the same. Small differences in the input pulse or difficulty in reading the photographs accurately could easily account for more variation than is shown in Table 6-2. The ratio (P_R/P_N) was previously predicted to be about 1.1 for this resonator configuration. The measured values of P_R/P_N given in Table 6-2 are in agreement with the predicted value and are about the same during both the forcing era and the free vibration era.

The Effect of Leakage

An interesting effect which was observed during this work concerns the consequences of the resonator cavity's not being air tight. The sonic boom application might very possibly involve attempting to calculate the Helmholtz resonant frequency of a typical room. It was mentioned previously that air leaks caused a noticeable rise in the natural frequency. This effect along with other complications such as non-rigid walls will have to be taken into account in any attempt to compute the Helmholtz frequencies for rooms and will make theoretical attempts more complicated and perhaps less reliable.

The two observed effects of the resonator cavity's not being air tight were an increase in damping and an increase in the natural frequency. The increase in damping is quite reasonable since there is air motion through small holes which may be expected to increase viscous

TABLE 6-2

COMPARISON OF MEASUREMENTS FROM FIGURES 6-19 AND 6-20

Peak Number	$\frac{\#5 \text{ Hole}}{\#1 \text{ Hole}}$		$\frac{P_R}{P_N}$
1	$\frac{2.2}{2.0}$	=	1.1
2	$\frac{3.9}{3.6}$	=	1.08
3	$\frac{3.1}{2.7}$	=	1.15
4	$\frac{3.4}{3.2}$	=	1.06
5	$\frac{3.0}{2.8}$	=	1.07
6	$\frac{2.9}{2.7}$	=	1.074
7	$\frac{2.6}{2.35}$	=	1.11
8	$\frac{2.7}{2.5}$	=	1.08
9	$\frac{2.2}{2.0}$	=	1.1

losses. The increase in the natural frequency may be explained by considering a problem for which the air leak is controlled. The resonator configuration as in Figure 6-4 was used with the cavity length reduced to 4 inches and the no. 5 hole left open. Figure 6-21 shows an input and response trace for this configuration. The natural frequency has increased considerably, to 203 cps, as compared to 169 cps with the no. 5 hole sealed. The damping has increased only slightly to $\zeta = 0.03$; a much greater increase in damping might be expected if large numbers of small holes or narrow slots formed the leakage passage.

A predicted response curve was computed in exactly the same manner as was previously done. The general shape of the response curve is in agreement with the predicted curve, all the peaks occurred in the right places but the predicted values were about 30% higher than the measured values.

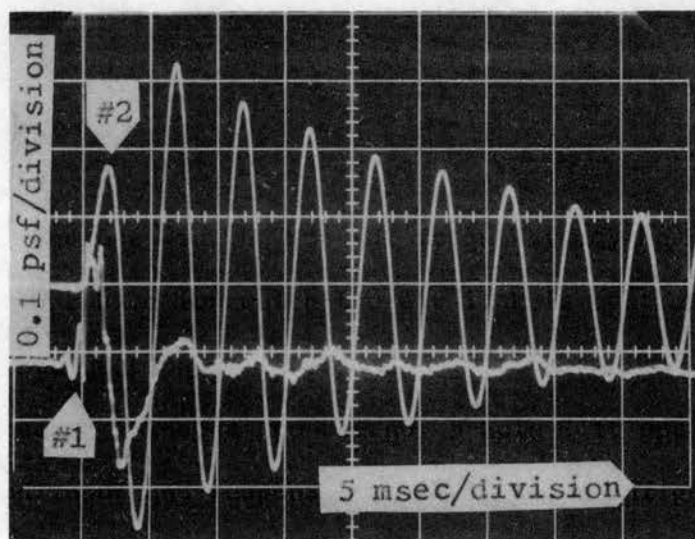


Figure 6-21. Time Response Measurement With Leakage on a Second Mass

The situation here is no longer the simple, one-degree-of-freedom oscillator. The acoustical and equivalent mechanical circuit is shown in Figure 6-22.

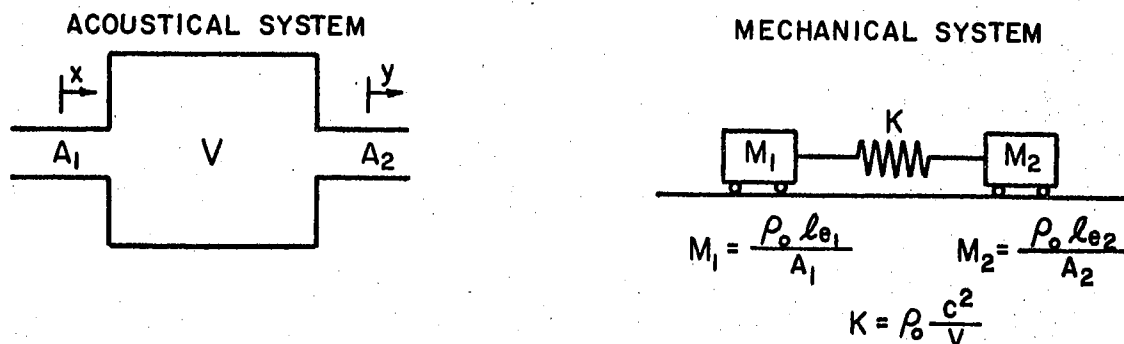


Figure 6-22. Acoustical and Mechanical Systems
With Leakage or a Second Mass

The differential equation for the acoustical system may be written as

$$(\rho_0 l_{e1} A_1) \frac{d^2 x}{dt^2} + \frac{\rho_0 c^2 A_1}{V} (A_1 x - A_2 y) = A_1 P(t), \quad (6-3)$$

and

$$\frac{\rho_0 c^2 A_2}{V} (A_2 y - A_1 x) + \rho_0 l_{e2} A_2 \frac{d^2 y}{dt^2} = 0, \quad (6-4)$$

where x and y are real displacements in the necks. If the equations are written in terms of volume displacements,

$$X = A_1 x \quad (6-5)$$

$$Y = A_2 y,$$

transformed into the frequency domain, and written in matrix form, they become

$$\begin{bmatrix} \left\{ \frac{(\rho_0 L_{e1})}{A_1} s^2 + \frac{\rho_0 c^2}{V} \right\} & -\frac{\rho_0 c^2}{V} \\ -\frac{\rho_0 c^2}{V} & \left\{ \frac{(\rho_0 L_{e2})}{A_2} s^2 + \frac{\rho_0 c^2}{V} \right\} \end{bmatrix} \begin{bmatrix} X(s) \\ Y(s) \end{bmatrix} = \begin{bmatrix} P_1(s) \\ 0 \end{bmatrix}, \quad (6-6)$$

which may be solved for the volume displacements

$$X(s) = \frac{(m_2 s^2 + K) P_1(s)}{m_1 m_2 s^4 + (m_1 + m_2) K s^2}, \quad (6-7)$$

and

$$Y(s) = \frac{K P_1(s)}{m_1 m^2 s^4 + (m_1 + m^2) K s^2}, \quad (6-8)$$

where m_1 , m_2 , and K are defined in Figure 6-22. A Newtonian force balance on each of the acoustic masses yields the equations

$$\left(\frac{\rho_0 L_{e1}}{A_1} \right) s^2 X(s) = P_1(s) - P(s), \quad (6-9)$$

and

$$\left(\frac{\rho_0 L_{e2}}{A_2} \right) s^2 Y(s) = P(s). \quad (6-10)$$

Equations (6-7) through (6-10) may be solved for the pressure inside resonator cavity as

$$P(s) = \frac{\left(\frac{m_2}{m_1 + m_2} \right) P_1(s)}{\frac{m_1 m_2 s^2}{(m_1 + m_2)K} + 1}. \quad (6-11)$$

The nonzero natural frequency of the system is

$$\omega_0^2 = \frac{(m_1 + m_2)K}{m_1 m_2}. \quad (6-12)$$

If a numerical estimate is made as was done in the first part of this chapter, the estimated natural frequency is 196 cps. This is in reasonable agreement with the measured value. Equation (6-11) may now be written as

$$P(S) = \frac{\left(\frac{m_2}{m_1 + m_2}\right) P_1(S)}{\frac{S^2}{\omega_0^2} + 1}, \quad (6-13)$$

which is identical to the response equation for the simple resonator given by Equation (C-94) except for the term $m_2/(m_1 + m_2)$ in the numerator. Thus, prediction of the response on the basis of the simple resonator model is acceptable but should be in error by the multiplier $m_2/(m_1 + m_2)$. The relative magnitudes of m_1 and m_2 are given by $m_1 \approx 1.85$ and $m_2 \approx 4.27$. Therefore, $m_2/(m_1 + m_2)$ is approximately 0.7 which agrees with the experimental results.

The expressions for the acoustic masses

$$m_1 = \frac{\rho_0 L e_1}{A_1}, \quad (6-14)$$

and

$$m_2 = \frac{\rho_0 L e_2}{A_2}, \quad (6-15)$$

indicate that a small cross sectional area leads to a large acoustic mass. Thus, for small leaks the factor $m_2/(m_1 + m_2)$ may be expected to be closer to unity.

Several time response studies were made with various resonator configurations which were not sealed with wax so that there were leaks particularly around the annulus between the back plate and cylinder walls. As long as measured natural frequencies and damping

factors were used, the prediction of the response using the simple oscillator theory was quite good except for the constant amplitude factor. If the leaks are relatively minor, this factor will not cause differences of more than about 10%.

The presence of leaks in the resonator thus has three main effects. The natural frequency increases, the damping increases, and the response amplitudes decrease. If the leaks are minor the effect on the natural frequency and response amplitudes will not be great. Damping may be increased considerably. Although the damping factor might easily be doubled, the doubled value would still be considered small relative to the inertia and elastic effects. The damping for the sealed rigid resonator is so small that the addition of only a little damping can double or triple the total amount of damping.

CHAPTER VII

CONCLUSIONS AND RECOMMENDATIONS

The following conclusions have been reached from the results of this study:

1. In sonic boom response investigations, the lumped parameter representation of the Helmholtz resonator should be adequate as a model for transient response studies. As is often the case with the Helmholtz resonator, determination of the effective neck length will be an important and critical part of the prediction of natural frequencies. The fact that the walls of a structure are nonrigid will have some effect on the validity of the model simplification. The presence of air leaks may have marked effects if the amount of leakage is great. Still, it should not be difficult to make reasonable estimates of the natural frequency. If measured estimates of the natural frequency and damping are used it should be possible to predict responses to booms quite well.
2. The Helmholtz resonance phenomena should be an important part of any analysis or prediction of sonic boom damages. Pressure magnifications may cause damage because of increased level of loading. The ringing associated with the Helmholtz response may possibly act as a secondary source driving other properly tuned systems to considerable amplitudes.

3. The proposed supersonic transport, which will produce a longer boom duration than those produced in the Oklahoma City tests, will cause no new problem as far as Helmholtz resonance is concerned. If the shape of the boom is modified to resemble one cycle of a sine wave, amplification by Helmholtz resonance or response of any simple oscillator will be greater for near critical tuning but less for non-critical tuning. The maximum magnification possible for the sine wave is about three, while that for the N-wave is about two. The N-wave can theoretically produce pressure magnifications on the order of 1.5 to 2 in any resonator which has a period less than about twice the length of the boom.
4. The lumped parameter representation of the Helmholtz resonator will generally be adequate for the analysis of transient responses. If the resonator walls are reasonably rigid and there are no air leaks the natural frequencies may be predicted within about 3%. If measured natural frequencies and damping factors are used and the resonator geometry is reasonable, the response to a pressure pulse can be predicted accurately. Reasonable resonator geometry requires that the cavity be compact as opposed to elongated, that the neck cross section be compact, that the neck cross section be small compared to the cavity cross section, and that the neck length be less than the large dimension of the cavity but preferably not zero. The input pulses must not contain over two or three push-pull cycles however. Frequency limitations are not as critical as in the steady state response problem and the frequency of interest is the natural frequency of the resonator, rather than any particular frequency associated with the transient input.

5. Higher mode response is not generally important for the transient problem. Sharp rise inputs do not produce significant higher mode response; the higher mode response is usually less than 5% of the fundamental mode response.
6. The effects of air leaks on the resonator response include increasing the natural frequency, increasing the damping, and reducing response amplitudes. These effects may be minor or quite significant depending on the extent of air leakage.
7. The plane wave tube used in this study is a very useful and workable tool for the study of acoustic transient response problems and particularly sonic boom simulation studies.

Recommendations

It is recommended that further investigations be carried out in the following areas:

1. The verification of the lumped parameter representation of the Helmholtz resonator for the simple, one-degree-of-freedom resonator seems to answer the multi-degrees-of-freedom question at least partially. An experimental verification of a lumped parameter description of a several-degree-of-freedom system would probably not be wasted effort however. A study of several-degrees-of-freedom systems with interest in maximum possible responses would be of interest to the sonic boom applications. The complications arising from pressure amplitude variations in the fundamental mode from point to point within the simple resonator could lead to some interesting problems with the several-degrees-of-freedom system.

2. The difference between normal incidence and oblique incidence of the pulse should be minor due to the rapid passage of the pulse over the neck opening; however, the problem probably warrants closer study and some experimental investigation.
3. The theoretical basis for predicting the importance of the higher modes is weak. This is a very difficult problem in the case of the acoustic system and is not simple for any other type of distributed system.
4. In a typical residence it is sometimes very difficult to identify the lumped parameters because of difficult geometry. The solution of this problem will be necessary if attempts are made to study the acoustic response of buildings as a whole to sonic booms.
5. The effects caused by the nonrigid walls deserve investigation.
6. The plane wave tube used in this work offers excellent possibilities in sonic boom simulation. Refinements in the driving mechanism such as a rigid diaphragm and servo control which could be programmed as desired should permit really good simulation.

SELECTED BIBLIOGRAPHY

1. Rayleigh, J. W. S., The Theory of Sound, Vol. II, Dover Publications, New York, 1945.
2. Olson, H. F., Dynamical Analogies, D. Van Nostrand Company, Inc., Princeton, New Jersey, 1958.
3. Beranek, L. L., Acoustics, McGraw-Hill Book Company, Inc., New York, 1954.
4. Kinsler, L. E., and Frey, A. R., Fundamentals of Acoustics, John Wiley & Sons, Inc., New York, 1962.
5. Jacobsen, L. S., and Ayre, R. S., Engineering Vibrations, McGraw-Hill Book Company, Inc., New York, 1958.
6. Ingard, Uno, "On The Theory and Design of Acoustic Resonators," Journal, Acoustic Society of America, Vol. 25, Number 16, November, 1953.
7. ———, "The Near Field of a Helmholtz Resonator Exposed to a Plane Wave," Journal, Acoustic Society of America, Vol. 25, Number 6, November, 1953.
8. Lambert, R. F., "A Study of the Factors Influencing the Damping of an Acoustical Cavity Resonator," Journal, Acoustic Society of America, Vol. 25, Number 6, November, 1953.
9. McGinnis, C. S., and Albert, V. F., "Multiple Helmholtz Resonator," Journal, Acoustic Society of America, Vol. 24, Number 4, July, 1952.
10. Thompson, W. T., Laplace Transformation, Prentice-Hall Inc., Englewood Cliffs, New Jersey, 1960.
11. Cheng, D. H., "Some Dynamic Effects on Sonic Booms on Building Structural Elements," Langley Working Paper No. 25, NASA.
12. Arde Associates, Response of Structures to Aircraft Generated Shock Waves, WADC Technical Report 58-169, April, 1959.

13. Andrews Associates, Inc., and Hudgins, Thompson, Ball and Associates, Inc., "Final Report on Studies of Structural Response to Sonic Booms" for the Federal Aviation Agency, Vol. I, February 5, 1965.
14. Simpson, J. D., and Lowery, R. L., "The Response of Acoustic Resonators to Sonic Booms," Presented to the 70th meeting of the Acoustical Society of America, St. Louis, November 5, 1965.
15. Ingard, Uno, "On The Radiation of Sound into a Circular Tube, With an Application to Resonators," J.A.S.A., Volume 20, Number 5, September, 1948.
16. Lee, U. W., Statistical Theory of Communication, John Wiley & Sons, Inc., New York, 1960.

BIBLIOGRAPHY

1. Samulon, H., "Investigations on Acoustic Resonators," The Journal of the Acoustical Society of America, 19, January, 1947, 191-193.
2. Wood, John K. and Thurston, George B., "Acoustic Impedance of Rectangular Tubes," The Journal of the Acoustical Society of America, 25, September, 1953, 858-860.
3. Ingard, Uno and Lyon, Richard H., "The Impedance of a Resistance Loaded Helmholtz Resonator," The Journal of the Acoustical Society of America, 25, September, 1953, 854-857.
4. Bies, David A. and Wilson, O. B., Jr., "Acoustic Impedance of a Helmholtz Resonator at Very High Amplitude," The Journal of the Acoustical Society of America, 29, June, 1957, 711-714.
5. Edge, Philip M., Jr. and Mayes, William H., "Description and Research Capabilities of the Langley Low-Frequency Noise Facility," Presented at the 69th meeting of the Acoustical Society of America, Washington, D. C., June 2-5, 1965.
6. Schriever, W. R., "Effects of Sonic Boom on Buildings," Materials Research and Standards, ASTM, 4, November, 1964, 581. — C F
7. Lyster, H. N. C., "The Nature of the Sonic Boom," Materials Research and Standards, ASTM, 4, November, 1964, 582-587.
8. Mayes, W. H. and Edge, P. M., Jr., "Effects of Sonic Boom and Other Shock Waves on Buildings," Materials Research and Standards, ASTM, 4, November, 1964, 588-593.
9. Power, J. K., "Some Results of the Oklahoma City Sonic Boom Tests," Materials Research and Standards, ASTM, 4, November, 1964, 617-623.
10. McKinley, R. W., "Response of Glass Windows to Sonic Booms," Materials Research and Standards, ASTM, 4, November, 1964, 594-600.
11. Newberry, C. W., "Measuring the Sonic Boom and Its Effect on Buildings," Materials Research and Standards, ASTM, 4, November, 1964, 601-611.

12. Ramsay, W. A., "Damage to Ottawa Air Terminal Building Produced by a Sonic Boom," Materials Research and Standards, ASTM, 4, November, 1964, 612-616.
13. Parrott, T. L., "Experimental Studies of Glass Breakage Due to Sonic Booms," Sound, 1, May-June, 1962, 18-21.
14. Maglieri, Domenic J. and Hubbard, Harvey H., "Ground Measurements of the Shock-Wave Noise from Supersonic Bomber Airplanes in the Altitude Range from 30,000 to 50,000 Feet," NASA, Technical Note D-880, 1961.
15. Maglieri, Domenic J., Hubbard, Harvey H., and Lansing, Donald L., "Ground Measurements of the Shock-Wave Noise from Airplanes in Level Flight at Mach Numbers to 1.4 and at Altitudes to 45,000 Feet," NASA, Technical Note D-48, 1959.
16. Nichols, Marc R., "The Supersonic Transport - Required Characteristics of Configurations," Society of Automotive Engineering, 1961.
17. Teichman, G. A. and Westwater, R., "Blasting and Associated Vibrations," Engineering, April 12, 1957, 460-465.
18. Burger, Raymond L., "Some Effects of Flight Path and Atmospheric Variations on the Boom Propagated from a Supersonic Aircraft," NASA, Technical Report-191.
19. Whitham, G. B., "The Behavior of Supersonic Flow Past a Body of Revolution, Far from the Axis," Proceedings, Royal Society (London), Series A, Vol. 201, No. 1064, March 7, 1950, 89-109.
20. Rao, P. Sambasivia, "Supersonic Bangs - Part 1, Aeronautical Quarterly, Vol. 7, pt. 1, February, 1956, 21-44.
21. _____, "Supersonic Bangs - Part 2, Aeronautical Quarterly, Vol. 7, pt. 1, May, 1956, 135-155.
22. Power, J. Kenneth, "Some Considerations of Sonic Boom," Federal Aviation Agency, Office of Plans, Washington, D. C., May, 1961.
23. Friedman, Manfred P., "Sonic Boom Studies," Massachusetts Institute of Technology DSR No. 8750, February, 1962.
24. McKinley, R. W., "The Response of Glass to Sonic Booms," Paper for Sonic Boom Symposium, ASTM, 67th Annual Meeting, Chicago, Illinois, June 25, 1964.
25. Morrow, Charles T., "Shock Spectrum as a Criterion of Severity of Shock Impulses," Journal, Acoustical Society of America, 29, May, 1957, 596-602.

26. Nisbet, J. S. and Brennon, J. N., "Some Secondary Effects Related to Impact Wave Forms," Journal, Acoustical Society of America, 29, July, 1957, 837-842.
27. Bleakney, Walker, White, D. R., and Griffith, W. C., "Measurements of Diffraction of Shock Waves and Resulting Loading of Structures," Journal of Applied Mechanics, December, 1950, 439-445.
28. Kornhouser, M., "Prediction and Evaluation of Sensitivity to Transient Accelerations," Journal of Applied Mechanics, December, 1954, 371-380.
29. Crede, C. E., "The Effect of Pulse Shape on Simple Systems Under Impulsive Loading," Transactions of the ASME, August, 1955.
30. Bowles, R. B. Sugarman, "The Strength and Deflection Characteristics of Large Rectangular Glass Panels Under Uniform Pressure," Glass Technology, Vol. 3, No. 5, October, 1962.
31. Fung, Y. C., "Statistical Aspects of Dynamic Loads," Journal, Aero Science, 20, May, 1953, 3-17, 330.
32. Biot, M., "Acoustics Spectrum of an Elastic Body Submitted to Shock," Journal, Acoustical Society of America, 5, January, 1934, 206-207.
33. Wilson, H. A., Jr., "Sonic Boom," Scientific American, 206, January, 1962, 36-43.
34. Maglieri, Domenic J. and Parrot, Tony L., "Atmospheric Effects on Sonic-Boom Pressure Signatures," Sound, Vol. 2, No. 4, July-August, 1963, 11-14.
35. Maglieri, Domenic J. and Lansing, D. L., "Sonic Booms from Aircraft in Manuevers," Sound, Vol. 2, No. 4, March-April, 1963, 39-42.
36. Freynik, Henry S., Jr., "Response of Windows to Random Noise," Sound, Vol. 2, No. 3, May-June, 1963, 31-33.
37. Fung, Y. C. and Barton, M. V., "Some Characteristics and Uses of Shock Spectra," Journal, Applied Mechanics, 25, 1958, 365-372.
38. Ungar, E. E., "Response of Plates to Moving Shocks," Aerospace Engineering, March, 1961, 16-17 and 78-84.

APPENDIX A

LIST OF SYMBOLS

A	Cross sectional area of the neck of a Helmholtz resonator. Also used as an arbitrary constant in Appendix C.
B	An arbitrary constant used in Appendix C.
C	Capacitance
c	Velocity of sound
D	Characteristic dimension, also the diameter of the cavity cylinder in Appendix C.
E	Voltage
$f_n(\frac{r_o}{R_o})$	Function defined by Equation (C-28)
$f_n'(\frac{r_o}{R_o})$	Function defined by Equation (C-52)
f_L	Limit frequency on lumped parameter model
f_o	Natural frequency of a resonator
j	$\sqrt{-1}$
J_o	Bessel function of the first kind of order zero
L	Length of the circularly symmetric cavity shown in Figure C-1
L'	Length of the neck shown in Figure C-1
L_e	Effective length of the neck
\bar{L}	Inductance
p	Acoustic pressure

P_1	Pressure at the open end of the neck as shown in Figure C-3. Input Pressure
P_a	Pressure at the mouth of the cavity
P	Pressure inside the resonator
\bar{q}	Vector velocity
R_0	Radius of the cavity shown in Figure C-1
r_0	Radius of the neck shown in Figure C-1
r	Radius and radial coordinate used in Appendix C
$R(r)$	Function defining pressure variation as a function of radius defined by Equation (C-3)
S	The Laplace operator
t	Time
$T(t)$	Function defining pressure variation as a function of time defined by Equation (C-3)
U	Volume velocity
\bar{u}_x	Unit vector in the axial direction used in Appendix C
\bar{u}_r	Unit vector in the radial direction used in Appendix C
V_x	Velocity component along \bar{u}_x
V_r	Velocity component along \bar{u}_r
V_a	Velocity at the mouth of the cavity in Appendix C
V_1	Velocity at the open end of the neck in Appendix C
X	Volume displacement
x	Axial coordinate shown in Figure C-2
X_F	Maximum displacement during forcing era
X_S	Static displacement
$X(x)$	Function defining pressure variation as a function of x defined by Equation (C-3)
Y_0	Bessel function of the second kind of order zero

y	Axial component along neck defined by Figure C-3
α	Parameter defined by Equation (C-18)
β	Parameter defined by Equation (C-6)
ΔL_1	Neck correction at the open end
ΔL_2	Neck correction at the closed end
Δ	Parameter defined by Equation (C-80)
γ_n	Parameter defined by Equation (C-38) and (C-41)
λ	Wave length of pressure oscillations
ω	Angular frequency in radians per second
ϕ_n	Parameter defined by Equation (C-70)
ρ_0	Mean density of air
σ_n	Parameter defined by Equation (C-38)
τ	Time duration of a sonic boom

APPENDIX B

LIST OF MAJOR INSTRUMENTATION

Microphone System--Model 21BR150 Condensor Microphone, Serial No. 3854; 165 A Base; Model 526 B Power Supply, Serial No. 608; Manufacturer; Altec Lansing Corporation.

Microphone System--Model 21BR150 Condensor Microphone, Serial No. 3892; 165 A Base; Model 526 B Power Supply, Serial No. 606; Manufacturer, Altec Lansing Corporation.

Dual Beam Oscilloscope--Model 502; Manufacturer, Textronix; Serial No. 022893.

Low Frequency Function Generator--Model 202A; Manufacturer, Hewlett-Packard; Serial No. 037-09559.

Audio Oscillator--Model 200 AB; Manufacturer, Hewlett-Packard; Serial No. 003-13132.

Tone Burst Generator--Type 1396-A; Manufacturer, General Radio Company; Serial No. 354.

Power Amplifier--Model MC 75; Manufacturer, McIntosh.

Microphone--Model 98A108 Crystal Microphone; Manufacturer, Shure Brothers; Serial No. 2241.

Microphones (4)--Model 141-11, Crystal Microphone; Manufacturer, Turner.

APPENDIX C

DERIVATIONS RELATING TO FREQUENCY LIMITATIONS

A more detailed analysis of a particular resonator which is geometrically simple is warranted for several reasons. The analysis allows establishment of frequency limitations on the lumped parameter model in a reasonably straightforward manner, at least for the steady state situation. How these frequency limitations may be applied to the transient situation is not clarified by the discussions in this appendix. The frequency limitations so established may then be assumed to apply to other geometric configurations at least in a general way. This extension to other geometric configurations is restricted to shapes which are not too extreme. The cavity should not be greatly elongated, i.e., it should be roughly spherical. The neck cross section could be round, elliptical, square but should not be, for example, a narrow slot. The establishment of frequency limitations and their extension to permit application to the general Helmholtz resonator follows along the lines used by Beranek [3]. The analysis is essentially a solution of the wave equation for a particular geometric configuration. The solutions obtained reduce to the lumped parameter description when approximations permitted by a low frequency assumption are introduced into the equations.

The analysis also illustrates the tremendous mathematical difficulties involved in detailed analysis of the Helmholtz resonator.

Even for the very simple geometric situation studied here, it is necessary to make several simplifying assumptions. Attempts at a more sophisticated solution often encounter insurmountable mathematical difficulties. The geometry of the resonator if not extremely simple can present great difficulties.

The analysis also demonstrates how the consideration of higher frequencies and higher modes ties the solution to the geometric details of a particular resonator. Any solution thus obtained at tremendous cost in terms of time and effort is very restricted in its application.

The geometric configuration of the resonator to be studied is shown in Figure C-1. The volume or cavity of the resonator is a circular cylinder of radius R_0 and length L closed at both ends.

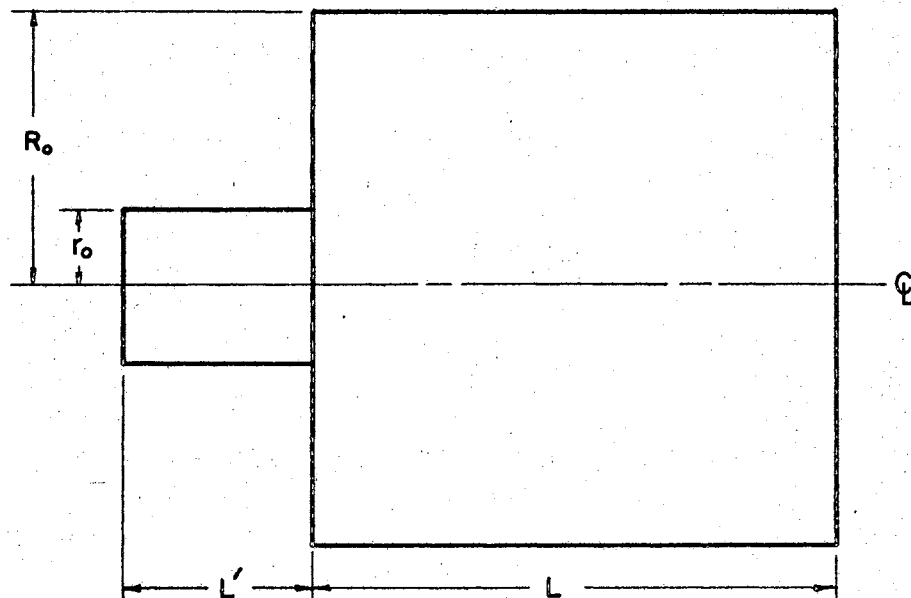


Figure C-1. Cross Section of a Circular Symmetric Resonator Configuration

The neck is a circular cylinder of radius r_0 and length L' and is attached to one end of the cavity along the axis of circular symmetry. The walls and neck of the resonator are assumed to be rigid.

The wave equation,

$$\nabla^2 p = \frac{1}{c^2} \frac{\partial^2 p}{\partial t^2}, \quad (C-1)$$

will be assumed to apply and damping will be neglected. Because of the discontinuity where the neck joins with the cavity, it is advantageous to analyze the neck and the cavity separately. The physical configuration of the cavity is shown in Figure C-2. The axial component of velocity is to be specified in the neck as a function of radius and time.

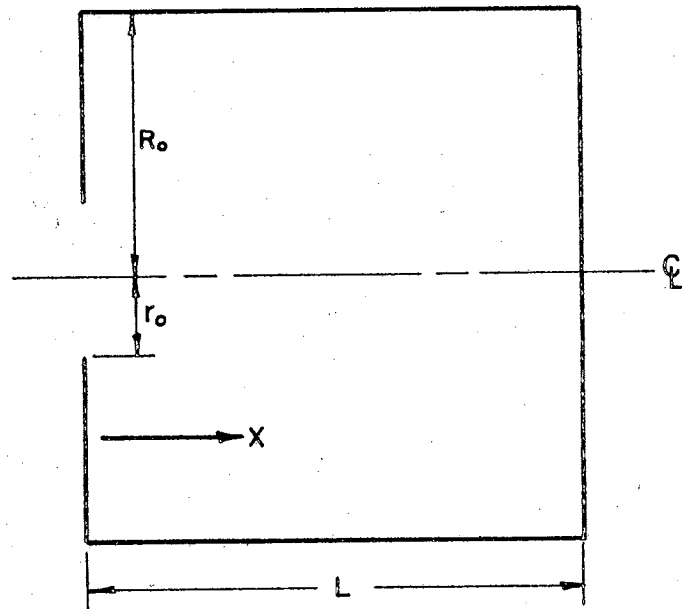


Figure C-2. Geometric Configuration of the Cavity of the Resonator

The property of circular symmetry suggests that polar coordinates would be appropriate. The wave equation applicable to this case may be written as

$$\frac{\partial^2 p}{\partial r^2} + \frac{1}{r} \frac{\partial p}{\partial r} + \frac{\partial^2 p}{\partial x^2} = \frac{1}{c^2} \frac{\partial^2 p}{\partial t^2}, \quad (C-2)$$

where

p = the pressure

x = the distance along the axis of the cylinder

r = the radius

c = the velocity of sound.

The solution of Equation (C-2) may be taken in the form

$$p(r, x, t) = R(r) X(x) T(t). \quad (C-3)$$

Equation (C-2) can then be written as

$$\frac{1}{R} \left\{ \frac{d^2 R}{dr^2} + \frac{1}{r} \frac{dR}{dr} \right\} + \frac{1}{X} \frac{d^2 X}{dx^2} = \frac{1}{c^2 T} \frac{d^2 T}{dt^2}. \quad (C-4)$$

If the Laplace transformation is applied to Equation (C-4) with respect to the time variable the equation becomes

$$\frac{1}{R} \left\{ \frac{d^2 R}{dr^2} + \frac{1}{r} \frac{dR}{dr} \right\} + \frac{1}{X} \frac{d^2 X}{dx^2} = \frac{S^2}{c^2}, \quad (C-5)$$

where S is the Laplace operator. The function $R(r)$ is given by the solution of the ordinary differential equation

$$\frac{d^2 R}{dr^2} + \frac{1}{r} \frac{dR}{dr} + \beta^2 R = 0, \quad (C-6)$$

which is Bessel's differential equation. The general solution of Equation (C-6) is

$$R(r) = C_1 J_0(\beta r) + C_2 Y_0(\beta r) , \quad (C-7)$$

where C_1 and C_2 are arbitrary constants, $J_0(\beta r)$ is the Bessel function of the first kind of order zero, and $Y_0(\beta r)$ is the Bessel function of the second kind of order zero. The Bessel function of the second kind $Y_0(\beta r)$ goes to infinity for a zero argument. Since pressure along the axis will be finite in the problem under discussion, the constant C_2 must equal zero and Equation (C-7) may therefore be reduced to

$$R(r) = C J_0(\beta r) . \quad (C-8)$$

The pressure and velocity are related through the equation

$$-\text{grad}(p) = \rho_0 \frac{\partial \bar{q}}{\partial t} , \quad (C-9)$$

where \bar{q} is the vector velocity and ρ_0 is the mean density. In the cylindrical coordinates of this problem, Equation (C-9) may be written as

$$-\frac{\partial p}{\partial x} \bar{u}_x - \frac{\partial p}{\partial r} \bar{u}_r = \rho_0 \frac{\partial V_x}{\partial t} \bar{u}_x + \rho_0 \frac{\partial V_r}{\partial t} \bar{u}_r , \quad (C-10)$$

where \bar{u}_x and \bar{u}_r are unit vectors directed in the x and r directions and V_x and V_r are the velocity components. Equation (C-10) can be divided into separate equations

$$\frac{\partial p}{\partial x} = - \rho_0 \frac{\partial V_x}{\partial t} \quad (C-11)$$

$$\frac{\partial p}{\partial r} = - \rho_0 \frac{\partial V_r}{\partial t} . \quad (C-12)$$

At the cylinder wall the radial velocity V_r becomes zero as does the time derivative of V_r . This boundary condition in Equation (C-12) leads to

$$\frac{\partial P}{\partial r} = \frac{\partial R(r)}{\partial r} X(x) T(t) = 0 \quad (C-13)$$

or

$$\frac{\partial R(r)}{\partial r} = 0, \quad (C-14)$$

and

$$J_1(\beta R_0) = 0, \quad (C-15)$$

where J_1 is the Bessel function of first kind and order one.

Equation (C-15) defines the values which the parameter β may have. Thus, the successive values of β are

$$\beta = 0, \frac{3.832}{R_0}, \frac{7.0155}{R_0}, \frac{10.1753}{R_0}, \frac{13.324}{R_0}, \frac{16.471}{R_0} \dots \quad (C-16)$$

The function $X(x)$ is given by the solution of the differential equation

$$\frac{d^2 X}{dx^2} - \alpha^2 X = 0, \quad (C-17)$$

where

$$\alpha^2 = \frac{s^2}{c^2} + \beta^2. \quad (C-18)$$

The general solution of Equation (C-17) is given by

$$X = Ae^{\alpha x} + Be^{-\alpha x} \quad (C-19)$$

The solution of Equation (C-5) which is the Laplace transform of the solution of Equation (C-2) is given by

$$\bar{P}(r, x, s) = \sum_{n=0}^{\infty} J_0(\beta r) \left\{ A_n e^{\alpha_n x} + B_n e^{-\alpha_n x} \right\} T(s). \quad (C-20)$$

The velocity V_x in the x direction will be zero at $x = L$. This boundary condition in Equations (C-11) and (C-20) leads to the equation

$$\left. \frac{\partial \bar{P}}{\partial x} \right|_{x=L} = \sum_{n=0}^{\infty} J_0(\beta_n r) \alpha_n \left\{ A_n e^{\alpha_n L} - B_n e^{-\alpha_n L} \right\} T(S) \quad (C-21)$$

or

$$A_n e^{\alpha_n L} - B_n e^{-\alpha_n L} = 0. \quad (C-22)$$

At the end $x = 0$, the boundary conditions are

$$V_x = 0 \text{ for } r > r_0 \quad (C-23)$$

and

$$V_x = V(r, t) \text{ for } r < r_0. \quad (C-24)$$

These boundary conditions may be applied by substituting Equation (C-20) into Equation (C-11) with the result

$$\left. \frac{\partial \bar{P}}{\partial x} \right|_{x=0} = \sum_{n=0}^{\infty} J_0(\beta_n r) \alpha_n \left\{ A_n - B_n \right\} T(S) = -\rho_0 S V_a(r) V_a(S) \quad (C-25)$$

where the variables have been separated in the velocity function on the right hand side. V_a is the velocity input at the mouth of the cavity. The radial component of this velocity is assumed to be zero. The difference between the coefficients $\{A_n - B_n\}$ may be separated from Equation (C-25) by using a Fourier Bessel series expansion. The procedure is to multiply both sides of the equation by $r J_0(\beta_n r)$ and then to integrate with respect to the r variable from zero to R_0 .

The result is in this case

$$A_n - B_n = \frac{-2\rho_0 S V_a(S) \int_0^r r V_a(r) J_0(\beta_n r) dr}{\alpha_n T(S) R_0^2 J_0^2(\beta_n r)} \quad (C-26)$$

or

$$A_n - B_n = \frac{-\rho_0 S V_a(S)}{\alpha_n T(S)} f_n\left(\frac{r_0}{R}\right), \quad (C-27)$$

where

$$f_n\left(\frac{r_0}{R}\right) = \frac{2 \int_0^{r_0} r V_a(r) J_0(\beta_n r) dr}{R_0^2 J_0^2(\beta_n R_0)}. \quad (C-28)$$

If the velocity in the opening is not a function of the radius then

$$\begin{aligned} V_a(r) &= 1 & r < r_0 \\ V_a(r) &= 0 & r > r_0 \end{aligned}, \quad (C-29)$$

and Equation (C-28) becomes

$$f_n\left(\frac{r_0}{R}\right) = \frac{2r_0 J_1(\beta_n r_0)}{R^2 \beta_n J_0^2(\beta_n R_0)}. \quad (C-30)$$

Several values of this function have been tabulated in Table C-1.

TABLE C-1
VALUES OF f_n

n	Φ_n	$f_n(.1)$	$f_n(.2)$	$f_n(.3)$	$f_n(.4)$	$f_n(.5)$
0	0	.01	.04	.09	0.16	.25
1	3.83	.0613	.232	.475	.733	.95
2	7.0155	.1045	.343	.54	.515	.21
3	10.1735	.1405	.362	.298	-.116	-.53
4	13.324	.166	.286	-.062	-.436	-.169
5	16.471	.181	.139	-.304	-.158	.413
6	19.619	.182	-.022	-.282	.266	.147

Equations (C-22) and (C-27) may be solved for the coefficients

A_n and B_n as

$$A_n = \frac{\rho_0 SV_2(S) f_n \left(\frac{r_0}{R_0}\right) e^{-\alpha_n L}}{\alpha_n T(S) 2 \sinh(\alpha_n L)}, \quad (C-31)$$

and

$$B_n = \frac{\rho_0 SV_2(S) f_n \left(\frac{r_0}{R_0}\right) e^{\alpha_n L}}{\alpha_n T(S) 2 \sinh(\alpha_n L)}. \quad (C-32)$$

Substitution of these coefficients into the solution equation yields

$$\bar{P}(r, x, s) = \sum_{n=0}^{\infty} \frac{J_0(\beta_n r) \rho_0 SV_2(S) f_n \left(\frac{r_0}{R_0}\right) \{e^{-\alpha_n(L-x)} + e^{\alpha_n(L-x)}\}}{2 \alpha_n \sinh(\alpha_n L)} \quad (C-33)$$

or

$$\bar{P}(r, x, s) = \rho_0 SV_2(S) \sum_{n=0}^{\infty} \frac{J_0(\beta_n r) \cosh(\alpha_n(L-x)) f_n \left(\frac{r_0}{R_0}\right)}{\alpha_n \sinh(\alpha_n L)}. \quad (C-34)$$

The axial and radial components of velocity can be derived from

Equations (C-11) and (C-12) as

$$V_x(r, x, s) = V_2(S) \sum_{n=0}^{\infty} \frac{J_0(\beta_n r) \sinh(\alpha_n(L-x)) f_n \left(\frac{r_0}{R_0}\right)}{\sinh(\alpha_n L)} \quad (C-35)$$

and

$$V_r(r, x, s) = V_2(S) \sum_{n=0}^{\infty} \frac{\beta_n J_1(\beta_n r) \cosh(\alpha_n(L-x)) f_n \left(\frac{r_0}{R_0}\right)}{\alpha_n \sinh(\alpha_n L)}. \quad (C-36)$$

At $x = 0$, Equation (C-34) becomes

$$\bar{P}(r, 0, s) = \rho_0 SV_2(S) \sum_{n=0}^{\infty} \frac{J_1(\beta_n r) \cosh(\alpha_n L) f_n \left(\frac{r_0}{R_0}\right)}{\alpha_n \sinh(\alpha_n L)}. \quad (C-37)$$

These solutions agree with Ingard [15] who made his derivations in the time domain. Several assumptions are involved in this solution. The wave equation was assumed and damping was neglected. The resonator was assumed to be rigid. The radial component of the input velocity was assumed to be zero and the axial component was assumed invariant over the neck cross section to facilitate a simple solution. More complicated velocity assumptions greatly complicate the solution.

The neck may be studied by considering an open end circular tube where the pressure variation as a function of radius and time is specified at one end and the velocity variation as a function of radius and time specified at the other end.

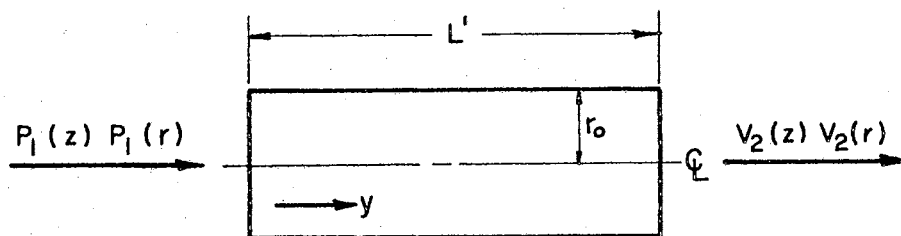


Figure C-3. Neck Configuration

The solution of the wave equation for this case may be written as

$$\bar{P}(r, y, s) = \sum_{n=0}^{\infty} J_0(\gamma_n r) \left\{ A_n e^{\sigma_n y} + B_n e^{-\sigma_n y} \right\} T(s) . \quad (C-38)$$

The radial velocity must be zero at the walls of the tube so that

$$J_1(\gamma_n r) = 0 . \quad (C-39)$$

This expression defines the permissible values of γ_n as

$$\gamma_n = 0, \frac{3.832}{r_0}, \frac{7.0155}{r_0}, \dots \quad (C-40)$$

The parameter σ_n is defined by the expression

$$\sigma_n = \left\{ \left(\frac{S}{c} \right)^2 + \gamma_n^2 \right\}^{\frac{1}{2}} \quad (C-41)$$

If the pressure variation at the open end of the neck is assumed to be a function of time only, then

$$P_1(S) = \sum_{n=0}^{\infty} J_0(\gamma_n r) \{A_n + B_n\} T(S) \quad (C-42)$$

If both sides of Equation (C-42) are multiplied by $r J_0(\gamma_n r)$ and integrated with respect to r from zero to r_0 , the coefficients are given by

$$A_n + B_n = \frac{2 \int_0^{r_0} r \left(P_1(S) / T(S) \right) J_0(\gamma_n r) dr}{r_0^2 J_0^2(\gamma_n r_0)} \quad (C-43)$$

or after carrying out the integration

$$A_n + B_n = \frac{2 P_1(S) J_1(\gamma_n r_0)}{T(S) r_0 \gamma_n J_0^2(\gamma_n r_0)} \quad (C-44)$$

Since $J_1(\gamma_n r_0) = 0$, the sum $\{A_n + B_n\}$ must equal zero for all n greater than zero. The value of $A_0 + B_0$ can be evaluated from Equation (C-44) by taking the limit as γ_n approaches zero,

$$A_0 + B_0 = \frac{2 P_1(S)}{T(S) r_0} \lim_{\gamma \rightarrow 0} \left(\frac{J_1(\gamma r_0)}{\gamma} \right) \quad (C-45)$$

The limit can be evaluated using L'Hospital's rule as

$$\lim_{\gamma \rightarrow 0} \frac{J_1(\gamma r_0)}{\gamma} = \lim_{\gamma \rightarrow 0} \left\{ J_0(\gamma r_0) - \frac{J_1(\gamma r_0) r_0}{\gamma r_0} \right\} \quad (C-46)$$

which can be written as

$$\lim_{\gamma \rightarrow 0} \frac{J_1(\gamma r_0)}{\gamma} = \frac{1}{2} \lim_{\gamma \rightarrow 0} r_0 J_0(\gamma r_0) = \frac{r_0}{2} . \quad (C-47)$$

This results in

$$A_0 + B_0 = \frac{P_1(S)}{T(S)} . \quad (C-48)$$

The boundary condition on the right leads to the equation

$$-\rho_0 S V_2(S) V_2(r) = \sum_{n=0}^{\infty} \sigma_n J_0(\gamma_n r) \left\{ A_n e^{\sigma_n L'} - B_n e^{-\sigma_n L'} \right\} T(S) . \quad (C-49)$$

Using the Fourier Bessel series expansion, leads to

$$A_n e^{\sigma_n L'} - B_n e^{-\sigma_n L'} = \frac{-2 \rho_0 S V_2(S) \int_0^{r_0} r V_2(r) J_0(\gamma_n r) dr}{\sigma_n T(S) r_0^2 J_0^2(\gamma_n r_0)} \quad (C-50)$$

or

$$A_n e^{\sigma_n L'} - B_n e^{-\sigma_n L'} = \frac{-\rho_0 S V_2(S) f_n'(r_0)}{\sigma_n T(S)} \quad (C-51)$$

where

$$f_n'(r_0) = \frac{2 \int_0^{r_0} r V_2(r) J_0(\gamma_n r) dr}{r_0^2 J_0^2(\gamma_n r_0)} . \quad (C-52)$$

If the velocity at the neck end which joins with the resonator cavity is not a function of the radius, that is $V_2(r) = 1$, then the function $f_n'(r_0)$ becomes

$$f_n'(r_0) = \frac{2 J_1(\gamma_n r_0)}{\gamma_n r_0 J_0^2(\gamma_n r_0)} . \quad (C-53)$$

The condition of constant pressure at one end and constant velocity at the other leads to the results

$$A_n + B_n = 0 \quad (C-54)$$

and

$$A_n e^{\sigma_n L'} - B_n e^{-\sigma_n L'} = 0 \quad (C-55)$$

for $n > 0$. These equations have no solution except $A_n = B_n = 0$

for $n > 0$. Equation (C-38) thus becomes

$$\bar{P}(y, s) = \left\{ A e^{\frac{S}{c} y} + B e^{-\frac{S}{c} y} \right\} T(S) \quad (C-56)$$

Equation (C-51) becomes

$$A e^{\frac{S}{c} L'} - B e^{-\frac{S}{c} L'} = \frac{-\rho_0 c V_2(S)}{T(S)} \quad (C-57)$$

Equations (C-48) and (C-57) may be solved for the coefficients A

and B as

$$A = \frac{-P_1(S) e^{\frac{S}{c} L'} + \rho_0 c V_2(S)}{-2 \cosh\left(\frac{S}{c} L'\right) T(S)} \quad (C-58)$$

and

$$B = \frac{-P_1(S) e^{-\frac{S}{c} L'} - \rho_0 c V_2(S)}{-2 \cosh\left(\frac{S}{c} L'\right) T(S)} \quad (C-59)$$

Substitution of these results into Equation (C-56) results in the solution

$$\bar{P}(y, s) = \frac{P_1(S) \cosh\left(\frac{S}{c}(L' - y)\right) - \rho_0 c V_2(S) \sinh\left(\frac{S}{c} y\right)}{\cosh\left(\frac{S}{c} L'\right)} \quad (C-60)$$

The velocity can be derived from Equation (C-11) as

$$\bar{V}(y, s) = \frac{\frac{P_1(S)}{\rho_0 c} \sinh\left(\frac{S}{c}(L' - y)\right) + V_2(S) \cosh\left(\frac{S}{c} y\right)}{\cosh\left(\frac{S}{c} L'\right)} \quad (C-61)$$

At $y = L'$, Equation (C-60) becomes

$$P_2(S) = \frac{P_1(S) - \rho c V_2(S) \sinh\left(\frac{S}{c} L'\right)}{\cosh\left(\frac{S}{c} L\right)} . \quad (C-62)$$

Having obtained solutions for the wave equation for the cavity and for the neck, one next examines these solutions and determines under what conditions they may be combined to obtain a complete solution for the resonator. The solution equations for the cavity show that in general the pressure across the mouth is not constant but is a function of the radius r . The solution for the neck with a constant pressure input at the open end and a constant velocity at the cavity end indicates that the pressure and velocity in the neck are independent of the radius. Thus, at the mouth of the cavity Equations (C-33) or (C-34) indicate that the pressure is a function of the radius while Equations (C-60) or (C-62) indicate that the pressure is not a function of the radius. Thus, the solutions will be of value when this discrepancy can be avoided or reduced to a minor effect. From a mathematical point of view this difficulty arises because it is impossible to impose three arbitrary end conditions on the solution of the wave equation for the neck. Thus, it is not possible to impose simultaneously the boundary conditions of the pressure at the open end being $P_1(S)$, the velocity at the cavity end being $V_2(S)$, and also that the pressure at the cavity end being $P_2(r,s)$. Actually neither the pressure nor velocity will be constant across any cross section of the neck. A better approximation for the velocity and pressure distribution might be obtained for a few geometrically simple cases, but the mathematical difficulties become excessive and any general solution is impossible.

Since the objective of this work is the study of the transient response of resonators in general rather than a detailed study of the modes and responses of a particular configuration, the solutions already obtained are adequate for their intended purpose.

The equations which describe the characteristics of the neck may be improved somewhat by taking into account the movement of the gas in the immediate vicinity of either end of the neck. Reasoning from the continuity viewpoint, some of the gas outside must move in unison with that in the neck. Kinsler and Frey [4] show that a piston vibrating in an infinite baffle is loaded by the adjacent medium with a mass equal to that of the fluid contained in a cylinder of the same diameter as the piston and length $\Delta L = 8r_0/3\pi$, where r_0 is the radius of the piston. At low frequencies it is usual to assume $\Delta L = 8r_0/3\pi = 0.85r_0$ for a neck terminated in a wide flange and $\Delta L = 0.6r_0$ for an unflanged termination. Thus, in the equations describing the neck, the actual length of the neck L' can be replaced by an effective length L_e where

$$L_e = L' + \Delta L_1 + \Delta L_2 \quad . \quad (C-63)$$

Kinsler and Frey show that there is a frequency limitation on this approximation which is given by

$$\lambda > 4\pi r_0 \quad . \quad (C-64)$$

The correction factor does not vary rapidly however so that the frequency limitation is neither rigid nor critical. The correction factor also depends on the shape of the neck although it does not vary much for shapes which are not extreme. As the length of the

neck is increased the correction factors become relatively less important.

The solution equations for the cavity are fully compatible with the solution equations for the neck if pressure or velocity variation with the radius is small for r less than r_0 . Some idea of how important the dependency on the radius is, can be developed by considering the frequency properties of the oscillations. For pressure oscillations which are sinusoidal in time, a variation of 18° in Figure C-4 which corresponds to $\lambda/20$ represents about five percent variation. Thus, if the pressure or velocity variation with the

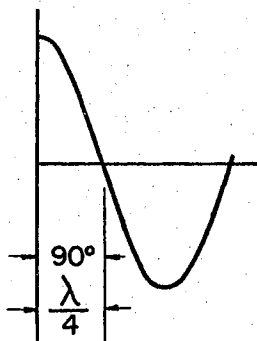


Figure C-4. Wave Length and Frequency Relationship for Sinusoidal Motion

radius is to be less than five percent for $r < r_0$, r_0 is related to the wavelength by the equation

$$r_0 < \frac{\lambda}{20}, \quad (C-65)$$

or the diameter of the neck should be less than $\lambda/10$. If the diameter of the neck is less than half the diameter of the cylinder, then this condition can be expressed as

$$D < \frac{\lambda}{5} \quad (C-66)$$

where D is the diameter of the cylinder.

The solution equation for the cylindrical cavity may be written as

$$V_2(S) = \frac{P_2(r, s)}{\rho_0 S \sum_{n=0}^{\infty} \frac{J_0(\beta_n r) \cosh(\alpha_n L)}{\alpha_n \sinh(\alpha_n L)} f_n\left(\frac{r_0}{R_0}\right)} \quad (C-67)$$

or

$$V_2(S) = \frac{P_2(r, s)}{\rho_0 c \frac{\cosh\left(\frac{S}{c} L\right)}{\sinh\left(\frac{S}{c} L\right)} \left(\frac{r_0}{R_0}\right)^2 + \rho_0 S \sum_{n=1}^{\infty} \frac{J_0(\beta_n r) \cosh(\alpha_n L)}{\alpha_n \sinh(\alpha_n L)} f_n\left(\frac{r_0}{R_0}\right)} \quad (C-68)$$

where $P_2(r, s)$ may now be considered to be the input and $V_2(S)$ to be the response. If the condition expressed by Equation (C-65) or Equation (C-66) holds, then the variation with the radius is unimportant. For $r = 0$ Equation (C-68) becomes

$$V_2(S) = \frac{P_2(S)}{\rho_0 c \frac{\cosh\left(\frac{S}{c} L\right)}{\sinh\left(\frac{S}{c} L\right)} \left(\frac{r_0}{R_0}\right)^2 + \rho_0 S \sum_{n=1}^{\infty} \frac{1 \cosh(\alpha_n L)}{\alpha_n \sinh(\alpha_n L)} f_n\left(\frac{r_0}{R_0}\right)} \quad (C-69)$$

The parameter α_n is defined by Equation (C-18) as

$$\alpha_n = \left\{ \frac{S^2}{c^2} + \beta_n^2 \right\}^{\frac{1}{2}} = \left\{ \frac{S^2}{c^2} + \frac{\phi_n^2}{R_0^2} \right\}^{\frac{1}{2}} \quad (C-70)$$

If $j\omega$ is substituted for S in Equation (C-70) the result is

$$\alpha_n = \left\{ -\left(\frac{2\pi}{\lambda}\right)^2 + \left(\frac{\phi_n}{R_0}\right)^2 \right\}^{\frac{1}{2}} \quad (C-71)$$

If the second term of the above expression is much larger than the first, then the first may be neglected. The parameter ϕ_1 may be evaluated from Table C-1 as $\phi_1 = 3.83$, so that the first term on the right of Equation (C-71) may be neglected if

$$\left(\frac{3.83}{R_0}\right)^2 \gg \left(\frac{2\pi}{\lambda}\right)^2 \quad (C-72)$$

If the first term is to be less than five percent of the second, then

$$\lambda^2 > \frac{20(2\pi)^2}{(3.83)^2} R_0^2 \quad (C-73)$$

or

$$\lambda > 7.4 R_0 \quad (C-74)$$

or approximately

$$\lambda > 4D \quad (C-75)$$

If Equation (C-75) holds then α_n is approximated by the relation

$$\alpha_n \approx \beta_n = \frac{\phi_n}{R_0} \quad (C-76)$$

If $\phi_n L/R_0$ is greater than about 2, the ratio

$$\frac{\cosh \alpha_n L}{\sinh \alpha_n L} \approx 1 \quad (C-77)$$

since the hyperbolic functions are very nearly equal for large arguments. With this condition the second term in the denominator of Equation (C-69) becomes

$$\rho_0 S \sum_{n=1}^{\infty} \frac{f_n\left(\frac{r_0}{R}\right)}{\alpha_n} = \rho_0 S \sum_{n=1}^{\infty} \frac{f_n\left(\frac{r_0}{R_0}\right)}{\beta_n} = \rho_0 S \sum_{n=1}^{\infty} \frac{r_0^2 J_1(\beta_n r_0)}{\phi_n^2 J_0^2(\beta_n R_0)} \quad (C-78)$$

or

$$\rho_0 S \sum_{n=1}^{\infty} \frac{f_n \left(\frac{r_0}{R_0} \right)}{\alpha_n} = \rho_0 S r_0 \Delta \quad (C-79)$$

where

$$\Delta = \sum_{n=1}^{\infty} \frac{2 J_1(\beta_n r_0)}{\beta_n^2 J_0^2(\beta_n R_0)} \quad (C-80)$$

The hyperbolic functions may be expanded in infinite series form as

$$\sinh x = x + \frac{x^3}{3!} + \frac{x^5}{5!} + \frac{x^7}{7!} + \dots \quad (C-81)$$

and

$$\cosh x = 1 + \frac{x^2}{2!} + \frac{x^4}{4!} + \frac{x^6}{6!} + \dots \quad (C-82)$$

It is sometimes useful to use only the first term of these series approximations. Some notion of the accuracy and limitations of this approximation may be gained by comparing the one term approximation with the two term approximation. For $\coth x$ the approximation becomes

$$\frac{\cosh x}{\sinh x} \approx \frac{(1 + \frac{x^2}{2!} + \dots)}{x(1 + \frac{x^2}{6})} \approx \frac{(1 + \frac{x^2}{2!} + \dots)(1 - \frac{x^2}{6} + \dots)}{x} \quad (C-83)$$

If the term $x^2/3$ is less than perhaps five percent of the 1, then the one term approximation of

$$\frac{\cosh \frac{S}{c} (L-x)}{\sinh \frac{S}{c} L} \approx \frac{1}{\frac{SL}{c}} \quad (C-84)$$

will be accurate within about five percent. Thus

$$(\frac{SL}{c})^2/3 \leq \frac{1}{20} \quad (C-85)$$

Substitution of $\omega = 2\pi f$ for S , where ω and f are the frequency of the sound in radians per second and cycles per second respectively and

$$f\lambda = c, \quad (C-86)$$

where λ is the wavelength of the sound, allows Equation (6-85) to be written as

$$\lambda > 2\pi \sqrt{\frac{20}{3}} L \approx 16 L. \quad (C-87)$$

With these simplifications the response equation for the cavity becomes

$$V_a(S) = \frac{P_a(S)}{\frac{\rho_0 c^2 r_0^2}{SL R_0^2} + \rho_0 r_0 \Delta S} \quad (C-88)$$

which could be expressed as

$$V_a(S) = \frac{P_a(S)}{\rho_0 c^2 \frac{A}{VS} + S \rho_0 r_0 \Delta} \quad (C-89)$$

where A is the area of the neck and V is the volume of the cavity. Thus, the acoustical system shown in Figure C-2 (the cavity alone) is analogous to the electrical system in Figure C-5.

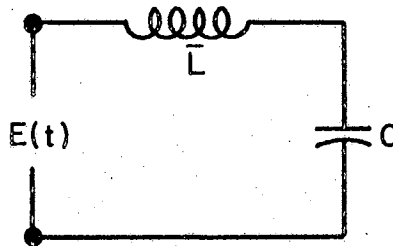


Figure C-5. Electrical Circuit Analogous to an Helmholtz Resonator at Low Frequencies

where the voltage input is analogous to the pressure input, current is analogous to velocity at the piston, the inductance is $\bar{L} = \rho_0 r_0 \Delta$ and the capacitance is $C = \rho_0 c^2 A/V$. This agrees with the analogous representation as presented by many other authors except for the inductance term. This term is in fact the end correction term for the cavity end of the neck. In the previous discussion of the neck it was mentioned that additional mass loading ranging from about $.85 r_0$ to $.6 r_0$ should be added. The value of Δ for various values of (r_0/R_0) is given in Table C-2 and is seen to be in rough agreement with the above values.

TABLE C-2
SELECTED CALCULATED VALUES OF Δ

$\frac{r_0}{R_0}$	Δ
.1	.85
.2	.77
.4	.56

There are indications that the neck correction factors are not simply a function of the neck shape and the assumed velocity distribution as is implied by Rayleigh [1] for example, but also depend on the geometry of the cavity and the location of the neck opening into the cavity.

If the effective length of the neck is less than $\lambda/16$, then Equation (C-62) may be reduced to

$$V(S) = \frac{P_1(S) - P_2(S)}{\rho_0 L_e S}, \quad (C-91)$$

where $V(S)$ is the mean velocity in the neck. The second term in the denominator of Equation (C-89) may now be dropped since $r_0 \Delta = \Delta_2$ in Equation (C-63). This leads to the equation

$$\frac{P_2(S)}{\rho_0 c^2 \frac{A}{VS}} = V_2(S) = V(S) . \quad (C-92)$$

Equations (C-91) and (C-92) may now be combined to yield

$$V(S) = \frac{P_1(S)}{\rho_0 S L_e + \frac{\rho_0 c^2 A}{VS}} . \quad (C-93)$$

In terms of pressures this result becomes

$$P_2(S) = P(S) = \frac{P_1(S)}{\frac{S^2}{\left(\frac{c^2 A}{VL_e}\right)} + 1} . \quad (C-94)$$

From either of these equations it can be seen that the Helmholtz resonator is analogous to a simple oscillator as shown in Figure C-5 where the inductance is now ρL_e . If the mechanical analogy is desired rather than the electrical, the equivalent system is shown in Figure C-6.

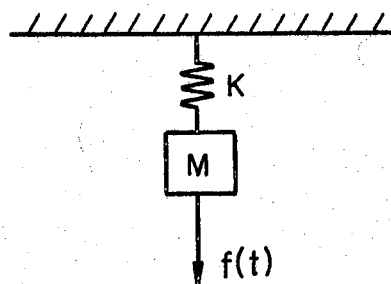


Figure C-6. Mechanical System Analogous to a Helmholtz Resonator at Low Frequencies

Here the forcing function is analogous to pressure input, the mass is $m = \rho L_e$ and the spring constant is $K = \frac{\rho_0 c^2 A}{V}$. The natural frequency is given by

$$f_n = \frac{c}{2\pi} \sqrt{\frac{A}{VL_e}} \quad (C-95)$$

The results given by Equations (C-93), (C-94), and (C-95) and the analogous electrical and mechanical circuits are in agreement with the simple results obtained by Rayleigh and others. This model is subject to the restriction that the sound wavelength be greater than sixteen times any of the characteristic dimensions of the resonator.

If the ratio of the hyperbolic functions is approximated as

$$\frac{\cosh x}{\sinh x} \approx \frac{1 + x^2/3}{x} \quad (C-96)$$

an estimate of what the wavelength restriction should be may be obtained by examining the effect of adding another term. Thus, the approximation could be written as

$$\begin{aligned} \frac{\cosh x}{\sinh x} &\approx \frac{(1 + \frac{x^2}{2!} + \frac{x^4}{4!} \dots)}{(x + \frac{x^3}{3!} + \frac{x^5}{5!} \dots)} \approx \\ &\frac{(1 + \frac{x^2}{2!} + \frac{x^4}{4!} \dots) \cdot (1 - \frac{x^2}{3!} - \frac{x^4}{5!} + (\frac{x^2}{6} + \frac{x^4}{5!})^2 + \dots)}{x} \\ &\approx \frac{1 + \frac{x^2}{3} - \frac{x^4}{45}}{x} \quad (C-97) \end{aligned}$$

The approximation

$$\frac{\cosh \frac{S}{c} L}{\sinh \frac{S}{c} L} \approx \frac{1 + (\frac{S}{c} L)^2/3}{\frac{SL}{c}} \quad (C-98)$$

will be accurate within approximately five percent if

$$\frac{1}{45} \left(\frac{SL}{c} \right)^4 < \frac{1}{20} \frac{1}{3} \left(\frac{SL}{c} \right)^2 \quad (C-99)$$

which reduces to

$$\lambda > 2\pi \sqrt{\frac{4}{3}} L \approx 7.3L \quad (C-100)$$

or

$$\lambda > 8L \quad (C-101)$$

If the approximation given by Equation (C-96) is used in Equation (C-69) which describes the response of the cavity, the result is

$$V_2(S) = \frac{P_2(S)}{\frac{\rho_0 c^2}{SL} \left(\frac{r_0}{R_0} \right)^2 + \frac{\rho_0 SL}{3} \left(\frac{r_0}{R_0} \right)^2 + \rho_0 S(r_0 \Delta)} \quad (C-102)$$

The analogous circuit for this case would be the same as that shown in Figure C-5 where the inductance and capacitance are given by

$$\bar{L} = \frac{\rho_0 L}{3} \left(\frac{r_0}{R_0} \right)^2 + \rho_0 (r_0 \Delta) \quad (C-103)$$

and

$$C = \frac{\rho_0 c^2 A}{V} \quad (C-104)$$

This circuit representation of the cavity is valid for wavelengths greater than 8 times the characteristic dimensions of the cavity.

If the cavity dimensions are less than $\lambda/8$, it is very likely that the neck dimensions would be less than $\lambda/16$. The equivalent

circuit for Equation (C-91) is shown in Figure C-7.

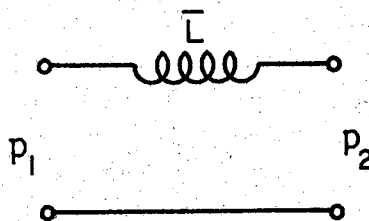


Figure C-7. Analogous Electrical Circuit for the Neck for
 $\lambda > L_e/16$

The combination of the analogous circuits from Figures C-7 and C-5, being careful not to include end effects more than once, again results in the simple oscillator circuit shown in Figure C-5 where the inductance and capacitance are given by

$$\bar{L} = \rho_0 L_e + \frac{\rho_0 L}{3} \left(\frac{r_0}{R_0} \right)^2 \quad (\text{C-105})$$

and

$$C = \frac{\rho_0 c^2 A}{V} \quad (\text{C-106})$$

The equation for the circuit can be written down from the circuit or can be obtained by combining Equations (C-91) and (C-102). In this case Equation (C-91) should be written as

$$V_2(S) = \frac{P_1(S) - P_2(S)}{\rho_0 S L_2} \quad (\text{C-107})$$

where

$$L_2 = L' + \Delta_1 \quad (\text{C-108})$$

is used instead of

$$L_e = L' + \Delta_1 + \Delta_2 = L_2 + \Delta_2 ; \quad (C-109)$$

where Δ_1 is the end correction term for the open end of the neck and Δ_2 is the end correction for the end which joins with the cavity. The reason for this change is that the end correction term for the cavity end is included in Equation (C-102). Elimination of $P_2(S)$ from Equation (C-102) and (C-107) yields

$$V_2(S) = V(S) = \frac{P_1(S)}{\frac{\rho_0 c^2}{SL} \left(\frac{r_0}{R_0}\right)^2 + \frac{\rho_0 SL}{3} \left(\frac{r_0}{R_0}\right)^2 + \rho_0 SL_e} . \quad (C-110)$$

The pressure inside the cavity is given by

$$P(x,s) = \frac{P_1(S) \left\{ \rho_0 c \frac{\cosh \frac{S}{c} (L-x)}{\sinh \frac{S}{c} L} \left(\frac{r_0}{R_0}\right)^2 + \rho_0 S \Delta_2 \right\}}{S \left\{ \rho_0 L_e + \frac{\rho_0 L}{3} \left(\frac{r_0}{R_0}\right)^2 \right\} + \frac{\rho_0 c^2 A}{SV}} . \quad (C-111)$$

Equations (C-110) and (C-111) are valid if the dimensions of the cavity are less than $\lambda/8$, the diameter of the neck is less than $\lambda/10$, and the length of the neck or more exactly the effective length of the neck is less than $\lambda/16$.

In the simple model which is valid if all dimensions are less than $\lambda/16$, the geometric details of the resonator were not relevant. The response Equation (C-94) involved only the volume of the cavity and the area and length of the neck. The shape of the neck provided that it is not distorted badly enters only as a minor effect in determining the end corrections. Equation (C-110) may be written as

$$V(S) = \frac{P_1(S)}{\frac{\rho_0 c^2 A}{SV} + S(\rho_0 L_e + \frac{\rho_0 L^2}{3} \frac{A}{V})} \quad (C-112)$$

From either form, Equation (C-110) or (C-112), it can be seen that the relative geometry of the cavity has entered into the problem.

It was shown that pressure or velocity variation with radius in the neck would be less than five percent for $(r_0/R) < .5$ and $\lambda > 5D$. If $(r_0/R_0) \leq .4$ then the wavelength limitation can be relaxed to $\lambda > 4D$. Equating Equations (C-37) and (C-62) leads to

$$\begin{aligned} \rho_0 S V_2(S) \sum_{n=0}^{\infty} \frac{J_0(\beta_n r)}{\alpha_n} \frac{\cosh(\alpha_n L)}{\sinh(\alpha_n L)} f_n \left(\frac{r_0}{R_0} \right) + \rho_0 c V_2(S) \frac{\sinh(\frac{S}{c} L')}{\cosh(\frac{S}{c} L')} \\ = \frac{P_1(S)}{\cosh(\frac{S}{c} L')} \end{aligned} \quad (C-113)$$

which can be solved for $V_2(S)$ as

$$\begin{aligned} V_2(S) = \frac{P_1(S)}{\cosh(\frac{S}{c} L')} \Bigg/ \left\{ \rho_0 c \frac{\cosh(\frac{S}{c} L)}{\sinh(\frac{S}{c} L)} \left(\frac{r_0}{R_0} \right)^2 \right. \\ \left. + \rho_0 S \sum_{n=1}^{\infty} \frac{J_0(\beta_n r)}{\alpha_n} \frac{\cosh(\alpha_n L)}{\sinh(\alpha_n L)} f_n \left(\frac{r_0}{R_0} \right) + \frac{\rho_0 c \sinh(\frac{S}{c} L')}{\cosh(\frac{S}{c} L')} \right\} \end{aligned} \quad (C-114)$$

No attempt has yet been made here to include an end correction term for the open end of the neck. The correction for the cavity end is the second term in the brackets in the denominator of Equation (C-111).

With the substitution

$$L_2 = L^1 + \Delta_1 \quad (C-115)$$

where $\Delta_1 \approx 0.85 r_o$ is the end correction for the open end into Equation (C-111) for L^1 , a reasonable correction is made. Equation (C-111) may then be substituted into Equation (C-34) to yield an expression for the pressure in the cavity,

$$\bar{P}(r, x, s) = \left[\frac{P_1(s)}{\cosh\left(\frac{S}{c} L_2\right) \left\{ c \frac{\cosh\left(\frac{S}{c} L\right)}{\sinh\left(\frac{S}{c} L\right)} \left(\frac{r_o}{R_o}\right)^2 + c \frac{\sinh\left(\frac{S}{c} L_2\right)}{\cosh\left(\frac{S}{c} L_2\right)} + s r_o \Delta \right\}} \right] \times$$

$$\left[s \sum_{n=0}^{\infty} \frac{J_0(\beta_n r)}{\alpha_n} \frac{\cosh \alpha_n (L-x)}{\sinh(\alpha_n L)} f_n \left(\frac{r_o}{R_o}\right) \right]. \quad (C-116)$$

This equation is valid for λ greater than 4 times any dimension of the resonator. The difficulty encountered in relaxing the wavelength limitation arises from the need to limit the pressure or velocity variation with radius at the junction of the neck with the cavity.

The solution given by Equation (C-116) is valid for higher frequencies than is the simple lumped parameter solution but it has several weaknesses. The geometry of the resonator under consideration was exceedingly simple; however, the solution given by Equation (C-116) is exceedingly complicated, almost too complicated to be of much use. The solution is chained to the geometry of the particular case; an application to a different geometrical situation could be impossible. Damping has not been included and will become more important at higher frequencies.

TABLE C-3

SUMMARY OF FREQUENCY DEPENDENT APPROXIMATIONS

Approximation	Wavelength Restriction	Approximate Accuracy
1. $\alpha_n \approx \beta_n = \frac{\phi_n}{R}$	$\lambda > 4 \text{ Dia.}$	5%
2. $\frac{\sinh \frac{SL}{c}}{\cosh \frac{SL}{c}} \approx \frac{SL}{c}$	$\lambda > 16 L$	5%
3. $\frac{\sinh \frac{SL}{c}}{\cosh \frac{SL}{c}} \approx \frac{\frac{SL}{c}}{1 + (\frac{SL}{c})^2/3}$	$\lambda > 8 L$ $\lambda > 5 L$	5% 10%
4. $\sinh \frac{SL}{c} \approx \frac{SL}{c}$	$\lambda > 11.5 L$	5%
5. $\sin \frac{SL}{c} \approx \frac{SL}{c}$	$\lambda > 11.5 L$	5%
6. $\sinh \frac{SL}{c} \approx \frac{SL}{c} + (\frac{SL}{c})^3/6$	$\lambda > 2\pi L$	5%
7. $\sin \frac{SL}{c} \approx \frac{SL}{c} + (\frac{SL}{c})^3/6$	$\lambda > 2\pi L$	5%
8. $\cosh \frac{SL}{c} \approx 1$	$\lambda > 20 L$	5%
9. $\cos \frac{SL}{c} \approx 1$	$\lambda > 20 L$	5%
10. $\cosh \frac{SL}{c} \approx 1 + (\frac{SL}{c})^2/2$	$\lambda > 8 L$ $\lambda > 5.7 L$	5% 10%

APPENDIX D

CALIBRATIONS

Two factory-calibrated Altec microphones and a Textronic oscilloscope were used to make the measurements. The calibration curves for the microphones indicate that the sensitivities of both microphones are -54.5 DB (reference 1 volt per dyne per centimeter) from 20 to 4000 cps which includes the frequencies encountered in this study. The above sensitivity corresponds to approximately 1.095 psf/volt. Tests indicated however that there was a slight difference in the sensitivities of the microphone. Microphone No. 3892 was used to record inputs mostly and is also referred to as microphone No. 1. Microphone No. 3854 was used to measure responses mostly and is also referred to as microphone No. 2. Table D-1 shows the relative sensitivities at various frequencies which cover the range of testing for this work. A photograph such as was used to compare the sensitivities is shown in Chapter V. Because of the inherent difficulty of reading a scope to more than two figures, the use of three figures in Table D-1 is probably not justified. On the average the sensitivity of the No. 2 microphone is about 1.1 times that of the No. 1 microphone. In labeling the figures throughout the work, the sensitivity of the microphone was taken as 1.0 psf/volt instead of the 1.095 psf/volt given above.

TABLE D-1

MICROPHONE SENSITIVITY COMPARISON

Frequency cps	$\frac{\text{\#2 Sensitivity}}{\text{\#1 Sensitivity}}$
60	1.06
70	1.05
80	1.08
90	1.1
100	1.1
110	1.13
120	1.09
130	1.09
140	1.09
150	1.08
160	1.09
170	1.1
180	1.08
190	1.09
200	1.09
210	1.1
220	1.1
230	1.09
240	1.1
250	1.1
260	1.1
300	1.1

This is justifiable since precise calibration is not of interest; instead the significant factor is the relative sensitivities of the two microphones.

The sweep rate calibration and linearity of the oscilloscope were checked by means of an oscillator and a Beckman counter. The calibration and linearity were good enough so that it was not possible to read any error from the scope trace. The amplitude calibration was checked with the internal calibrator of the scope and found to be good. The important consideration for this work was not absolute amplitude calibration but that the sensitivities of the two beams were identical. It was not possible to see any difference between the sensitivities or linearity of the two beams for all of the scales used in this work. In short, the scope calibration was good enough to be considered perfect since whatever errors were present could not be seen.

VITA

James Donald Simpson, Jr.

Candidate for the Degree of

Doctor of Philosophy

Thesis: THE TRANSIENT RESPONSE OF A HELMHOLTZ RESONATOR WITH APPLICATION
TO SONIC BOOM RESPONSE STUDIES

Major Field: Mechanical Engineering

Biographical:

Personal Data: Born in Okemah, Oklahoma, November 29, 1939, the son of James D. and Anna Ruth Simpson. Married to Patricia Ann Watson, June 3, 1961. Father of two sons, Jimmy and Robby.

Education: Graduated from Nowata High School, Nowata, Oklahoma, 1957; received the Bachelor of Science Degree in Mechanical Engineering from Oklahoma State University in January, 1962; received the Master of Science Degree in Mechanical Engineering from Oklahoma State University in August, 1963; completed requirements for the Doctor of Philosophy Degree in October, 1965.

Professional Experience: Engineering aid, Bureau of Indian Affairs, summer of 1959. Design draftsman, Phillips Petroleum Co., summers of 1960 and 1961. Research engineer, Autonetics, North American Aviation, February 1962 to September 1962. Graduate assistant, Oklahoma State University, September 1962 to September 1965.

Organizations: Member of Sigma Tau, and Pi Mu Epsilon.